Novel insights into

Flt1 mediated sprouting angiogenesis

in zebrafish

Inaugural-Dissertation
to obtain the academic degree
Doctor rerum naturalium (Dr. rer. nat.)

Submitted to the Department of Biology, Chemistry and Pharmacy
of Freie Universität Berlin

by
Janna Krüger
from Aachen (Germany)

2012

I completed my doctorate studies from March 01, 2008 to May 02, 2012 under the supervision of Prof. Dr. F. le Noble at the Max Delbrück Center for Molecular Medicine, Berlin.

1st Reviewer: Prof. Dr. Ferdinand le Noble

2nd Reviewer: Prof. Dr. Rupert Mutzel

Date of defense: September 12, 2012

Acknowledgement

First of all I would like to thank my supervisor Prof. Dr. F. le Noble for the opportunity to work on an exciting project. I am very grateful for the resources he offered, his encouragement, and the scientific discussions. The experience I got from his lab has provided me with lifetime benefits.

I thank Prof. Dr. R. Mutzel of the Freie Universität Berlin for his interest in my doctorate studies and the supervision at the university.

I am grateful to all the current and former members of the le Noble lab for their kindness and helpfulness. I really enjoyed working in this group. I especially want to thank Katja Scholz for expert technical assistance and her constructive remarks. I thank Dr. Christian Klein for the thoughtful advices. Additionally, I'm very thankful to Stefan Kunert, and Dr. Mariana Lagos-Quintana for their time to read my thesis to refine my work. Dr. Yu Shi I want to thank for designing the TaqMan probes and Dr. Dong Liu for valuable suggestions. Furthermore, I'm especially grateful to Dr. Katharina da Silva Lopes for the critical reading of my thesis as well as for her helpfulness and our creative discussions.

My gratitude to Dr. Arndt Siekmann from the MPI for Molecular Biomedicine and Dr. Francesca Peri from the EMBO for providing me chances to work in their labs shortly on my thesis project. I thank also Dr. Stefan Schulte-Merker for sharing the double transgenic zebrafish line Tg(*flt1*^{BAC}*:yfp*) x Tg(*kdrl:ras-cherry*)^{s916}.

I would like to gratefully acknowledge the Center for Stroke Research Berlin (CSB) for providing me with a PhD scholarship.

I'm very thankful to my family and friends for their cheerful support and enthusiasm. Besides, I'm heartily grateful to my parents who gave me the moral I required for my dissertation. Special thanks deserve my partner Vladimir Andrey Gimenez Rivera and my brother Johann Krüger for their encouragement and patience in me and my work. Without their love, understanding and support I would never have come so far.

Table of contents

1 Abstract

In vertebrates, the formation of blood vessels is fundamental for development, tissue growth and repair. New blood vessels are formed from pre-existing vessels in a process termed sprouting angiogenesis. Endothelial cells with distinct cell fates and behaviour guide the angiogenic sprouts. The leading endothelial cell, called tip cell, extends filopodia protrusions to explore the local environment for guidance cues such as vascular endothelial growth factor (VEGF), while the adjacent stalk cell is responsible for lumen formation. VEGF mediates its signal through binding to its cognate receptors VEGFR-1 and -2 that are expressed on tip and stalk cells. Several studies have linked the expression levels of VEGFR-1, also called Flt1, with the capacity to form new vessels in pathologies like ischemic cardiovascular diseases, retinopathies and tumour growth. However, the precise function of Flt1 during sprouting angiogenesis is unknown. Using transgenic zebrafish embryos as model system, we aimed to characterize the role of Flt1 during vascular growth *in vivo*. Here we show that Flt1 negatively regulates tip cell formation.

Initial analysis of Flt1 in zebrafish revealed expression of membrane-bound Flt1 (mFlt1) and a so far unknown soluble isoform of Flt1 (sFlt1). Knockdown of Flt1 in zebrafish embryos increased tip cell behaviour within the angiogenic sprout resulting in hyperbranching of segmental arteries. In line with increased sprouting, we observed a reduced expression of the Notch signalling pathway; a signalling casacade that suppresses tip cell differentiation. Conditional overexpression of Notch in Flt1 deficient embryos could restore the segmental artery pattering indicating a contribution of Notch to the vascular phenotype. In addition to the vascular expression domain of Flt1, we detected Flt1 expression in neurons of zebrafish embryos. Knockdown of Flt1 resulted not only in aberrant vessels but also in a reduced neuronal cell number, pointing to a role of Flt1 also in developing neurons. Surprisingly, vascular specific overexpression of the secreted isoform sFlt1 led to a distribution throughout the neural tube. This suggests that the nervous system may contribute to establishing VEGF gradients required for segmental artery outgrowth.

These results demonstrate that Flt1 acts in a Notch dependent manner as negative regulator for tip cell formation and branching morphogenesis. Moreover, Flt1 affects neurogenesis and can most likely function at the interface of vascular and neuronal development.

2 Zusammenfassung

Die Bildung von Blutgefäßen ist essentiell für die Entwicklung, das Wachstum und die Regeneration von Gewebe in Vertebraten. Neue Blutgefäße können durch den Prozess der Angiogenese aus bereits bestehenden Gefäßen entstehen. Die Endothelialzellen im Gefäßspross besitzen abhängig von ihrer Lokalisation unterschiedliche Eigenschaften. Die an der Spitze des Gefäßsprosses liegende Endothelialzelle wird als „tip cell“ bezeichnet. Diese erkennt mithilfe von Filopodien die Umgebung nach vaskulären Wachstumsfaktoren, wie z.B. VEGF („vascular endothelial growth factor“) und bestimmt somit die Wachstumsrichtung des Gefäßsprosses. Die angrenzende Endothelialzelle, die „stalk cell“, dient der Lumenbildung. VEGF vermittelt sein Signal durch die Bindung an die VEGF-Rezeptoren-1 und -2, welche auf der „tip cell“ und der „stalk cell“ lokalisiert sind. Verschiedene Studien belegen einen Zusammenhang zwischen der Expression des VEGF-Rezeptors-1 (Flt1) und der Pathologie von Herz-Kreislauferkrankungen, der Ausbreitung von Tumoren und Retinopathien. Die genaue Funktion von Flt1 in Gefäßen und ihrer Enstehung ist jedoch weitgehend unbekannt. Zur Charakterisierung der Rolle von Flt1 während der Angiogenese *in vivo*, wählten wir transgene Zebrafischembryos als Modellsystem. In dieser Arbeit wurde Flt1 als negativer Regulator bei der Bildung von „tip cells“ identifiziert.

Erste Untersuchungen im Zebrafischembryo ergaben die Expression einer membrangebundenen Flt1 Isoform (mFlt1) und einer bisher nicht annotierten löslichen Isoform von Flt1 (sFlt1). Die Depletion von Flt1 im Zebrafischembryo zeigte eine vermehrte Bildung von „tip cells“ im angiogenen Gefäßsproß. Dies führte während der Entwicklung zu einem verstärkten Verzweigungsmuster der intersomitischen Gefäße. Konsistent zu diesem Phänotyp wurde in diesen Zebrafischembryos eine reduzierte Expression des Notch-Signalweges beobachtet, eine Signalkaskade, die die „tip cell“ Differenzierung steuert. Die konditionelle Überexpression von Notch in Flt1-defizienten Zebrafischembryos verringerte signifikant die aberranten Gefäßverzweigungen und deutet auf eine Beteiligung von Notch im vaskulären Phänotyp von Flt1 an. Zusätzlich zu der vaskulären Expression von Flt1, wurde eine Expression in Neuronen detektiert. Neben aberranten Gefäßen resultierte die Depletion von Flt1 in einer reduzierten Anzahl an Neuronen. Interessanterweise führte eine gefäßspezifische Überexpression der löslichen

Isoform sFlt1 zu einer Distribution im Neuralrohr. Eine Beteiligung des Nervensystems bei der Etablierung des VEGF Gradienten, welcher für das Wachstum der intersomitischen Gefäße essentiell ist, wäre daher möglich.

Die Ergebnisse der vorliegenden Untersuchungen zeigen, dass Flt1 in Abhängigkeit von Notch die Bildung von „tip cells“ und die arterielle Gefäßmorphologie negativ reguliert. Darüber hinaus verringert Flt1 die Anzahl der Neuronen und agiert wahrscheinlich an der Schnittstelle der Gefäß- und Nervenentwicklung.

3 Introduction

A functional blood vessel network nurtures all tissues in the higher vertebrate body and is essential for its survival. An abnormal growth of blood vessels is associated with the pathophysiology of cancer, hypertension, ischemic heart diseases and stroke, which subsume the most common causes of death in the civilized western society (Carmeliet, 2003; Carmeliet, 2000; Folkman, 1995). So far, more than 70 disorders have been implicated as angiogenesis-dependent diseases. Therapeutic approaches that target angiogenesis have thus far not led to desired results, showing drug resistance, limited efficiency and angiogenic escape mechanisms. Meeting that challenge, recent studies gained insights into the formation of vascular networks with focus on interactions of endothelial cells (ECs) with each other and their environment. Understanding the vascular outgrowth at the cellular and molecular levels enables the generation of new principles that provide perspectives for therapeutic applications.

3.1 Blood vessel development

The cardiovascular system is the first functional organ system to develop in the vertebrate embryo (Carmeliet, 2003; Flamme et al., 1997; Palis et al., 1995; Risau et al., 1995). In the earliest stages of embryonic development the nutrition and oxygen supply is provided by diffusion, but as the embryo grows, diffusion distances for a sufficient nutrient distribution become too long. Evolution met these requirements through the formation of the cardiovascular system. The highly branched vessel network of the cardiovascular system serves mainly to nurture the demanding tissues, to transport hormones and to provide gateways for immune surveillance of the vertebrate body (Adams and Eichmann, 2010).

The development of the vascular system is classically subdivided into three temporally distinguishable processes. Vasculogenesis characterizes the *de novo* formation of a primitive vascular labyrinth, whereas angiogenesis describes the remodelling of the primitive vascular plexus into a functional network of arteries and veins. The process by which the vessel identity is determined is called arterial-venous differentiation.

In the adult, the vascular system is arranged in a hierarchical order of tube-like structures (Figure 1). Arteries, smaller arterioles and capillaries carry oxygenized blood from the heart to the tissue. The latter form a highly branched capillary network that optimizes the release of nutrients and oxygen to the surrounding tissue. Small venules and veins return the blood back to the heart (Herbert and Stainier, 2011; Adams and Eichmann, 2010). Due to the essential role of blood vessels for the vertebrate survival, a dysfunction can cause several diseases.

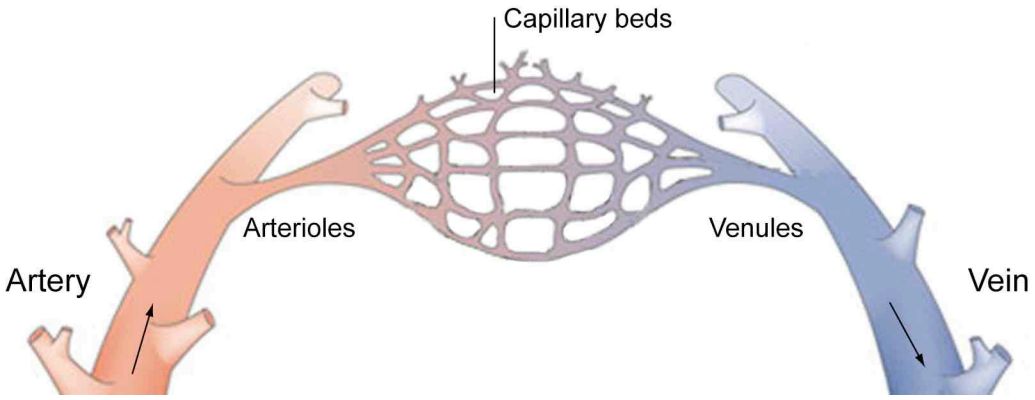

Figure 1. Schematic organization of the blood vessel network. Blood vessels are arranged in a hierarchical network. Oxygenated blood flows through arteries and arterioles into the capillary beds. Small venules and veins return the blood back to the heart (modified from Herbert and Stainier, 2011).

3.1.1 Vasculogenesis

Vasculogenesis describes the *de novo* formation of a primitive vascular network in early embryonic development (Figure 2; Adams and Alitalo, 2007; Risau, 1997). The highly regulated process characterizes the initial step of the formation of the cardiovascular system. During vasculogenesis, mesoderm-derived precursors of endothelial and hematopoietic cells (hemangioblasts) assemble to aggregates in the extra embryonic tissue, known as blood islands. Within the blood island, the outer hemangioblasts differentiate into angioblasts, while the inner hemangioblasts are committed to become hematopoietic progenitors. From early developmental stage onward the angioblasts are specified as either arterial or venous. Subsequent fusion of angioblasts results in the formation of a honeycomb-shaped primary vascular plexus (Figure 2; Flamme et al., 1997). This event goes along with the differentiation of angioblasts into arterial or venous-fated ECs (Rocha and Adams, 2009).

Within the embryo itself angioblasts assemble along the body axis, coalesce into a cord with lumen and form the dorsal aorta and cardinal vein (Coultas et al., 2005; Zhong et a., 2001). Thus, angioblasts aggregate into vascular structures, with no need of pre-existing ones. The remodelling and growth of the primitive vascular plexus is continued by angiogenesis.

3.1.2 Angiogenesis

After the primary vascular plexus has been established in the embryo, blood vessels expand and remodel into a highly orchestrated network. This mechanism by which new vessels are formed from pre-existing ones is termed angiogenesis (Figure 2; Coultas et al., 2005; Folkman and Shing, 1992). The vessel network enables blood circulation into previously avascular regions, consequently, angiogenesis is a crucial process to prevent or reverse tissue hypoxia (Patan et al., 2001). Angiogenesis is not temporally restricted to embryonic development, but can also occur in response to several physiological and pathological conditions like female reproduction cycle, tissue repair and tumour growth in the adult (Wang and Olson, 2009; Carmeliet, 2003; Meduri et al., 2000; Folkman, 1995).

Angiogenesis can be subdivided into two different mechanisms, namely sprouting angiogenesis and splitting angiogenesis, also known as intussusception (Figure 2). The well-studied sprouting angiogenesis is induced by hypoxia, which leads to an upregulation of several angiogenic genes, such as VEGF. Induced by VEGF, the endothelium becomes permeable as ECs loose their cell-cell junctional contacts and acquire a motile behaviour to initiate vessel sprouting (Mehta and Malik, 2006; Moses, 1997). The so-called tip cell spearheads the developing sprout and guides its outgrowth direction, while the following stalk cell proliferates and forms the lumen (Gerhardt et al., 2003). When tip cells of newly formed sprouts reach their target, they fuse and anastomose to functional vessel circuits. In mammals, macrophages may contribute to this anastomosis process by acting as `bridge cells´ that facilitate the contact between neighbouring tip cells (Rymo et al., 2011; Fantin et al., 2010).

While sprouting angiogenesis characterizes the outgrowth of ECs from pre-existing vessels, intussusceptive angiogenesis describes the insertion of translumen pillars in already existing vessels (Figure 2). The formation of these interstitial tissue columns

promotes the splitting of one blood vessel into two (Burri et al., 2004; Djonov et al., 2003). This process can be found, for instance, in lungs and the developing yolk sac of chicken embryos (Patan et al., 1993; Zeltner and Burri, 1987). The underlying molecular mechanism is still poorly understood.

Both forms of angiogenesis stabilize the nascent vessels by recruitment of mural cells, allowing blood circulation within the vessel.

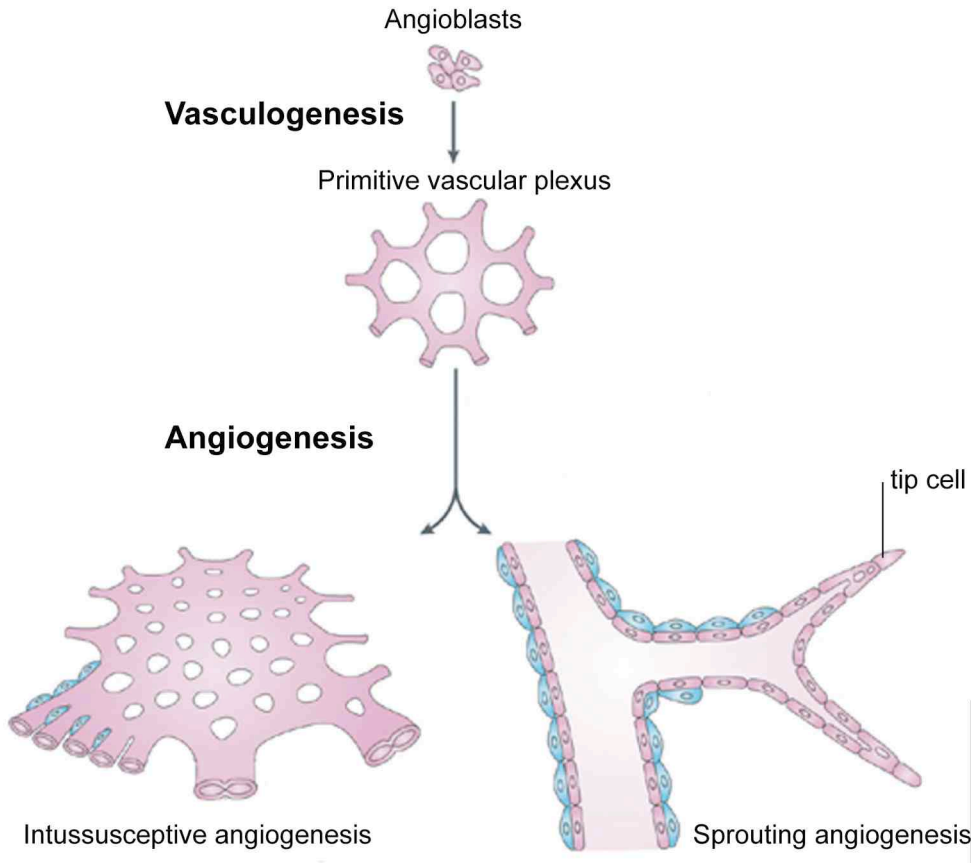

Figure 2. Development of a functional vasculature. During vasculogenesis angioblasts differentiate to ECs and form a primitive vascular plexus, which remodels and expands by angiogenesis. Angiogenesis can be subdivided into intussusceptive and sprouting angiogenesis. Intussusceptive angiogenesis involves the splitting of already existing vessels. In sprouting angiogenesis the leading EC, termed tip cell, explores the environment for vascular guidance cues and navigates the outgrowth of the sprout (modified from Dijke and Arthur, 2007).

3.1.3 Arterial-venous differentiation

The arterial-venous differentiation describes the process by which the vessel identity as either arterial or venous is determined. Two distinct mechanisms regulate the vessel identity: genetic hardwiring and hemodynamics (Jones et al., 2006; le Noble et al., 2005).

The genetic basis of the arterial-venous differentiation has been investigated in chick, mouse and zebrafish. Both specifications for arterial and venous identity require selective signalling pathways. For venous differentiation the orphan nuclear receptor COUP transcription factor-2 represses the Notch signalling pathway and stimulates the ephrinB-4 expression. By contrast, for arterial specification VEGF activates the Notch signalling pathway in arterial-fated angioblasts, thereby leading to ephrinB-2 expression and hence, to arterial differentiation. Thus, the growth factor VEGF and the signalling receptor Notch have been well characterized during the establishment of the vessel identity (Swift and Weinstein, 2009). Overexpression of VEGF in mice leads to an increase, while reduction of VEGF in zebrafish causes a decrease of arteries (Lawson et al., 2002; Visconti et al., 2002). The Notch signalling pathway appears to specify the arterial fate too, since inhibition of Notch in zebrafish results in ectopic expression of the venous marker VEGFR-3 (Lawson et al., 2001).

Besides the genetic programming of the arterial-venous differentiation, increasing evidence pointed out that hemodynamic factors like blood flow play a critical role in regulating vessel identity involving the expression of ephrinB-2 and neuropilin-1 (le Noble et al., 2005; le Noble et al., 2004).

3.2 Cellular and molecular regulation of sprouting angiogenesis

Sprouting angiogenesis is the most studied mechanism of blood vessel formation. It is not only important under normal conditions, but is also involved under pathologic conditions, for instance during primary tumour growth and metastasis formation (Hanahan and Weinberg, 2000). The expansion and remodelling of the vascular network require a tightly controlled and coordinated EC behaviour (Carmeliet, 2003; Folkman and D`Amore, 1996). Induced by VEGF, the developing vessel can be subdivided into the leading tip cell and the adjacent stalk cell. When a tip cell has

contact with another tip cell of a neighbouring vessel, these cells undergo anastomosis and form a functional vessel loop that allows blood circulation.
Numerous factors can influence the highly balanced formation of tip and stalk cells and therefore the developing vascular network. For instance, changes of the VEGF gradient in the microenvironment or altered Dll4-Notch signalling in ECs results in a modified outgrowth of the developing sprout. Consequently, only a well-coordinated combination of extrinsic and intrinsic cues leads to a functional vascular network.

3.2.1 The key cell types: tip and stalk cells

The formation of a functional vascular network is based on the tight coordination of specialized ECs within the developing sprout. The behavioural heterogeneity of those ECs allows a directional outgrowth and lumen formation of nascent sprouts.
The leading cell of an angiogenic sprout, named tip cell, is highly motile and polarized (Figure 3). Tip cells extend long filopodia to sense the microenvironment for attractive and repulsive guidance cues and hence serve to guide the sprout in a certain direction (De Smet et al., 2009; Lu et al., 2004; Gerhardt et al., 2003; Ruhrberg et al., 2002). The following cell is called stalk cell (Figure 3). Stalk cells proliferate and form the nascent vascular lumen, essential for blood flow delivery (Gerhardt et al., 2003). Although the tip cell migration can take place without proliferation of stalk cells and *vice versa*, only a tight balance of both cell phenotypes leads to an adequate functional vessel network (Gerhardt et al., 2003; Ruhrberg et al., 2003; Ruhrberg et al., 2002). Once a vessel loop is established and carries blood flow, the migratory and proliferative ECs become quiescent and are termed phalanx cells (Mazzone et al., 2009). While tip cells are adjacent to stalk cells, no clear positional relationship between stalk cells and phalanx cells has been defined yet.
The specification of tip and stalk cells is genetically determined. Analysis of the gene expression profile of tip cells shows an enrichment of VEGFR-2, VEGFR-3 and the Notch ligand Delta-like 4 (Dll4). In contrast, stalk cells display a higher expression of VEGFR-1, the receptor Notch1, and Notch-regulated ankyrin repeat protein a/b (Nrarpa/b) (Figure 3; Strasser et al., 2010; Phng et al., 2009). However, until present no single gene that can be utilized as an unambiguous molecular marker for tip or stalk cells has been identified.

Tip and stalk cells acquire transient phenotypes and are under constant challenge to maintain their position within the sprout. Over the last years it has been suggested that the dynamic competition is dependent on the relative levels of VEGFR-1 and VEGFR-2, which alter the expression of Dll4 and hence, the ability of the EC to become a tip or a stalk cell (Jakobsson et al., 2010). A recent study from Benedito and co-workers revised the simplistic model. In contrast to the previous model, they showed that Dll4 expression is only weakly modulated by VEGFR-2 and that angiogenesis can occur without VEGF-VEGFR-2 signalling in mice (Benedito et al., 2012). Additionally, a tight link between the Notch signalling pathway and VEGFR-3 has been demonstrated, making the molecular crosstalk between tip and stalk cells more complicated (Benedito et al., 2012).

Thus, guidance of the angiogenic sprout is a result of dynamic shuffling between the tip and stalk cell position, but the molecular explanation is still under investigation. Due to the differential binding affinities of the VEGFRs to VEGF, the dynamic behaviour of ECs within the sprout enhance their ability to determine the direction of the VEGF gradient, thus increasing the robustness of the vessel patterning.

3.2.2 The key pathway: Dll4-Notch signalling

The tip and stalk cell specification is tightly regulated by the Dll4-Notch signalling pathway (Bentley et al., 2008; Hellstrom et al., 2007; Leslie et al., 2007; Siekmann and Lawson, 2007; Suchting et al., 2007). Notch signalling is an evolutionary conserved pathway that determines fundamental cell fate decisions in all metazoas (Gazave et al., 2009). Moreover, it controls essential processes in almost all vertebrate tissues. Beside its relevance in vessels as for instance during tip cell/stalk cell differentiation and arterial-venous specification, Notch signalling is a critical mechanism in neuronal tissue (Kim et al., 2008; Louvi and Artavanis-Tsakonas, 2006; Yoon and Gaiano, 2005; Duarte et al., 2004; Lawson et al., 2001). In general, Notch mediates its function through lateral inhibition, a process that depends on the cell-cell contact, by which one cell with a certain phenotype inhibits the neighbouring cell from acquiring the same fate (Lewis, 1998; Chitnis, 1995). Lateral inhibition leads therefore to two cell phenotypes, while all cells initially shared the same developmental potential.

In vertebrates, four known Notch receptors (Notch1 to 4) and five Notch ligands (Dll1, Dll3 to 4, Jagged1 to 2) exist. Several studies in mouse and zebrafish revealed prominent Notch1 expression in stalk cells and lower expression in tip cells. Conversely, Dll4 is highly abundant on tip cells and hardly detectable on stalk cells (Hellstrom et al., 2007). Over the last years, evidence is accumulating showing the requirement of the Dll4-Notch signalling pathway for tip cell/stalk cell differentiation. Normally, all ECs of the endothelium are exposed to VEGF, but only some ECs respond with directional migration. Due to stochastically differences in the local VEGF concentration, only the ECs that are exposed to the highest VEGF levels will promote Dll4 expression and therefore be selected as tip cells. Dll4 expression is stimulated by VEGF binding to its cognate receptors (Hellstrom et al., 2007; Liu et al., 2003). Subsequently, Dll4 activates Notch at the adjacent stalk cell that consequently represses the tip cell fate by regulating the VEGFR level (Figure 3; Phng and Gerhardt, 2009). Thus, tip cells reinforce their own leading position by activating a feedback loop, which permits the leading cell to maintain its position, while avoiding adjacent cells from leaving their position as stalk cells. The feedback loop between VEGF and the Dll4-Notch-signalling pathway establishes therefore a “salt and pepper” distribution of tip and stalk cells within the angiogenic sprout (Bentley et al., 2008; Hellstrom et al., 2007; Leslie et al., 2007; Siekmann and Lawson, 2007; Suchting et al., 2007).

While the Notch-Dll4 signalling pathway functions as negative regulator for tip cell formation, another Notch ligand, Jagged1, has been identified to stimulate tip cell formation and angiogenesis. Expressed in stalk cells, Jagged1 antagonises Notch activation by competing with Dll4 for Notch binding in tip cells (Benedito et al., 2009). The coordinated control of Dll4 and Jagged1 strengthens the tip cell/stalk cell differentiation and hence, the crucial process of angiogenic sprouting.

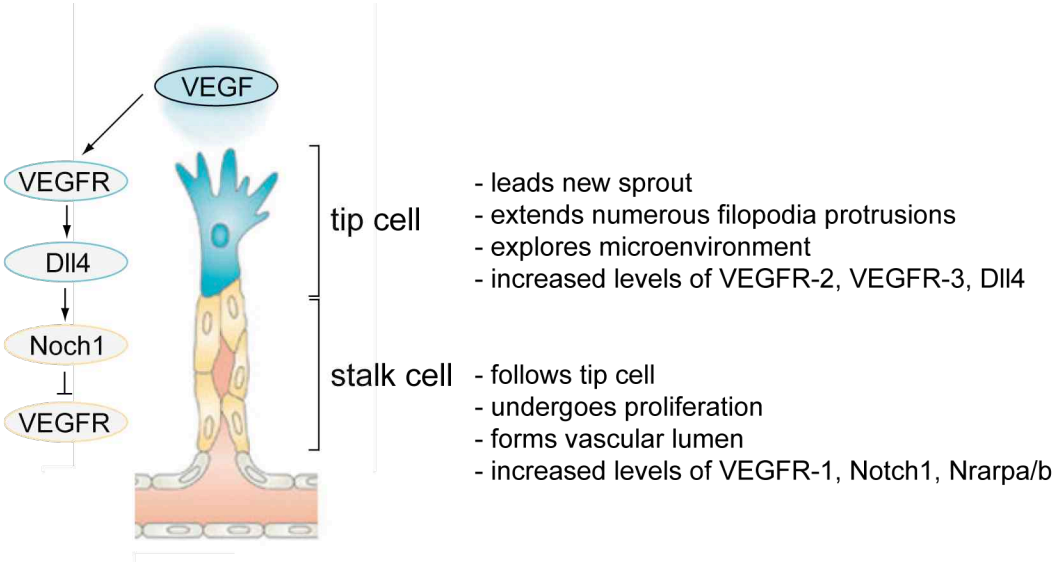

Figure 3. Cellular and molecular regulation of new sprouts. ECs of new sprouts are organized into the leading tip cell and the adjacent stalk cell. The tip cell formation is induced by VEGF. Subsequent activation of the Dll4-Notch signalling pathway represses VEGFR signalling in the stalk cell. The tip cell extends filopodia protrusions to explore the microenvironment for guidance cues and expresses high levels of VEGFR-2, VEGFR-3 and Dll4. The stalk cell undergoes proliferation, forms the vascular lumen and expresses high levels of VEGFR-1, Notch1 and Nrarpa/b (modified from Herbert and Stainier, 2011).

The significance of the Dll4-Notch signalling pathway during tip cell/stalk cell differentiation has been confirmed in several independent mouse and zebrafish studies. Activation of Notch signalling promotes the stalk cell phenotype and inhibits the tip cell formation. In contrast, genetic or pharmacological inactivation of Notch or Dll4 resulted in excessive sprouting. The increased tip cell formation indicates the default response of the activated endothelium after inhibition of Notch signalling, while Notch activation is required for the stalk cell formation (Hellstrom et al., 2007; Leslie et al., 2007; Lobov et al., 2007; Siekmann and Lawson, 2007; Suchting et al., 2007).

3.2.3 Dynamic interaction between the key pathway Dll4-Notch and VEGF

During sprouting angiogenesis, the key pathways Dll4-Notch and VEGF-VEGFR signalling co-operate in an intercellular feedback loop, thereby regulating tip cell/stalk cell differentiation. This process includes the regulation of all VEGFRs by Notch signalling (Figure 4).

In the past it has been believed that binding of VEGF to VEGFR-2 in tip cells promotes Dll4 expression that subsequently activates Notch1 in the adjacent stalk cell. Recently, Benedito and co-workers showed that VEGFR-2 expression is not essential for Dll4 activation in tip cells, pointing towards other upstream regulators such as cell matrix signalling factors (Benedito et al., 2012). In response to ligand binding, Notch1 undergoes a series of proteolytic cleavages. The final cleavage of Notch1 through γ-secretase releases the Notch intracellular domain (NICD), which then translocates to the nucleus. NICD functions as a key transcriptional regulator during cell fate specification by, for instance, downregulating the transcription of EphrinB2a and VEGFR-2 in stalk cells (Jakobsson et al., 2010; Sawamiphak et al., 2010; Wang et al., 2010; Hellstrom et al., 2007). The NICD mediated downregulation of VEGFR-2 has been revised in a current study, in which only a weak modulation of VEGFR-2 expression by Notch was measured (Benedito et al., 2012). Instead, VEGFR-3 expression was strongly affected by Notch, suggesting that VEGFR-2 and VEGFR-3 are regulated in a differential manner by Notch (Figure 4; Benedito et al., 2012). Over the last years scientists had assumed that the downregulation of VEGFR-2 by NICD in stalk cells reduces the VEGF-induced expression of Dll4 in these cells and consequently suppresses the tip cell phenotype in stalk cells (Hellstrom et al., 2007). Due to new findings, the previous concept of the crosstalk between VEGF and Notch has been fundamentally changed. In disagreement with the previous model, VEGFR-2 is not essential for Dll4 activation and is only weakly modulated by Notch. Surprisingly, Notch strongly regulates VEGFR-3 expression. The Notch dependent VEGFR-3 upregulation allows angiogenesis without ligand binding and without VEGF-VEGFR-2 signalling, pointing towards a potential growth factor independent vessel growth (Benedito et al., 2012). The new insights concerning the regulation of VEGFR-2 and VEGFR-3 during tip cell/stalk differentiation revises the previous simplistic model and opens new perspectives for future studies.

In contrast to the Notch mediated downregulation of VEGFR-2 and VEGFR-3 in stalk cells, VEGFR-1 is upregulated by Notch leading to increased levels of VEGFR-1 and its soluble isoform sVEGFR-1 in stalk cells (Figure 4; Funahashi et al., 2010). sVEGFR-1 can form inactive heterodimers with VEGFR-2, thereby limiting its downstream signalling cascade and hence, reducing the angiogenic response to VEGF. Additionally VEGFR-1 functions as decoy receptor of VEGF. One study suggested that sVEGFR-1 is distributed adjacent to the developing sprout and influences the sprout guidance by acting as spatial cue (Chappell et al., 2009). Hence, the Dll4-Notch signalling pathway would therefore indirectly modulate local guidance cues by increasing sVEGFR-1 levels.

Collectively, molecular regulation of VEGFRs by Notch activation decreases the sensitivity of stalk cells to VEGF and enhances therefore the robustness of tip cell/stalk cell differentiation.

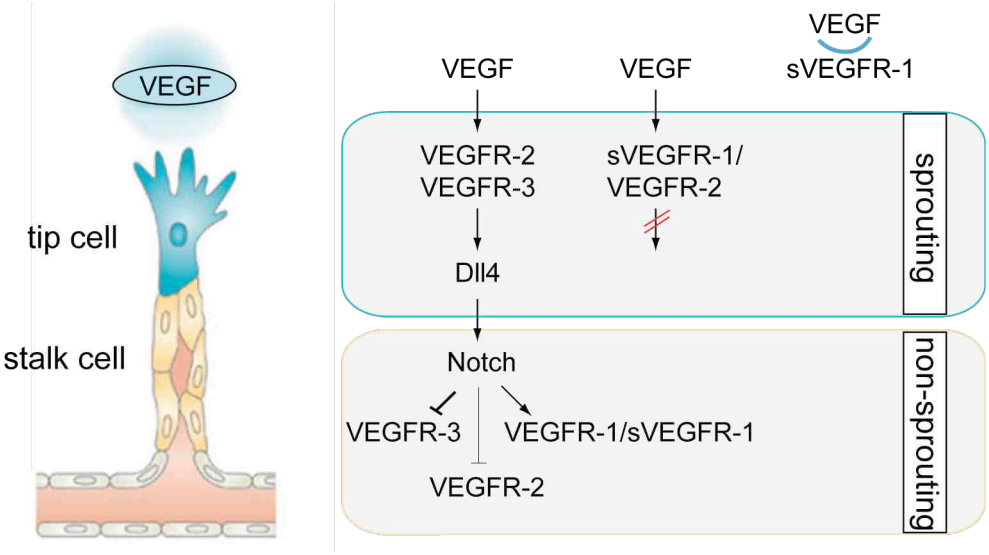

Figure 4. Interaction of Dll4-Notch signalling pathway and VEGFRs during tip cell/stalk cell differentiation. VEGF binds to VEGFR-2 and VEGFR-3, which induces Dll4 expression in the tip cell. Dll4 activates Notch on the adjacent stalk cell that in turn leads to a weak modulation of VEGFR-2 and strong downregulation of VEGFR-3, while VEGFR-1 expression is stimulated. sVEGFR-1 can form inactive heterodimers with VEGFR-2. Additionally, sVEGFR-1 can scavenge VEGF in the microenvironment (modified from Herbert and Stainier, 2011).

3.3 Vascular guidance signals: the VEGF family

Extrinsic guidance cues are required for initial sprouting from the parental vessel. Furthermore, they attract or repel the developing sprout (le Noble et al., 2008; Eichmann et al., 2005). The balance between attractant and repulsive cues determines the direction in which the sprout will expand. One of the best described attractive guidance cues and inductor of angiogenic sprouting is VEGF.

3.3.1 The VEGF ligands

The VEGF family and its cognate receptors are one of the most important and intensively studied pathways in promoting angiogenesis and tumour angiogenesis. In mammals, the VEGF family includes five members, VEGF-A, VEGF-B, VEGF-C, VEGF-D, and placental growth factor (PLGF). Additionally, two other structurally related proteins, which are termed VEGF-E and VEGF-F, have been identified in parapoxviruses and snake venoms (Suto et al., 2005; Takahashi and Shibuya, 2005). VEGF-A, commonly called VEGF, encodes several splicing isoforms that are freely diffusible or sequestered in the extracellular matrix (Houck et al., 1991). Its expression is stimulated by hypoxia, thus as response to low oxygen levels in tissues. Besides acting as a prominent attractor for developing vessels, VEGF-A induces EC proliferation and tube formation during blood vessel formation (Olsson et al., 2006; Gerhardt et al., 2003; Ruhrberg et al., 2002; Conway et al., 2001; Carmeliet et al., 1996; Flamme et al., 1995). VEGF dosage is highly critical as mice with homozygous as well as heterozygous deletion of *Vegf-a* (*Vegf-a*$^{-/-}$, *Vegf-a*$^{+/-}$) result in embryonic lethality due to severe vascular defects (Carmeliet et al., 1996; Ferrara et al., 1996). The tight spatial regulation of VEGF-A and therefore its bioavailability is a key control point for vascular development. Deficiency of other VEGF family members in mice displayed milder defects in the vasculature compared to *Vegf-a*$^{-/-}$ and *Vegf-a*$^{+/-}$ mice. Homozygous deletion of *Vegf-b* showed no defects during embryogenesis, while adult mice exhibited dysfunctional coronary vasculature (Aase et al., 2001). VEGF-C and VEGF-D are more relevant for lymphangiogenesis, since homozygous deletion of *Vegf-c* cause embryonic lethality due to absence of lymphatic vessels and *Vegf-d* deficient mice display a reduced number of lymphatic vessels (Baldwin et al., 2005; Karkkainen et al., 2004; Jeltsch et al., 1997).

The VEGF family exerts distinct functions during vascular development. As VEGF-A is the best-known pro-angiogenic signal during blood vessel formation, its production and bioavailability require a strongly controlled regulation.

3.3.2 The VEGF receptors

VEGF ligands mediate their effect through binding to their cognate receptors, namely VEGFR-1 (encoded by Flt1), VEGFR-2 (encoded by Kdr) and VEGFR-3 (encoded by Flt4). In addition to the soluble isoforms, longer isoforms of these receptors are structured in an extracellular, transmembrane-spanning and an intracellular domain. While the extracellular domain is composed of immunoglobulin (Ig)-like domains essential for VEGF binding, it is the tyrosine kinase intracellular domain that is important for downstream signalling. Upon binding of VEGF, the VEGFRs form homo- or heterodimers that subsequently activate their downstream signalling pathways. Co-receptors, like heparan sulphate proteoglycan and neuropilin, can act in conjunction with VEGFRs to support the receptor activation (Olsson et al., 2006).
Not all VEGF ligands can bind to all VEGFRs. VEGF-A binds to VEGFR-1 and VEGFR-2, while VEGF-B and VEGF-F binding is restricted to VEGFR-1. VEGF-E can selectively activate VEGFR-2, whereas VEGF-C and VEGF-D interact with VEGFR-2 and VEGFR-3 (Figure 5).

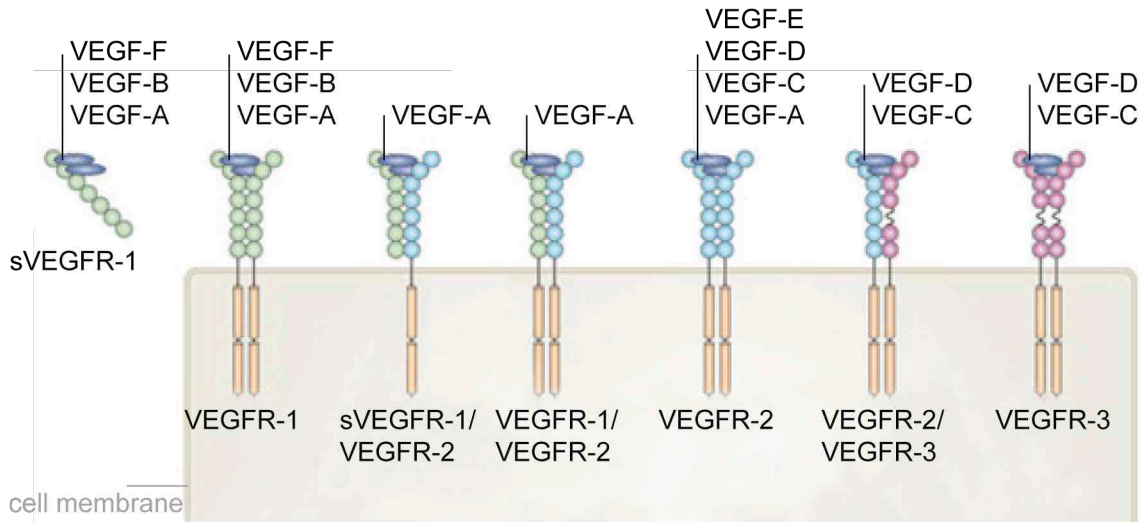

Figure 5. Schematic overview of VEGF ligands and receptors. VEGF ligands bind specifically homo- and heterodimers of VEGF receptors (modified from Herbert and Stainier, 2011).

VEGFR-1 and VEGFR-2 were originally found to be expressed on ECs, while recent studies demonstrated additional expression on hematopoietic cells and on neurons (Poeson et al., 2008; Shibuya et al., 1999; Terman et al., 1992). VEGFR-3 is expressed by embryonic ECs and in the adult it becomes restricted to the lymphatic endothelium (Kaipainen et al., 1995).

VEGFR-1 is required for vascular development since homozygous *Vegfr-1* deficient mice (*Vegfr-1*$^{-/-}$) display a disorganized vasculature resulting in embryonic lethality (Fong et al., 1995). Mice lacking the tyrosine kinase domain of *Vegfr-1* (*Vegfr-1*$^{TK-/-}$) display normal vessels, indicating that the extracellular and the transmembrane-spanning domains are sufficient for vascular development (Hiratsuka et al, 1998). Because the extracellular domain of VEGFR-1 binds VEGF-A with high affinity, and the intracellular domain possesses a weak tyrosine kinase activity, VEGFR-1 has been described to function as decoy receptor for VEGF-A. Moreover, alternative splicing generates a truncated form of VEGFR-1, sVEGFR-1, that is considered to act as sink for free VEGF-A, thereby regulating the amount of VEGF-A that binds to VEGFR-2 (Hiratsuka et al., 2005). However, VEGFR-1 and VEGFR-2 can form heterodimers that mediate angiogenic signals upon binding of VEGF-A/PLGF (Autiero et al., 2003).

VEGFR-2 is the principal regulator for VEGF-A signalling. Binding of VEGF-A to VEGFR-2 leads to activation of downstream signals, such as mitogen-activated protein kinases (MAPKs), phosphoinositide 3-kinases (PI3Ks), and AKT. As a result, VEGFR-2 induces EC proliferation, migration and survival (Ferrara et al., 2003). Accordingly, homo- and heterozygous deletion of *Vegfr-2* (*Vegfr-2*$^{-/-}$; *Vegfr-2*$^{+/-}$) display defects in blood island formation that causes embryonic lethality, reminiscent to *Vegf-a*$^{-/-}$ mice (Shalaby et al., 1997; Shalaby et al., 1995).

VEGFR-3 plays important roles during angiogenesis and lymphangiogenesis since homozygous deletion of *Vegfr-3* exhibits a defective assembly of blood islands, which leads to embryonic lethality (Tammela et al., 2010; Tammela et al., 2008; Dumont et al., 1998). During sprouting angiogenesis, VEGFR-3 can form heterodimers with VEGFR-2 on tip cells, positively influencing angiogenic sprouting (Nilsson et al., 2010).

The complex interplay of VEGF ligands and their distribution as well as the VEGF receptors and their dimerization are essential for vascular development.

Homozygous deletion of each VEGF ligand or receptor leads in most cases to embryonic lethality, emphasising its significance.

3.3.3 The vascular guidance cue VEGF acts on the nervous system

VEGF has originally been characterized as an endothelial specific guidance cue that provides a template for tip cell attraction. Interestingly, recent studies suggest that VEGF may actually act as a neurotrophic factor as well. The notation that such well-known vascular growth factors like VEGF have a role in neurogenesis and that well-known neural genes like plexin exert proangiogenic effects, has led to the suggestion that neurogenesis and angiogenesis are governed by common cues and mechanisms. VEGF, known as key control point during angiogenesis, developed early during the evolution of the nervous system of invertebrates. Invertebrates, such as the nematode worm *Caenorhabditis elegans*, lack a vascular system and VEGF acts herein not as angiogenic but rather as neuronal signal in worms (Tarsitano et al., 2006). Recently in evolution, vertebrates developed a vascular system for oxygen and nutrient transport. There are striking similarities between the nervous and the vascular system. Major blood vessels and nerve fibres within the body grow in close proximity to each other, indicating that common pathways regulate the co-patterning (Figure 6). Moreover, axonal growth cones, which guide axons, share many morphological and functional similarities with the tip cell that leads the angiogenic sprout (Figure 6; Gerhardt et al., 2003; Dickson, 2002; Tessier-Lavigne and Goodman, 1996). Both explore their surroundings for guidance cues. VEGF acts as common guidance cue for axonal as well as for EC outgrowth and is therefore also described as angioneurin (Zacchigna et al., 2008). However, the functions of VEGF ligands and receptors in neurogenesis are far from clear. The work by the group of Carmeliet has shown that VEGF plays a central role in neurodegenerative diseases (Ruiz de Almodovar et al., 2009; Poesen et al., 2008; Storkebaum et al., 2005; Azzouz et al., 2004). More recent work showed that VEGF-B exerts neuroprotective effects through VEGFR-1 in primary motor neurons (Poesen et al., 2008). Another study showed that VEGF and VEGFR-2 can travel retrogradely and antegradely along peripheral axons (Storkebaum et al., 2005). Neither the functional relevance of this axonal transport nor the mechanism has been identified.

Collectively, VEGF exerts pleiotropic effects in the nervous and the vascular system. The precise role of VEGF ligands and receptors herein need to be examined in future studies.

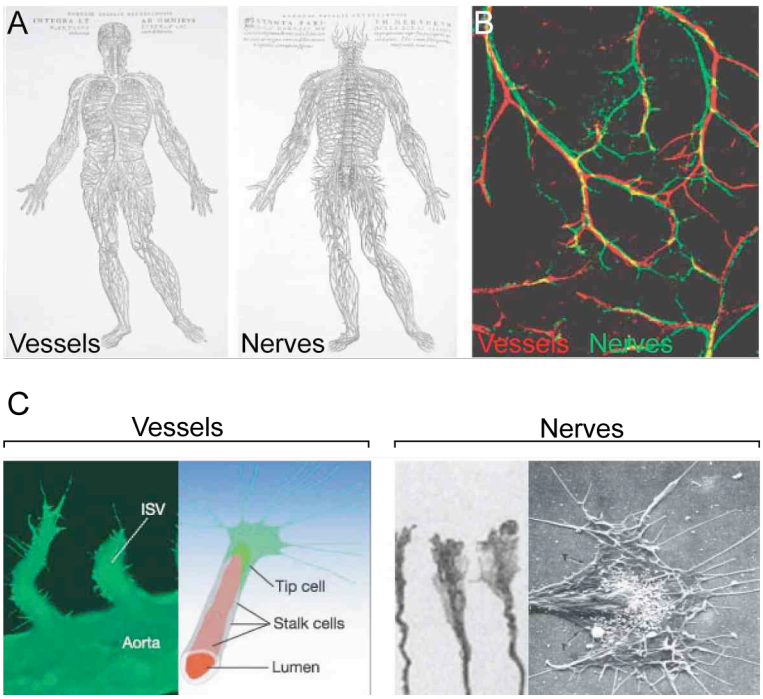

Figure 6. Parallels of vessels and nerves. (A) Drawings of the vascular and nervous network highlight their similar patterning. (B) Coalignement of vessels (red) and nerves (green). (C) Vessels and nerves share morphological similarities. Left side: Image of the intersomitic vessels of zebrafish shows numerous filopodia extensions, which are represented in the schematic overview of the tip cell and stalk cell. Right side: Photograpgh of axons terminating in a growth cone. The growth cone displays filopodia extensions as seen in the scanning electron micrograph. ISV, intersomitic vessel. (modified from Carmeliet and Tessier-Lavigne, 2005).

3.4 Flt1 and its role during vascular development

VEGF is a key regulator of physiological and pathological angiogenesis. The biological function of VEGF is mediated by its cognate receptors. Flt1, also commonly known as VEGFR-1, is one of the three VEGFRs, but its precise role during sprouting angiogenesis remains elusive.

In mammals, the gene *Flt1* encodes one membrane-bound protein (mFlt1) and several soluble isoforms (sFlt1). The distinct Flt1 isoforms are considered to be generated by alternative splicing. Flt1 shares structural similarities to the Fms family and was therefore originally designated as Fms-like tyrosine kinase-1 (Shibuya et al., 1990). The membrane-anchored Flt1 isoform is composed of seven extracellular Ig-like domains, a transmembrane-spanning and an intracellular tyrosine kinase domain (Shibuya et al., 1990; Matsushime et al., 1987). The extracellular Ig-like domains are necessary for high affinity ligand binding and receptor dimerization, while the tyrosine kinase is required for activation of downstream signalling pathways, such as MAPK and AKT (Piossek et al., 1999; Barleon et al., 1997; Davis-Smyth et al., 1996). In contrast to mFlt1, sFlt1 isoforms consist only of extracellular Ig-like domains and can be secreted to the environment.

Two decades ago, Flt1 expression has been found in vascular ECs (Shibuya et al., 1990). However, Flt1 is also abundant in trophoblast cells, monocytes and hematopoietic stem cells (Hirashima et al., 2003; Sawano et al., 2001). More recently, expression of Flt1 has been detected in motor neurons and dorsal root ganglia of mice (Poeson et al., 2008; Storkebaum et al., 2005).

Induced by hypoxia and Notch, Flt1 binds VEGF-A and selectively VEGF-B, VEGF-F and PLGF. Binding of a ligand leads to the formation of homo- or heterodimers. mFlt1 homodimers as well as mFlt1/VEGFR-2 heterodimers induce downstream signalling cascades, while sFlt1 homodimers and sFlt1/VEGFR-2 heterodimers bind the ligand without any further activation of signalling pathways. Due to these two opposing biological activities of Flt1, its role during angiogenesis has been controversial in the past. Whether Flt1 acts as transducer of VEGF signals or as decoy receptor, seems to depend on the developmental stage and cellular context.

Flt1 has the highest binding affinity for VEGF-A compared to other VEGFRs, although its tyrosine kinase activity is very weak (Sawano et al., 2001; Seetharam et al., 1995; Waltenberger et al., 1994). Thus, Flt1 is proposed to act as decoy receptor

for VEGF, thereby regulating the signalling capacities through VEGFR-2. By scavenging the ligand, sFlt1 modulates the bioavailability of VEGF and forms a corridor for further vessel outgrowth (Chappell et al., 2009). Consistent with this model, homozygous deletion of *Flt1* (*Flt1*$^{-/-}$) in mice causes a disorganized blood vessel network that results in embryonic lethality. In contrast, mice lacking the *Flt1* tyrosine kinase (*Flt1*$^{TK-/-}$) display normal blood vessels and are viable (Hiratsuka et al, 1998; Fong et al., 1995). These findings support the idea that VEGF sequestering through Flt1 is mainly essential during development. However, mice that lack the tyrosine kinase and transmembrane-spanning domain of *Flt1* (*Flt1*$^{TM-/-TK-/-}$) were in part viable or embryonic lethal, depending on the endogenous VEGFR-2 levels (Hiratsuka et al., 2005). In these mice, the recruitment of VEGF to VEGFR-2 was impaired, indicating that the membrane fixation of Flt1 is required for an efficient VEGFR-2 stimulation through VEGF. The mice with high VEGFR-2 levels were embryonic lethal, as VEGFR-2 activity is necessary for the formation of the cardiovasculature (Hiratsuka et al., 2005). Instead, mice with low VEGFR-2 levels survived, suggesting that sFlt1 can adopt some functions of mFlt1.

Besides the function as decoy receptor, some evidences indicate Flt1 as transducer of VEGF signals. In various disease models, Flt1 signalling is required, since *Flt1*$^{TK-/-}$ mice exhibit impaired inflammation and angiogenesis under pathological conditions. The ligand PLGF is generally upregulated in tumours. Upon binding to Flt1, PLGF activates the signalling cascade and induces EC migration.

VEGF-B is another ligand that binds selectively to Flt1, but the functional role during vascular development remains unclear. In motor neurons VEGF-B has been shown to exert neuroprotective effects that are dependent on the tyrosine kinase activity of Flt1 (Poesen et al., 2008). Furthermore, the signalling domain of Flt1 is also required for monocyte migration, which is impaired in *Flt1*$^{TK-/-}$ mice. Intriguingly, Flt1 expression in non-ECs can also affect angiogenesis. Expression of Flt1 in retinal myeloid cells has been demonstrated to suppress angiogenesis in the mouse retina (Stefater et al., 2011).

Flt1 has been identified two decades ago. Numerous studies gained insight into a function of Flt1 during vascular development, but the understanding how Flt1 regulates sprouting angiogenesis at cellular and molecular level is still missing.

3.5 Zebrafish as model system to study angiogenic sprouting

The vascular network develops in a conserved manner in all vertebrates. Nowadays, zebrafish embryos (*Danio rerio*) are used as relatively new model system to study vascular biology. Zebrafish are a powerful system that offers various advantages, as their embryos are readily accessible for genetic manipulations, have a rapid generation time and are so small that oxygen can passively diffuse through the tissues without the demand of a functional blood vessel network (Pelster and Burggren, 1996; Stainier et al., 1996). Very importantly, zebrafish embryos are optically clear, allowing to record individual cells and gene expression in transgenic lines *in vivo*.

The transgenic zebrafish line Tg(*fli1a:egfp*)^{y1} expresses the enhanced green fluorescent protein (eGFP) under the endothelial specific *fli1a* promoter (Figure 7; Lawson and Weinsten, 2002). Thus, Tg(*fli1a:egfp*)^{y1} embryos have been useful for a detailed analysis of blood vessel development. The spatiotemporally conserved pattern of intersomitic vessels (ISVs) as well as their sprouting from the dorsal aorta (DA) have been well characterised (Figure 7; Blum et al., 2008; Isogai et al., 2003; Childs et al., 2002).

As the signalling pathways during vascular development are conserved throughout vertebrates, insights about the function of specific genes will be applicable for future research in other vertebrates.

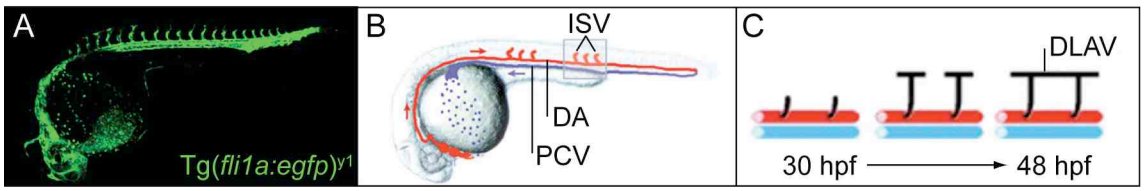

Figure 7. Zebrafish vasculature. (A) Transgenic zebrafish embryo Tg(*fli1a:egfp*)^{y1} at 30 hours post fertilization (hpf) showing endothelial specific eGFP expression. (B) Schematic representation of a zebrafish embryo at 30 hpf demonstrates the developed vasculature: the dorsal aorta (red), growing intersomitic vessels (red) and the posterior cardinal vein (purple). (C) Illustration of the intersomitic vessel formation. At 30 hpf, new sprouts (black) emerge from the dorsal aorta (red) and grow dorsally to form the dorsal longitudinal anastomotic vessel at 48 hpf. DA, dorsal aorta; ISV, intersomitic vessel; PCV, posterior cardinal vein; DLAV, dorsal longitudinal anastomotic vessel (modified from Lawson and Weinstein, 2002).

3.6 Clinical relevance of Flt1

A tightly balanced blood vessel formation is required for an adequate nutrient transport to all tissues of the vertebrate body. Accordingly, an insufficient or an increased blood vessel growth causes numerous diseases like myocardial infarction, stroke, neurodegeneration, tumourigenesis, and ocular disorders.

Flt1, the cognate receptor for the key pro-angiogenic factor VEGF, has been shown to be upregulated in ischemic and inflammatory diseases (Luttun et al., 2002). In addition, Flt1 is highly expressed in various tumours, such as lung cancer, breast, prostate and colon cancer, pulmonary adenocarcinoma, hepatocellular carcinoma, glio blastoma, multiple myeloma and nephroblastoma (Ghanem et al., 2003; André et al., 2000; Decausin et al., 1999; de Jong et al., 1998; Yoshiji et al., 1996; Plate et al., 1994). Another study highlighted Flt1 also in leukemia, since 76% of patients with leukemia exhibit Flt1 immunoreactivity (Bellamy et al., 2001; Fiedler et al., 1997). As prominent Flt1 expression is linked to cancers, Flt1 immunoreactivity in tumours is used as criteria regarding the prediction of the disease outcome (Pillozzi et al., 2007; Kaplan et al., 2005; Xiang et al., 2001). Flt1 has been investigated to function as anticancer drug target. Indeed, antibodies and inhibitors against Flt1 attenuate migration and invasion of malignant cells (Fan et al., 2005; Luttun et al., 2002). However, not all tumours respond equally well and require a combinational therapy including other anticancer drugs. Beside the function of Flt1 inhibitors and anti-Flt1 antibodies in tumorigenesis, its application also ameliorates inflammatory diseases such as atherosclerosis and arthritis (Luttun et al., 2002; Carmeliet and Jain, 2000). The anti-inflammatory effect of anti-Flt1 antibodies is mediated by affecting the mobilization of myeloid progenitors into the peripheral blood, the infiltration of Flt1-expressing leukocytes and the activation of myeloid cells (Luttun et al., 2002). Furthermore, ischemic diseases like choroidal neovascularisation in the eye are also treated with anti-Flt1 antibodies, as selective sFlt1 expression in the cornea is required for normal corneal avascularity allowing optical vision (Ambati et al., 2007; Ambati et al., 2006). Flt1, in particular sFlt1, has been associated with the pathogenesis of preeclampsia. Preeclampsia characterizes pregnancy-induced hypertension showing disturbed angiogenesis that is linked to an unbalanced ratio of sFlt1/PLGF expression (Verlohren et al., 2012; Jebbnik et al., 2011).

Taken together, a deregulated Flt1 expression can result in ischemic or inflammatory disorders. Flt1 plays a critical role in tumours; too, as its expression level is used for further prognosis of the disease outcome.

3.7 Aim of the study

The present study was aimed to determine the role of Flt1 in sprouting angiogenesis with focus on tip cell/stalk cell differentiation. To directly investigate the role of Flt1 during vascular development, loss- and gain-of-function as well as rescue experiments were performed in zebrafish embryos. Defects at the cellular level were observed by *in vivo* time-lapse imaging of vascular transgenic reporter lines, while molecular mechanisms were evaluated using in situ hybridization and real-time PCR. As recent studies emphasized an interdependence of vascular and neuronal development, we investigated the impact of Flt1 not only on vessels but also on neurons. Consequently, this study can help to elucidate the controversial function of Flt1 during blood vessel formation and has an implication for numerous diseases.

4 Material and methods

4.1 Material

4.1.1 Transgenic zebrafish lines

Transgenic zebrafish lines were used to visualize the development of the vascular and nervous system and the contribution of specific genes herein. The transgenic zebrafish lines are listed in Table 1. Tg indicates transgene, whereas the gene promoter is written in italic driving the expression of enhanced green fluorescent protein (eGFP), yellow fluorescent protein (YFP) or Cherry.

Table 1. **Transgenic zebrafish lines.**

Transgenic zebrafish line	Function
Tg(*fli1a:egfp*)^{y1}	EC marker
Tg(*kdrl:ras-cherry*)^{s916}	EC marker
Tg(*flt1^{BAC}:yfp*) x Tg(*kdrl:ras-cherry*)^{s916}	EC marker and expression of *flt1*
Tg(*uas:notch1a-ICD*) x Tg(*hsp70:gal4*)	Conditional overexpression of NICD
Tg(*huC:egfp*)	Neuronal marker
Tg(*huC:egfp*) x Tg(*kdrl:ras-cherry*)^{s916}	EC/ neuronal marker

EC: endothelial cell; NICD: notch1a intracellular domain

These transgenic lines were described in Hogan et al., 2009; Chi et al., 2008; Siekmann and Lawson, 2007; Isogai et al., 2003; Lawson and Weinstein, 2002 and Park et al., 2000.

4.1.2 Enzymes

Table 2. Enzymes.

Enzyme	Manufacturer	Restriction enzyme	Manufacturer
DNase	Promega	EcoRI	NEB
Proteinase K	Roche	EcoRV	NEB
Taq polymerase	Clontech	NotI	NEB
RNase	Roche	XhoI	NEB
Pronase	Roche		

4.1.3 Chemicals and kits

Chemicals were purchased from Invitrogen, Sigma-Aldrich and Roth if not stated otherwise.

Table 3. Kits.

Kit	Manufacturer
ThermoScript™ First-Strand System	Invitrogen
TaqMan® Gene Expression Assay	Applied Biosystems
Zyppy™ Plasmid Miniprep Kit	Zymo Research
mMESSAGE mMACHINE® Sp6 Kit	Ambion
Pierce®BCA Protein Assay Kit	Piercenet
Tyramide Signal Amplification™	PerkinElmer
SuperSignal West Femto Chemiluminescent Substrate	Piercenet
Zymoclean™ Gel DNA Recovery Kit	Zymo Research

4.1.4 Oligonucleotides

Table 4. Morpholino antisense oligonucleotides from GeneTools.

Morpholino	Used conc	Sequence 5´ - 3´	Target
Control	3.0 ng	CTCTTACCTCAGTTACAATTTATA	-
Flt1MO	3.0 ng	ATATCGAACATTCTCTTGGTCTTGC	ATG of *flt1*
3´ UTR-MO	1.5 ng	CTTGAGGGTGTTTGT TTGGAGATGA	3´ UTR of *flt1*
DLL4MO	6.0 ng	TAGGGTTTAGTCTTACCTTGGTCAC	splicing of *dll4*
Pu1MO	30.0 ng	GATATACTGATACTCCATTGGTGGT	splicing of *pu1*

conc: concentration

Table 5. Primer for 5´ and 3´ RACE.

RACE	Primer name	Sequence 5´ - 3´
5´ RACE	GSP1	CGTTTGGATGGACCACTGGTTACTTGAC
3´ RACE	GSP2	CTTACTGGGATCCAGCAGTACGGGCTTT

Table 6. Primer for generating expression constructs.

Final construct	Forward primer 5´ - 3´/ reverse primer 5´ - 3´
pTol*fliep:cherry-sflt1*	ACACCCTCAAGCAAGACCAA/ TGATTTTTCGCACAGG
pminiTol*kdrl:cherry-sflt1*	GCAGATATCACCATGGTGAGCAAGGGCGAGGAGGA/ CCCGATATCGCGCCGCGGCCGCGAATTAAAAAACC
pminiTol*kdrl:egfp-sflt1*	GCAGATATCACCATGGTGAGCAAGGGCGAGGAGCT/ CCGATATCGCGCCGCGGCCGCGAATTAAAAAACC
pCS2*mflt1*	CCGGAATTCTCCAAACAAACACCCTCAAGCAAGAC/ ACCGCTCGAGTAATGAGGAACCGAAAGCAGCAGCAG
pCS2*sflt1*	ATTCAATATGGCGTATATGGACTCATGC/ TATGATCACTTAGATTTCCAAGCAGCAAC

Table 7. Primer and probes for quantitative real-time PCR (qRT-PCR).

Gene	Forward primer 5` - 3`/reverse primer 5` - 3` Probe 5´ - 3´
mflt1	GTGAACACAAGGCTCTAATGACAGA/ TGCGCCGAGGAGATTGAC
	FAM- GAAGATTCTCAATCATATAGGTCACCACATCAATG -TAMRA
sflt1	CCCCGACGCGAGACA/ GACTGTGCCACGTTTGAAGAC
	FAM- CTTCCCAGCAGCGTGATTGTCCCT -TAMRA
dll4	GAATACTGCGAAGAACCGATCTG/ TACAGGCTGGATATGTTTTACA
	FAM- TGGAGGGATGCAGTGAGGCGAATG -TAMRA
ef1α	GTTGCCTTCGTCCCAATTTC/ CAATCTTCCATCCCTTGAACCA
	FAM- ATGTTTGAGCTGGCCTCCAGCATGTT -TAMRA
ephrinb2a	CCAGTGTCGGGAACAAGTGA/ GTACGGATGGTGTTCATGTTCTCA
	FAM- AGCAGTTGGGAAGAAGTAAGCGGCTACG -TAMRA
kdra	CAATGGCAGGATTCACTTTGAG/ GACCGGTGTGGTGCTAAAATG
	FAM- AGTTTCATAAGGAGCGGATCAATCG -TAMRA
kdrb	ACAGGTGCATCGCTACCAATAA/ GGACGCTTAGGTTGAGAAAACG
	FAM- GTTACTTGAAACACAATGACTCGCTG -TAMRA
notch1a	ATCTACTGCGACGTGCCTAGTG/ CCGCATGACGACACAAAACT
	FAM- AGGTCGCTGCCAGACAGCAAGGTG -TAMRA
notch1b	AGGCGTCTTCCAGATTTTGA/ CCTCGACCGCCAGTCTT
	FAM- ACGGAACCGCGCCACAGATCTA -TAMRA
notch3	GGTGGCTGGTCAGGTCGTTA/ TCTGGCGGCCTCTTTGTCT
	FAM- CTGCGACTTCACAGGACACTCCTG -TAMRA
nrarpa	AACATGACCAACTGCGAGTTTAAC/ AATATCGGCTCCAAATTTAAC
	FAM- GTTTCACGAGCTCCAGGTTCCCG -TAMRA
nrarpb	GCGCCCTGCACATAGCA/ TCGCCCGTGTGATGAGGTA
	FAM- CGTTTGGTGGACATCAAGACATCGTGC -TAMRA
β-actin	TGCTGTTTTCCCCTCCATTG/ TTCTGTCCCATGCCAACCA
	FAM- TGGACGACCCAGACATCAGGGAGTG -TAMRA

FAM: 6-carboxyfluorescein; TAMRA: 6-carboxytetramethylrhodamine

Table 8. Primer for in situ hybridization probes.

Gene	Forward primer 5´ - 3´/ reverse primer 5´ - 3´ or provider
mflt1	CTCGGCGCATGTACCAAATCAGG/ CATCCGAGTGCCGTGCTTCAGTC
sflt1	CTTCCCAGCAGCGTGATT/ GAGACCCGTAGAGTAGAAACAAAC
jagged1a	CTGCCTGCCGAACCCGTGTGA/ CCCTGTGGCATGGTGTCCTTGTT
jagged1b	GATACCAAGCCCCAAAACTGACTACC/ AGCCGCTGGATAAGGAAGAAACAAC
jagged2	TGCTCGCATCACCCTTATTTTCAA/ GGTCCGCGCTGCAGATTTAGAGTA
notch1a	GGCGGCGGTCTTGAAAATGAAA/ ACGAGCAGCGAGGAAAAGAGG
notch1b	CAATGAGCAGGAACTGAAGAAACAC/ CGTTTCAATCGGATGTAATGTTAGG
notch2	GGAAGGCATGGTGGAGGAACTGG/AGAATTGGCCGTGCTGGAGG
notch3	CAACACTGGCAACACGCACTACTG/ GCCCACCAAAGCCCTGAAT
ephrinB2a	Mione, M; Center for Molecular Medicine, Germany
dll4	Lewis, J; Cancer Research UK London Research Institute, UK
kdra	Lawson, ND; University of Massachusetts Medical School, USA
flt4	Lawson, ND; University of Massachusetts Medical School, USA
l-plastin	Herbomel, P; Ecole Normale Supérieure, France

4.1.5 Vectors

Table 9. Vectors.

Vector	Manufacturer or provider
pGEM®-T Easy	Promega
pCR8/GW/TOPO	Invitrogen
pCS2+	Seyfried, S; Max Delbrück Center Berlin, Germany
pTol*fliepcherry*Dest	Lawson, ND; University of Massachusetts Medical School, USA
pminiTol*kdrl*	Schulte-Merker S; Hubrecht Institute, Netherlands

4.1.6 Antibodies

Table 10. Antibodies.

Antibodies	Dilution	Manufacturer
Rabbit anti-phopho-Histone H3	IF: 1:800	Millipore
Rabbit anti-Flt1	IF: 1:1000, WB: 1:500	Eurogentec
Mouse anti-Zn-12	IF:1:500	ZIRC
Goat anti-rabbit-HRP	WB: 1:1000	Dako Cytomation
Alexa-Flour 633 goat anti-rabbit IgG	IF: 1:200	Invitrogen
Alexa-Flour 561 goat anti-mouse IgG	IF: 1:200	Invitrogen
Biotinylated horse anti-goat IgG	IF: 1:200	VectorLab
Goat anti-Digoxigenin	ISH: 1:4000	Roche

IF: immunofluorescence; WB: Western blot; ISH: in situ hybridization; HRP: horseradish peroxidase; Lab: Laboratories; ZIRC: Zebrafish International Resource Center

4.2 Methods

4.2.1 Zebrafish procedures

4.2.1.1 Maintenance of zebrafish and collecting embryos

Zebrafish were maintained under standard laboratory conditions (Westerfield, 1989). Embryos were collected in egg water from pair wise mating, kept at 26°C ambient temperature and staged by hours post fertilisation (hpf). When pigmentation started beyond 30 hpf, PTU (1-phenyl-2-thiourea, Sigma-Aldrich) were added to egg water to prevent the melanisation. At the desired stage between 24 hpf and 48 hpf the embryos were carefully dechorionated and fixed in 4% PFA for 2 h room temperature or over night (o/n) at 4°C.

Egg water	60^{-4} % Red Sea Salt
	10^{-5} % methylene blue, Ve-water
PTU	0.2 mM 1-phenyl 2-thiourea in egg water
4% PFA	4% paraformaldehyde in PBS, pH 7.5

4.2.1.2 Injections and Morpholino mediated gene knockdown

To analyse the functions of genes during early development *in vivo*, genetic manipulations were performed by injecting *in vitro* transcribed mRNA, expression constructs or antisense morpholino oligonucleotides (GeneTools) into one-cell stage embryos.

For the injection fertilized eggs were transferred to a 2% agarose ramp filled with egg water. The reagent was injected into the yolk sac or the ovule of the embryo using a glass micropipette with a microinjector (MPPI-2 Pressure Injector, ASI) (Figure 8) and subsequently distributed by cytoplasmic flow. Afterwards, embryos were transferred to a petri dish with egg water and incubated at 26 °C until the desired developmental stage was reached.

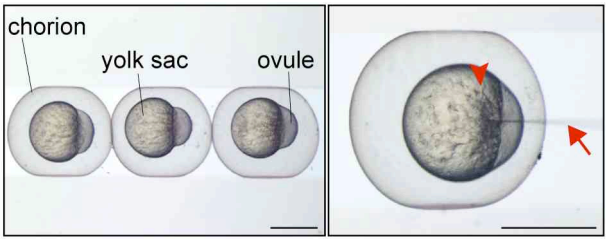

Figure 8. Microinjection of zebrafish embryos. On the left side fertilized eggs embedded in a 2% agarose ramp are shown. The fertilized egg consists of a chorion, a yolk sac, and the ovule. High magnification image on the right side indicates the glass micropipette (arrow) for microinjection and the cytoplasmic flow (arrowhead) within the yolk sac. Scale bar 400 µm.

The injected solutions contained *in vivo* transcribed mRNA (4.2.2.11) or expression constructs together with transposase that lead to ubiquitously or promoter driven overexpression of a specific gene. For gene knockdowns morpholino antisense oligonucleotides (GeneTools) were injected. Morpholino antisense oligonucleotides are translational blockers, which bind to the complementary sequences of mRNA. According to the manufactures protocol, the morpholino antisense oligonucleotides were designed against the start codon or the 5´UTR region of the gene of interest. To knockdown *flt1* function we used in general the *flt1* ATG-blocking morpholino, called Flt1MO. For validation of the *flt1* phenotype we employed a *flt1* 5`UTR-blocking morpholino. A morpholino with irrelevant sequence was utilized as control.

All injected mRNAs, constructs or morpholinos were diluted in Danieau Buffer and can be found with its used concentration in the Table 4 and Table 6.

Danieau Buffer (10x)	174 mM NaCl, 2.1 mM KCl, 1.2 mM $MgSO_4$, 1.8 mM $Ca(NO_3)$, 15mM HEPES, pH 7.6, used at 1x

4.2.1.3 *In vivo* imaging

For phenotype analysis living embryos were initially dechorionated and anaesthetized with 0.016% tricaine (Sigma-Aldrich). To immobilize the embryos for microscopy, the anaesthetic was removed and the embryos were embedded in 0.6% agarose (Sigma-Aldrich). *In vivo* imaging was performed using Zeiss LSM 510 microscopy with a 25 x (NA=0.8) water immersion objective (4.2.6.1, Carl Zeiss) and a Zeiss Axioscope A1 microscope with a 20x water immersion objective (4.2.6.2, Carl Zeiss). To record growing intersomitic vessels between 26 hpf - 46 hpf or blood flow at 72 hpf the living, but immobilized zebrafish embryos were incubated at 26°C and covered with egg water.

0.016% Tricaine	200 mg/50 ml tricaine in system water
0,6% Agarose	0.6% agarose in system water
System water	water out of the facility's water system

4.2.1.4 Application of γ-secretase inhibitor DAPT in zebrafish embryos

The γ-secretase inhibitor DAPT (N-[N-(3,5-Difluorophenacetyl)-L-alanyl]-S-phenylglycine t-butyl ester, Sigma-Aldrich) is an indirect inhibitor of Notch signalling and therefore used to analyse vascular defects after inhibition of Notch signalling. Zebrafish embryos were treated with DMSO-diluted DAPT (100 µM) at 20 hpf. Embryos in egg water containing DMSO (Serva) alone were utilized as control. Changes in the vasculature were observed by confocal microscopy (4.2.6.1).

4.2.2 Molecular biological methods

4.2.2.1 Polymerase chain reaction (PCR)

The PCR for DNA amplification was performed in a thermo cycler (Biometra). The general PCR reaction and cycle conditions are listed in Table 11. Based on different primer mixes, product sizes and further cloning steps, conditions for every PCR had to be adjusted. The final PCR product was confirmed by agarose gel electrophoresis (4.2.2.3).

Table 11. Polymerase chain reaction.

PCR reaction	**PCR cycle conditions**	
	Step	**Temperature and Time**
1x *Taq* DNA polymerase buffer	1. First denaturation	94°C 3 min
20 ng cDNA	2. Denaturation	94°C 30 s
0.4 µM primers mix	3. Annealing	60°C 30 s
0.2 mM dNTP	4. Elongation	68°C 2 min
0.02 U/µl *Taq* DNA polymerase	5. Storage	4°C ∞
ad 20 µl H_2O	Repeated steps: 2-4, 25 x	

4.2.2.2 Rapid amplification of cDNA-ends with polymerase chain reaction (RACE-PCR)

RACE-PCR is a technique for identifying unknown 5´- and 3´-end sequences from cDNA. During the procedure nucleic acid sequences between a defined internal site and an unknown 5´- or 3´-end are amplified (Scotto-Lavino et al., 2006a/b; Zhang and Frohman, 1997).

Using the SMARTer^{TM} RACE cDNA Amplification Kit (Clontech) we performed the 5´ and 3´ RACE-PCR in order to identify a putative soluble *flt1* isoform (*sflt1*) in zebrafish. Initially, mRNA from 30 hpf zebrafish was transcribed into cDNA according to manufacturer's instructions. To allow isolation of unknown 5´- or 3´-end sequences, synthesized cDNA contained anchor sequences appended to the unknown region. cDNA synthesis for the 3´ RACE takes the advantage of the natural polyA tail in the mRNA as generic priming site. Therefore mRNA was reversed

transcribed adding an oligo-dT adapter primer at the poly(A) tail. For 5` RACE cDNA was synthesized using reverse transcriptase and an anchored oligo-dT primer that enabled the addition of adaptor nucleotides at the 5`-end. These anchor sequences were later detected by PCR using the universal primer mix contained in the Kit. The corresponding primer that binds to a defined internal side of the cDNA was designed according following characteristics: 23-28 nt, 50-70% GC, Temperature > 68°C, located in the coding sequence and without stop codon. The primer sequences used for the 5` and 3` RACE-PCR are listed in Table 5.

For PCR reaction touchdown PCR was performed to increase the specificity, sensitivity and yield of the amplified products by using three different annealing temperatures (Table 12).

Table 12. Rapid amplification of cDNA-ends with polymerase chain reaction.

PCR reaction	PCR conditions	
	Steps	Temperature and time
1x Advantage 2 PCR buffer	1. First denaturation	94°C 5 min
3` or 5` RACE cDNA	2. Denaturation	94°C 30 s
10 µM Universal primer mix	3. Annealing	72°C 3 min
10 µM GSP1 or 2	4. Denaturation	94°C 30 s
0.2 mM dNTP	5. Annealing	70°C 30 s
1x Advantage 2 polymerase mix	6. Elongation	72°C 3 min
ad 30 µl H_2O	7. Denaturation	94°C 30 s
	8. Annealing	68°C 30 s
	9. Elongation	72°C 3 min
	10. Storage	4°C ∞
	Repeated steps: 2-3, 5 x; 4-6, 5 x; 7-9, 27 x	

PCR products were separated by agarose gel electrophoresis (4.2.2.3) and excised. The purified PCR fragments were then cloned into the pGEM®-T Easy vector (Promega) (4.2.2.4) and sequenced by MWG. The identified *sflt1* sequence can be found under the GenBank Accession Number JF330410.

4.2.2.3 Agarose gel electrophoresis

Agarose gel electrophoresis was used to separate PCR products and to analyse the quality of purified RNA. The 1% agarose gel was prepared by melting agarose powder (Sigma-Aldrich), 0.5x Tris-acetate EDTA (TAE) and ethidium bromide (0.5 µg). DNA or denaturised RNA samples were mixed with loading buffer and subsequently loaded onto the gel. If required, the DNA was excised from the gel using clean scalpels and purified via Zymoclean™ Gel DNA Recovery Kit (Zymo Research).

0.5 x TAE buffer	20 mM Tris-base, 0.05% acetic acid, 0.5 mM EDTA pH 8.0
Loading buffer	0.5% orange G, 50 % glycerol, 25 mM EDTA, pH 8.0

4.2.2.4 TA cloning

TA cloning was performed in order to generate in situ hybridization probes and to clone products of the RACE-PCR for further sequence analysis. TA cloning uses 3` adenine overhangs of the PCR products to enable easily its ligation into the linearized vector containing the complementary 3` thymine overhang. For the TA cloning we used *Taq* DNA polymerase (Fermentas) to amplify the desired insert with 3` adenine overhangs and the vector pGEM®-T Easy (Promega) according to manufacturer's instructions. Generated in situ probes are listed in Table 8.

4.2.2.5 Molecular cloning

For a ubiquitously overexpression of *in vitro* transcribed *mflt1* and *sflt1* mRNA we cloned *mflt1* and *sflt1* coding sequences into the vector pCS2+ (Seyfried, S; MDC, Germany). The vector is generally used for stable overexpression of genes because of its poly(A) signal downstream the cloning site. *mflt1* and *sflt1* cDNA were amplified using primers containing restriction endonucleases sites. The PCR products were purified, subsequently digested with EcoRI (NEB) and XhoI (NEB) and subcloned into the vector pCS2+ by using the restriction site linkers. Cloned *mflt1* and *sflt1* coding sequences were verified by sequence analysis from MWG. Sense-capped RNA was then synthesized as described in 4.2.2.11.

A similar strategy was applied to generate a construct for vascular specific overexpression of *sflt1* fused to egfp. The EcoRV (NEB) digested *egfp-sflt1* coding sequence was inserted into the EcoRV recognition site of the vector pminiTol*kdrl* (Schulte-Merker, S; Hubrecht Institute, The Netherlands) that contains the vascular specific promoter *kdrl*. Used primers, vectors and restriction enzymes can be found in Table 2, Table 6 and Table 9.

4.2.2.6 Gateway cloning

The Gateway® cloning technology from Invitrogen was used to clone *sflt1* in the vector pTol*fliepcherry*Dest (Lawson, ND; University of Massachusetts Medical School, USA) enabling vascular specific overexpression of *sflt1*. This destination vector contains the *fli1a* promoter in Tol2 backbone for N-terminal egfp fusion expression. The Gateway cloning procedure consists of two main reactions: the BP and LR reaction. These reactions are based on the recombination sites attB/attP and attL/attR that flank the gene of interest and facilitates its exchange. In general, the BP reaction is done between an expression clone (attB sites) and a donor vector (attP sites) to generate an entry clone containing the gene of interest flanked by attL sites. We produced the entry clone differently by ligating *sflt1* coding sequence directly into pCR8/GW/TOPO vector (Invitrogen). This resulted in an entry clone with *sflt1* flanked by attL sequences. The subsequent LR reaction was performed using the entry clone (attL sites) and the destination vector pTol*fliepcherry*Dest (attR sites) to generate the final expression construct pTol*fliepcherry-sflt1*. This expression construct (100 ng) was coinjected with transposase (50 ng mRNA) into zebrafish fertilized eggs. A more detailed description of the procedure can be found in the protocol for Gateway®cloning from Invitrogen. Primers and vectors are listed in Table 6 and Table 9.

4.2.2.7 Heat shock transformation

Plasmids were transformed into bacteria via heat shock in order to obtain enough template DNA for *in situ* hybridization probes, synthetic mRNAs or expression constructs. In general, we used *E. coli* DH-5α (Invitrogen) as competent cells that

were initially thawed on ice and mixed with 50 ng vector DNA before another incubation on ice. The heat shock was done at 42°C for 90 s. The transformed cells were incubated on ice and subsequently shaken in LB-media at 37°C for 1 h. Afterwards the cell suspension were spread out on LB-agar plates containing the corresponding antibiotics and incubated o/n at 37°C. Selected colonies were then transferred and shaken in LB-media o/n at 37°C, followed by plasmid DNA isolation (Zyppy™ Plasmid Miniprep Kit, Zymo Research) according to manufacturer's protocol. The DNA concentration and purity were determined using a NanoDrop spectrophotometer (Thermo Scientific).
Modifications concerning the usage of different competent cells were adapted to the corresponding manufacturer's protocol.

LB-media	20 g LB-Medium ad 1 l water
LB-agar	20 g LB-Medium ad 1 l water, 1.5% agar-agar
Antibiotics	100 µg/ml ampicilin, 25 µg/ml kanamycin, 50 µg/ml chloramphenicol
Supplement	1 mM IPTG, 80 µg/ml X-Gal

4.2.2.8 Preparation of RNA from zebrafish embryos

Total RNA was extracted from zebrafish embryos, isolated ECs and neurons. Snap frozen zebrafish embryos, ECs and neurons were homogenized in TriFast (peglab) using pp-pestle (Roth). The RNA was separated by phenol-chloroform extraction. Quantity and quality of the purified RNA were measured photometrically using NanoDrop (Thermo Scientific) according to the manufacturer's instructions. The integrity of the RNA was additionally assessed by agarose gel electrophoresis (4.2.2.3). Total RNA samples were stored at -80°C.

4.2.2.9 cDNA synthesis

Complementary DNA (cDNA) was required for cloning procedures (4.2.2.1) and quantitative real-time PCR (qRT-PCR, 4.2.2.10). Using cDNA First-Strand Kit

(Fermentas) the reverse transcription (RT) PCR was performed according to the manufacturer's instruction with 2.5 µg RNA as template and random hexamer primers as primers. cDNA samples were stored at -20°C or directly subjected.

4.2.2.10 Quantitative real-time PCR

In order to analyse the expression levels of specific genes we performed quantitative real-time PCR using TaqMan® Gene Expression Assay (Applied Biosystems). The principle relies on the 5` - 3` exonuclease activity of the Taq polymerase that cleaves the fluorophore (FAM and TAMRA) labelled TaqMan probes and its associated primer pair during hybridization. The cleavage of the TaqMan probe from the gene of interest releases the fluorophore that can then be measured.

The reaction mix was prepared according to the manufacturer's instruction. The primers and the probes were designed individually. Their sequences can be found in Table 7. Each gene was analysed in triplicates. The amplification was carried out in the ABI Prism 7000 thermo cycler (Applied Biosystems). PCR reaction mix and cycling conditions are listed in Table 13.

Table 13. Quantitative real time PCR.

PCR reaction	PCR conditions		
	Steps	Temperature and time	
1x TaqMan Universal PCR Master Mix	UNG incubation	50°C	2 min
100 µM Primer and probe mix	*Taq* activation,	95°C	10 min
12.5 ng/µl cDNA	UNG inactivation		
ad 10 µl H_2O	Denaturation	95°C	10 s
	Elongation	60°C	1 min
	Repeat steps 3-4: 50 x		

Gene expression data were normalized against elongation factor 1-apha (Ef1α). An additional housekeeping gene for the expression levels in neurons was beta-actin (β-actin) and assured the internal control Ef1α.

4.2.2.11 *In vitro* mRNA transcription of single-stranded RNA probes

In vitro transcribed mRNA was generated to obtain antisense/sense probes for in situ hybridization and to overexpress poly(A) capped mRNA *in vivo*.

For the synthesis of antisense and sense probes a desired insert sequence was amplified by PCR (4.2.2.1) and cloned into the pGEM®-T Easy vector (Promega) according to manufacturer's instructions. The used primer sequences for gene specific probes are listed in Table 8. Subsequent, 20 µg plasmid DNA containing the desired insert was linearized with restriction endonucleases for 2 h at 37°C. The linearized DNA was verified by agarose gel electrophoresis and purified via GeneJet Gel extraction kit (Fermentas, 4.2.2.3), before it was transcribed into a digoxigenin (DIG)-labelled mRNA *in vitro*. Using SP6 or T7 polymerase (Promega) to generate an antisense or sense probe the *in vitro* transcription reaction was performed as displayed in Table 14, followed by DNase (Promega) digestion. The antisense probe contained the complementary counterpart of the mRNA and enabled the detection of mRNA expression, whereby the sense probe was used as control.

Table 14. *In vitro* transcription of single-stranded RNA probes.

In vitro transcription reaction		DNase digestion
1 µg linearized template DNA		20 µl *in vitro* transcription reaction
1x Transcription buffer		1x DNase buffer
100 mM DTT		1 u/µl DNase
1x recombinant RNasine		ad 100 µl H_2O
1x DIG labelling mix	→	
20 u/µl RNA T7 or sp6 polymerase		
ad 20 µl RNase-free H_2O		
Incubation at 37°C for 2 h		Incubation at 37°C for 30 min

RNA purification and concentration was measured using NanoDrop (Thermo Scientific) and correct fragment size was checked via agarose gel electrophoresis (4.2.2.3).

For generation of poly(A) capped mRNA the desired insert sequence was cloned into the pCS2+ vector (Seyfried, S; MDC; Germany) as described in 4.2.2.5. The synthesis of *in vitro* capped mRNA was performed using mMESSAGE mMACHINE®

Sp6 Kit from Ambion. Before transcription, the plasmids containing the *mflt1* or *sflt1* coding sequence were linearized with the restriction enzyme NotI (NEB). The RNA purification and concentration were analysed as described above.

4.2.2.12 Whole mount in situ hybridization (WISH)

Whole mount in situ hybridization (WISH) was carried out with DIG-labelled mRNA probes (4.2.2.11) to detect the location of mRNA transcripts.

Zebrafish embryos were fixed in 4% PFA at the desired developmental stage and dehydrated in 100% methanol (Roth). Rehydration in 75%, 50%, 25% methanol/PBT (0.1% Tween) followed by proteinase K (2.5 µg/µl, Roche) treatment permeabilized the embryos. After re-fixation in 4% PFA for 20 min and 3 washing steps in PBT (0.1% Tween), the embryos were pre-hybridized with prewarmed hybridization buffer at least 2 h at 65°C. Subsequently, hybridization with the appropriate DIG-labelled RNA (500 ng) probe was performed for 16 h at 65°C. Next, the riboprobe and the hybridization buffer were removed via washing and RNase (100 µg/ml, Roche) digestion. For the antibody staining, the embryos were incubated in 2% Boehringer blocking reagent (Roche)/MABT for 2 h at room temperature before it was replaced with the antibody anti-DIG (1:4000, o/n, 4°C, Roche). The embryos were then rinsed with MABT and washed with substrate buffer NTMT. The staining was performed using BM purple (Roche) at 37°C and could be stopped by removing the substrate. The stained embryos were finally conserved in 80% glycerol/PBS.

Hybridization buffer	50% formamide, 5 x SSC, 100 µg/ml yeast RNA (tRNA), 0.1% tween-20, 50 µg/ml heparin, 4.6 citric acid (pH 6)
RNase buffer	0.1M hepes (pH7.5), 0.15 M NaCl, 0.1% tween-20
MABT	100 mM maleic acid, 150 mM NaCl, 0.1% tween-20, pH 7.5 buffered with NaOH
NTMT	0.1 M tris-HCl (pH 9.5), 0.1 M NaCl, 1% tween-20, 50 mM $MgCl_2$
PBT	PBS with 0.1% tween-20

4.2.3 Biochemical methods

4.2.3.1 Isolation of zebrafish protein

In order to isolate protein, zebrafish embryos were dechorionated and frozen at -80°C. After thawing them on ice, the embryos were homogenized with pistel (Roth) in Homo buffer and centrifuged at 8000 rcf, 10 min at 4°C. The supernatant contained soluble proteins, whereas the pellet was resuspended in Res buffer. Additional centrifugation of the resuspended pellet at 10000 rcf, 60 min at 4°C separated the membrane-bound proteins from the rest. The concentration of the isolated soluble and membrane-binding proteins were measured using the Pierce®BCA Protein Assay Kit (Piercenet) according to manufacturer's instructions.

Homo buffer	10 mM imidazole, 4 mM EDTA (pH 7.4), 1 mM EGTA, 0.2 mM DTT, 0.6 mM PMSF
Res buffer	6 M urea, 0.01 M Tris (pH 8), 1 mM EDTA, 0.15 M NaCl, 1 mM DTT, 0.6 mM PMSF

4.2.3.2 SDS polyacrylamide gel electrophoresis (SDS-PAGE)

SDS-PAGE was performed according to the protocol from Quiagen using a 10% separating and a 3.9% stacking gel. The protein samples (each 50 µg) were mixed with 4x loading buffer and heated for 5 min at 95°C prior to loading. The Spectra™ Multicolour Broad Range Protein ladder (Fermentas) served as molecular weight estimate. The gels run initially 20 min at 70 V and then for 90 min at 120 V in SDS-PAGE buffer. Subsequent, the proteins were passed to a PVDF membrane by wet transfer (4.2.3.3).

Separating gel (10%)	6.25 ml H_2O, 3.75 ml 4 x Tris (pH 8.8), 5.0 ml acrylamide, 10 µl temed, 50 µl 10% Aps
Stacking gel (3.9%)	3.05 ml H_2O, 1.25 ml 4 x Tris (pH 6.8), 0.65 ml acrylamide, 5 µl temed, 25 µl 10% Aps
Loading buffer 4x	200 mM DTT, 100 mM Tris-HCl (pH 6.8), 20 % glycerol, 4% SDS, 0.2% bromphenol blue
5x SDS Page buffer	25 mM Tris, 20 mM glycin, 0.1% SDS

4.2.3.3 Wet transfer

Wet transfer was performed to pass the by SDS-PAGE separated proteins (4.2.3.2) on a PVDF membrane (Millipore). Initially, the PVDF membrane was activated with methanol, shortly washed with H_2O and then placed under the gel that contained the proteins. The membrane and the gel were positioned carefully between 2 Whatman papers (Whatman) and 2 sponges (Biorad), soaked with Western blot buffer. The sandwich was closed and set into the Blot apparatus (Biorad) filled with Western blot buffer. The blot was run at 55 V for 20 h at 4°C, allowing all proteins to move from the gel onto the membrane, towards the positive pole. The transfer efficiency was monitored by reversible Ponceau Red solution of the PVDF membrane and by Coomassie staining of the gel. Afterwards the PVDF membrane was decolourised and used for immunodetection (4.2.3.4).

10x Western blot buffer	25 mM Tris, 200 mM glycine, 0.02% SDS, 5% methanol
Coomassie	0.1% Coomassie blue, 20% methanol, 10% acetic acid
Ponceau Red	0.1% ponceau S, 5% acetic acid

4.2.3.4 Immunodetection

Immobilized proteins on a PVDF membrane (Millipore) were analysed by immunodetection. To avoid unspecific binding of the Flt1 antibody, the blotted PVDF membrane was blocked in 5% milk (Roth)/PBT for 1 h at room temperature while shaking. Subsequently, the membrane was incubated with the primary antibody Flt1 (1:500, Eurogentec) in 1% milk/PBT solution at 4°C o/n. 3 washing steps with PBT for 15 min at room temperature were followed by incubation with the second antibody for 1 h at room temperature. The used antibodies are listed in Table 10. Additional 3 washing steps prepared the membrane for the chemoluminescense staining using Femto Chemoluminescent Substrate (Piercenet).

4.2.4 Histological methods

4.2.4.1 Immunofluorescence staining of whole mount zebrafish embryos

Whole mount zebrafish embryos were dechorionated and fixed in 4% PFA o/n at 4°C. Dehydration and rehydration through graded methanol series (25%, 50%, 75%, 100% methanol/PBT, Roth) were performed to permeabilize the fixed embryos followed by proteinase K digestion (10 µg/ml, Roche). After removing proteinase K by 3 washes with PBT the embryos were additionally fixed in 4% PFA for 20 min. Unspecific binding sides of the primary antibody were blocked with 1% BSA/1% goat serum/PBT for 1 h at room temperature before the primary antibody was added to the embryo and incubated o/n at 4°C. Unbound primary antibodies were removed by 2 washes with PBT for 30 min. Subsequently, embryos were incubated with a fluorescent-labelled secondary antibody for 1 h at room temperature. Used antibodies are listed in Table 10. After washing with PBT 3x for 5 min embryos were stored in the dark at 4°C or embedded in Vectashield®Mounting Medium (Vector laboratories) on coverslips for immediate analysis.

We performed three different negative controls. The first negative control contained all steps exceptional the incubation with the second antibody. In the second control the binding sides of the primary antibody were blocked using the corresponding peptide. The third negative control includes non-specific IgG.

4.2.4.2 Immunofluorescence staining using tyramide signal amplification (TSA)

In order to detect Flt1 antibody in zebrafish vasculature we used the tyramide signal amplification™ Kit (Perkin Elmer) according to the manufacturer's protocol. Fixed and rehydrated zebrafish embryos were permeabilized with acetone (Roth) 2x for 5 min. A series of different blocking solutions were used (1% H_2O_2/TBS, avidin-block, biotin-block, TNB-block, each 45 min) before the embryos were incubated with the primary antibody o/n at 4°C. After removing the primary antibody with TNT, the embryos were incubated with a biotin coated secondary antibody. The used antibodies can be found in Table 10. For an amplification staining, the second antibody was removed and the embryos were incubated first with streptavidin-HRP for 1 h followed by tyramide for 20 min. Subsequently the embryos were 3x washed in TNT for 30 min and embedded in Vectashield (Vector laboratories).

TBS	0.1 M Tris pH 7.5, 0.15 M NaCl
TNB-block	0.1 M Tris pH 7.5, 0.15 M NaCl, 0.5% blocking solution
TNT	0.1 M Tris-HCl pH 7.5, 0.15 M NaCl, 0.1% tween-20, pH

4.2.4.3 Generation of antibody

Flt1 protein was detected using a polyclonal Flt1 antibody produced by Eurogentec, utilising the AS-SUPR-DXP program. For rabbit immunization a peptide sequence of the extracellular domain of Flt1 (CQVTSGPSKRETNTT) was used. The antibody was purified by affinity matrix and used for Western blot analysis (1:500) and immunofluorescence staining (1:1000).

4.2.5 Cell biological method

As cell biological method we used the fluorescence-activated cell sorting (FACS) of GFP positive (GFP+) and GFP negative (GFP-) cells that served to isolate ECs and neurons. For this purpose 800 zebrafish embryos of the transgenic lines Tg(*fli1a:egfp*)^{y1} and Tg(*huC:egfp*) were dechorionated using 0.5 mg/ml pronase (Roche)/egg water, followed by 3 washes with egg water. The zebrafish embryos were dissociated to obtain a single cell suspension via trypsinization (Trypsin with 0.25% EDTA, Sigma-Aldrich) for 3 h at 26°C. After collecting the cells by centrifugation at 200 g, for 10 min at 4°C, the trypsinization was deactivated with 100% FSC (Biochrom). The centrifugation step was repeated, cells resuspended in 2% FCS/PBS and counted with Neubauer chamber. The cell suspensions were set to 5 x 10^7 cells/ml. Subsequently the cell suspensions were resuspended after additional centrifugation in sterile PBS and strained through a 75-µm filter into ice-cold falcons (Polystyrene Round Bottom Tube with cell strainer cup, BD Falcon). Using the FACS Sorter Aria1 (BD Biosciences, USA) the cell suspensions were separated into GFP+ and GFP- fractions. To assure the purity, the first 1000 cells were resorted. During sorting the cells were kept at 4°C. For the following RNA isolation (4.2.2.8), the samples were resuspended in TRIzol (Invitrogen) and stored at -80°C. The FACS data were analysed with FlowJo.

4.2.6 Microscopy

4.2.6.1 Confocal microscopy

To image the ISVs of a living and mounted zebrafish embryos (4.2.1.3), confocal microscopy was performed on the Zeiss LSM 510 microscopy with 25x (NA=0.8) and 63x (NA=1.2) water immersion objective. To acquire several focal planes one stack consisted of 20-30 single images that were scanned in a distance of 2 µm with an average number of 2. For the *in vivo* time-lapse imaging a stack was obtained in a time interval of 20 min. Images were processed using Zeiss ZEN 2009 Light Edition and ImageJ.

4.2.6.2 Intra vital microscopy

In vivo blood flow of the immobilized zebrafish embryos at 72 hpf (4.2.1.3) was imaged using a Zeiss intravital microscopy (Zeiss Axioscope A1, Carl Zeiss) with a 20x (NA=0.50) water immersion objective. Images were stored on digital tape (Sony DVCAM64) using a digital video recorder (Sony DVCAM DSR-25).

4.2.6.3 Light microscopy

Images of zebrafish embryos from whole mount in situ hybridizations were performed with Leica MZ 16 FA microscope and its attached colour camera CoolSnap^{TM} from Visitron Systems. Images were processed using Adobe Photoshop CS3 software and assembled using Adobe Illustrator CS3.

4.2.7 Statistical analysis

The data were analysed by Microsoft Excel 2008. All results are expressed as mean ± standard error of the mean (SEM). Significant differences between 2 experimental groups were determined by two-tailed Student's t-test. p-values were considered as *, $p<0.05$; **, $p<0.01$; ***, $p<0.001$.

5 Results

This study focused on VEGFR-1, namely Flt1, and its function during sprouting angiogenesis. Taking the advantage of transgenic zebrafish lines, changes in the vasculature and in the neuronal tissue caused by Flt1 knockdown or overexpression could be observed. Until now, one membrane-bounding isoform of Flt1 (mFlt1) has been annotated in zebrafish, while in mammals several distinct Flt1 isoforms are known. Due to these differences, we initially examined the existence of putative Flt1 isoforms in zebrafish. Indeed, using RACE-PCR we identified one additional, so far unknown, soluble Flt1 (sFlt1) isoform in zebrafish embryos. Flt1 loss- and gain-of-function experiments as well as in situ hybridization and real-time PCR revealed that Flt1 acts in a Notch dependent manner as negative regulator of tip cell formation. Furthermore, Flt1 expression was abundant in vessels and neurons. Accordingly, Flt1 affects branching morphogenesis and neuronal cell number. Vascular specific overexpression of sFlt1 showed distribution of sFlt1 protein adjacent to neurons, therefore regulating the VEGF gradient required for segmental artery outgrowth.

5.1 Characterization of Flt1 isoforms in zebrafish

5.1.1 Identification of a soluble isoform of Flt1 in zebrafish

In mammals the *Flt1* gene encodes several Flt1 isoforms that can be subdivided into one membrane-bound and numerous soluble isoforms (Heydarian et al., 2009; He et al., 1999; Kendall et al., 1993). Both the membrane-bound and the soluble Flt1 isoforms are composed of an extracellular VEGF-binding domain, while the membrane-bound isoform contains an additional intracellular tyrosine kinase domain. In zebrafish, only one membrane-bound isoform of Flt1 (mFlt1) was annotated in the database NCBI (GenBank Accession Number: GI72535147). To prove whether putative Flt1 isoforms are expressed in zebrafish, we performed 5´ and 3´ RACE-PCR using gene specific primers (GSP1/2, Figure 9A). The 5´ and 3´ RACE-PCR enable the identification of unknown 5´- and 3´-end sequences since nucleic acid sequences between a defined internal site and an unknown 5´- or 3´-end are amplified (Scotto-Lavino et al. 2006a/b; Zhang and Frohman, 1997). Based on the

well-known structure of the VEGF-binding domain of soluble Flt1 isoforms in mammals, we selected GSP1/2 according to the corresponding region of Flt1 in zebrafish. The GSP1/2 were chosen to bind within exon 8 and exon 9 of zebrafish Flt1 encoding the extracellular VEGF-binding domain (Figure 9A). 5´ RACE-PCR resulted in an amplified DNA of 1200 bp, whereas the product of the 3´ RACE-PCR was 1450 bp in length (Figure 9B). Analysis of the sequenced RACE-PCR products determined their structures: the 1200 bp 5´ RACE product consisted of exon 1 to exon 8, while the 1450 bp 3` RACE product consisted of exon 9 to the previously unknown exon 11a. Due to the experimental design, the 3` RACE PCR did not amplify an additional product encoding exon 9 to exon 30 corresponding to mFlt1 (Figure 9B). Detailed examination of both RACE products identified a new soluble isoform of Flt1 in zebrafish: sFlt1. The intron-exon structure of *flt1* precursor mRNA (pre mRNA) is illustrated in Figure 9A. *mflt1* and *sflt1* use a common transcription start site and share the first 10 exons. After exon 10 the *flt1* pre mRNA is alternatively spliced, which consequently leads to the formation of the two transcripts *mflt1* and *sflt1*. Splicing of exon 11b produces *mflt1*, whereas splicing of exon 11a generates *sflt1*. Although both transcripts use a common transcription start site, the stop codon for *mflt1* is encoded within exon 30, while *sflt1* utilizes poly(A) signal sequences within exon 11a to form a transcript that lacks downstream exons. A precise overview of the splicing region of *flt1* is demonstrated in Figure 9C. The existence of exon 11b and the so far unknown exon 11a was verified by PCR. Primers targeting exon 10 and exon 11b as well as exon 11a amplified the corresponding sequence of *mflt1* and *sflt1* (Figure 9D).

The newly identified sFlt1 isoform spans over 2878 bp including the coding sequence from 214-1635 bp. Translation of the cDNA sequence yields a 473 amino acids protein. The entire sFlt1 sequence can be found under the GenBank Accession Number JF330410. Due to the shared first 10 exons of mFlt1 and sFlt1 (Figure 9A), which encode the extracellular VEGF-binding domain, sFlt1 is a soluble isoform of Flt1 and may be secreted as a translated protein.

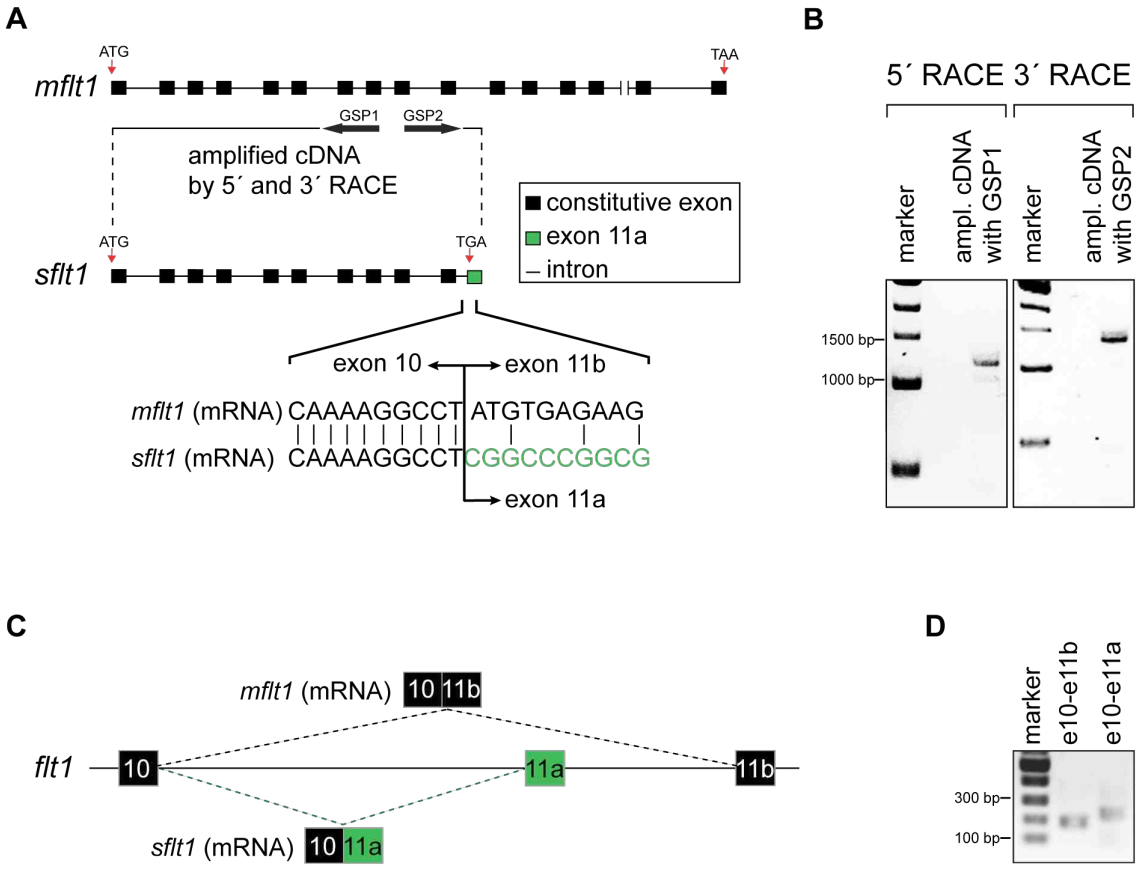

Figure 9. Identification of a soluble Flt1 isoform in zebrafish. (A) Representation of the intron-exon structure of pre mRNA of zebrafish *flt1* isoforms: membrane-bound *flt1* (*mflt1*) and soluble *flt1* (*sflt1*). *sflt1* was identified by 5´ and 3´ RACE-PCR using gene specific primers for *flt1*. Alternative splicing after exon 10 leads to two transcripts. Splicing to exon 11b produces *mflt1*, whereas splicing to exon 11a generates *sflt1*. Although both transcripts use a common transcription start site, *mflt1* encodes the stop codon within exon 30, while the stop codon for *sflt1* is within exon 11a. Both isoforms share the first 10 exons. (B) Gel electrophoresis of 5´ and 3´ RACE-PCR confirmed the expression of *sflt1* in zebrafish embryos. (C) Detailed illustration of the splicing region of *flt1* pre mRNA: *mflt1* is produced by exon skipping to exon 11b and *sflt1* is generated by exon retention of exon 11a. (D) The existence of exon 11a and exon 11b of *flt1* pre mRNA was verified by PCR. RACE-PCR, rapid amplification of cDNA-ends with polymerase chain reaction; GSP, gene-specific primer.

A novel isoform of Flt1, sFlt1, was identified in zebrafish. Since sFlt1 and mFlt1 are transcripts that arise from the same gene, we examined the expression levels and the expression pattern of each isoform.

5.1.2 Differential expression of Flt1 isoforms during development

We studied the expression levels of *mflt1* and *sflt1* mRNA in zebrafish using quantitative real-time PCR (Figure 10A). Based on the sequence differences of *mflt1* and *sflt1*, isoform-specific PCR probes were designed. Quantitative real-time PCR revealed a three to five fold higher expression level of *sflt1* compared with *mflt1* during the time period 24-48 hpf. The maximum of *sflt1* expression was achieved at 30 hpf, pointing to a eventually high relevance for angiogenic development.

The protein expression of Flt1 isoforms in zebrafish was determined by Western blot analysis (Figure 10B). Due to the lack of commercial Flt1 antibodies for zebrafish, we generated a custom made antibody directed against the extracellular domain of zebrafish Flt1 (4.2.4.3). Since both Flt1 isoforms contain the extracellular VEGF-binding domain, we performed Western blot analysis using the custom made antibody and detected mFlt1 in isolated membrane fraction as well as sFlt1 in zebrafish lysate (Figure 10B). The Western blot analysis confirmed the result of the RACE-PCR. sFlt1 was translated into a 52 kDa protein that corresponds to its coding sequence size of about 1538 bp. Furthermore, mFlt1 protein was detected at 140 kDa (Figure 10B).

To enable a structural illustration of the confirmed mFlt1 and sFlt1 proteins in zebrafish, we aligned the amino acid sequences of both isoforms and hence, identified their conserved domains. Their domain assembly is presented in Figure 10C. Both Flt1 isoforms are characterized by extracellular domains carrying immunoglobulin (Ig)-like domains for VEGF-binding. Additionally, mFlt1 is structured in a transmembrane-spanning and an intracellular tyrosine kinase domain, essential for receptor dimerization and signalling.

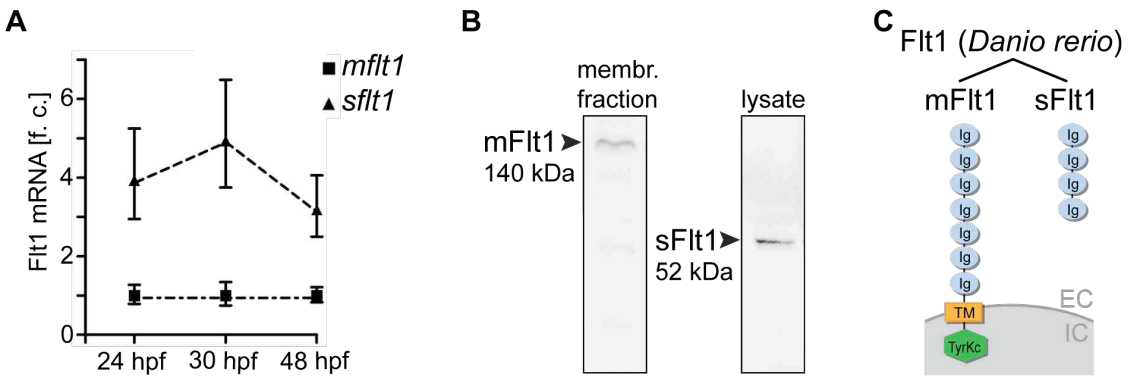

Figure 10. Differential expression levels of Flt1 isoforms during development. (A) Quantitative real-time PCR analysis demonstrated increased mRNA expression of *sflt1* compared to *mflt1* during development in zebrafish (n=3; 90 embryos/group). (B) Western blot analysis confirmed mFlt1 expression in isolated membrane fraction and sFlt1 expression in cell lysate of zebrafish embryos at 30 hpf. (C) Schematic representation of mFlt1 and sFlt1 protein in zebrafish (*Danio rerio*). Both isoforms share extracellular immunoglobulin-like domains. mFlt1 contains an additional transmembrane-spanning and an intracellular tyrosine kinase domain. F. c., fold change relative to *mflt1* expression; Ig, immunoglobulin-like domain; TM, transmembrane-spanning domain; TyrKc, tyrosine kinase domain; EC, extracellular; IC, intracellular.

The expression pattern of *flt1* was evaluated on DNA and mRNA level using the double transgenic zebrafish line Tg(*flt1*^{BAC}*:yfp*) x Tg(*kdrl:ras-cherry*)^{s916} (Hogan et al., 2009) and whole mount in situ hybridization (WISH, Figure 11).

The double transgenic zebrafish line Tg(*flt1*^{BAC}*:yfp*) x Tg(*kdrl:ras-cherry*)^{s916} was generated by J. Bussmann using a bacterial artificial chromosome (BAC) that contains the *flt1* gene including 86 kb of upstream and 4 kb of downstream sequence. A yellow fluorescent protein (YFP) reporter cassette was inserted at the ATG of *flt1* and enabled the visualisation of both *flt1* isoforms. The *flt1* promoter drives the expression of YFP, whereas the vascular specific promoter *kdrl* is expressed as cherry fluorescent protein (Cherry). Confocal microscopy of living Tg(*flt1*^{BAC}*:yfp*) x Tg(*kdrl:ras-cherry*)^{s916} embryos at 30 hpf revealed *flt1*^{BAC}*:yfp* expression mainly in the arterial domain including the dorsal aorta and segmental arteries, with *flt1*^{BAC}*:yfp* expression in the venous domain being less pronounced (Figure 11A). Interestingly, detailed examination of segmental arteries showed *flt1*^{BAC}*:yfp* expression in tip cells (arrowhead) and stalk cells (arrow, Figure 11A, bottom row). The vascular specific *kdrl* promoter expressed Cherry in the arterial and venous domain and referred as vascular marker.

To investigate the mRNA localization of each *flt1* isoform at 30 hpf, WISH with isoform-specific riboprobes was performed (Figure 11B). Both *flt1* isoforms were detected in the arterial domain. Additionally, *mflt1* was present in the venous domain. Detailed view of the posterior region of the zebrafish embryo revealed prominent *mflt1* and *sflt1* expression in the dorsal aorta and in segmental arteries at 30 hpf (Figure 11B, right panel). In addition, *mflt1* was expressed in low abundance in the posterior cardinal vein.

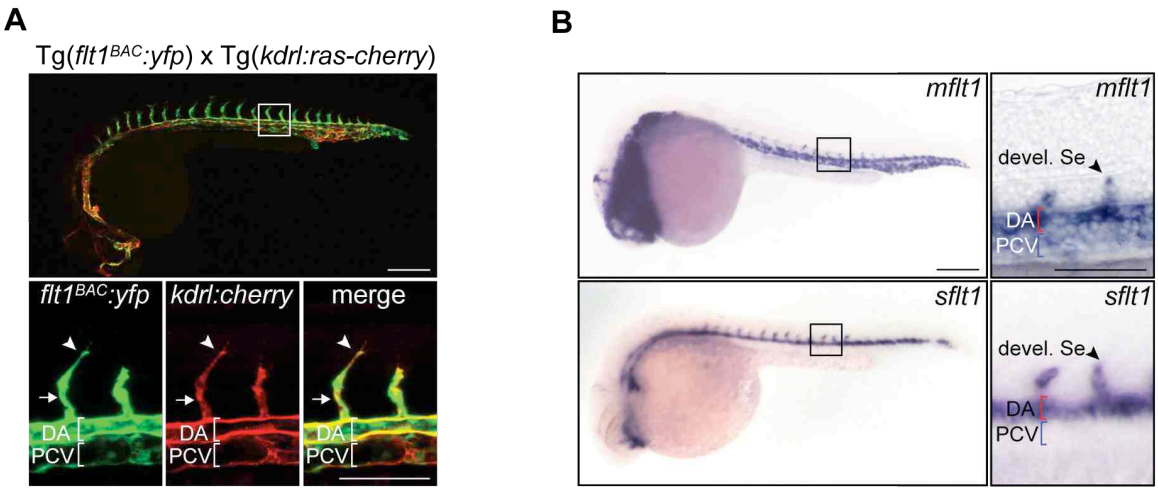

Figure 11. *flt1* expression pattern in zebrafish at 30 hpf. (A) The double transgenic zebrafish line Tg(*flt1*^{BAC}*:yfp*) x Tg(*kdrl:ras-cherry*)^{s916} expressed *flt1*^{BAC}*:yfp* in the dorsal aorta, the posterior cardinal vein and in the developing sprout at 30 hpf. Detailed information of the boxed region in the upper panel shows *flt1*^{BAC}*:yfp* expression in the tip cell (arrowhead) and the stalk cell (arrow). *kdrl:ras-cherry* signal was used as EC marker. (B) WISH with isoform specific riboprobes detected *mflt1* and *sflt1* mRNA expression in the dorsal aorta and the developing segmental artery (arrowhead). Expression in the posterior cardinal vein was restricted to *mflt1*. High magnification of the trunk region is shown on the corresponding right side. DA, dorsal aorta; PCV, posterior cardinal vein; devel. Se, developing segmental artery; scale bar 100 µm.

Analysis of the temporal and spatial expression of *flt1* DNA and mRNA as well as Flt1 protein showed expression during development and in the vasculature of 30 hpf zebrafish embryos. Based on these results, we expected a role for Flt1 during vascular development and performed knockdown and overexpression experiments.

5.2 Flt1 regulates segmental vessel branching

5.2.1 Flt1 loss-of-function results in hyperbranched segmental arteries

The identification and expression of Flt1 as well as its functional activity are of significant interest. In mice, it has been described that genetic loss of *Flt1* led to vessel dysmorphogenesis and overgrowth (Fong et al., 1995), but a detailed characterization of the underlying mechanisms is still missing. To gain insight into Flt1's function we initially investigated whether Flt1 plays a role during vascular

development in zebrafish. We knocked down Flt1 using morpholino antisense oligonucleotides. In zebrafish, the morpholino mediated knockdown is an effective approach to block the function of a specific gene by inhibiting its translation (Corey and Abrams, 2001). Therefore we designed a morpholino antisense oligonucleotide targeting the ATG of *flt1* (Flt1MO). The *flt1* morpholino injected embryos are called *flt1* morphants. A morpholino antisense oligonucleotide with an irrelevant sequence was used as control (control). In order to observe vascular changes after Flt1 knockdown, we used the transgenic zebrafish line Tg(*fli1a:egfp*)^{y1}, where the vascular specific promoter *fli1a* drives eGFP expression (Lawson and Weinstein et al., 2002). Using living Tg(*fli1a:egfp*)^{y1} embryos we were able to visualize the dynamic progression of branching morphogenesis from the onset expression of early angioblasts to the complete vascular system. Due to *flt1* mRNA expression at 30 hpf (Figure 10A), we monitored vessel development, especially the formation of segmental arteries, so called intersomitic vessels (ISVs). Using confocal microscopy we imaged the progression of segmental arteries in the posterior region of morpholino injected embryos (Figure 12A). Control morpholino injected embryos displayed no vascular defects (Figure 12A, top row). At 30 hpf, segmental arteries, which formed by sprouting from the dorsal aorta, reached the horizontal myoseptum in a stereotyped pattern. Subsequently, the segmental arteries navigated to the dorsal roof of the neural tube. Via fusion of the adjacent ISVs the dorsal-longitudinal anastomotic vessel (DLAV) was formed at 48 hpf. Blood flow within the vasculature was observed at 72 hpf. *flt1* morphants revealed no vascular defects during the initial sprouting at 30 hpf (Figure 12A, bottom row). Interestingly, at 48 hpf aberrant segmental artery branches were formed above the horizontal myoseptum, which showed lateral connections between adjacent sprouts, both in the anterior and posterior direction (Figure 12A, bottom row). These aberrant vessel connections formed a lumen, carried blood flow and were therefore functional at 72 hpf.

To quantify the effect of Flt1 knockdown on vessel formation, embryos that displayed hyperbranched segmental arteries were counted. Statistical analysis revealed a significant increase of embryos exhibiting aberrant branches in *flt1* morphants (78 ± 2%) compared to control morpholino injected embryos (2 ± 0.1%, Figure 12B).

The efficacy of the *flt1* ATG-blocking morpholino was confirmed by Western blot analysis. Reduced mFlt1 and sFlt1 protein levels were detected in *flt1* morphants

compared to control morpholino injected embryos. Equally loaded protein samples were detected by Coomassie staining (Figure 12C).

To demonstrate that the vascular phenotype was caused by the reduction in Flt1 expression, we designed a second *flt1* morpholino (Figure 12D). This morpholino antisense oligonucleotide targeting the 5` UTR region of *flt1* (5` UTR-Flt1MO) did not overlap with the *flt1* morpholino that blocked the ATG region of *flt1* (Flt1MO). Injection with either Flt1MO or 5` UTR-Flt1MO revealed similar branching defects of segmental arteries at 48 hpf, verifying the specificity of the vascular branching phenotype caused by Flt1 knockdown (Figure 12D).

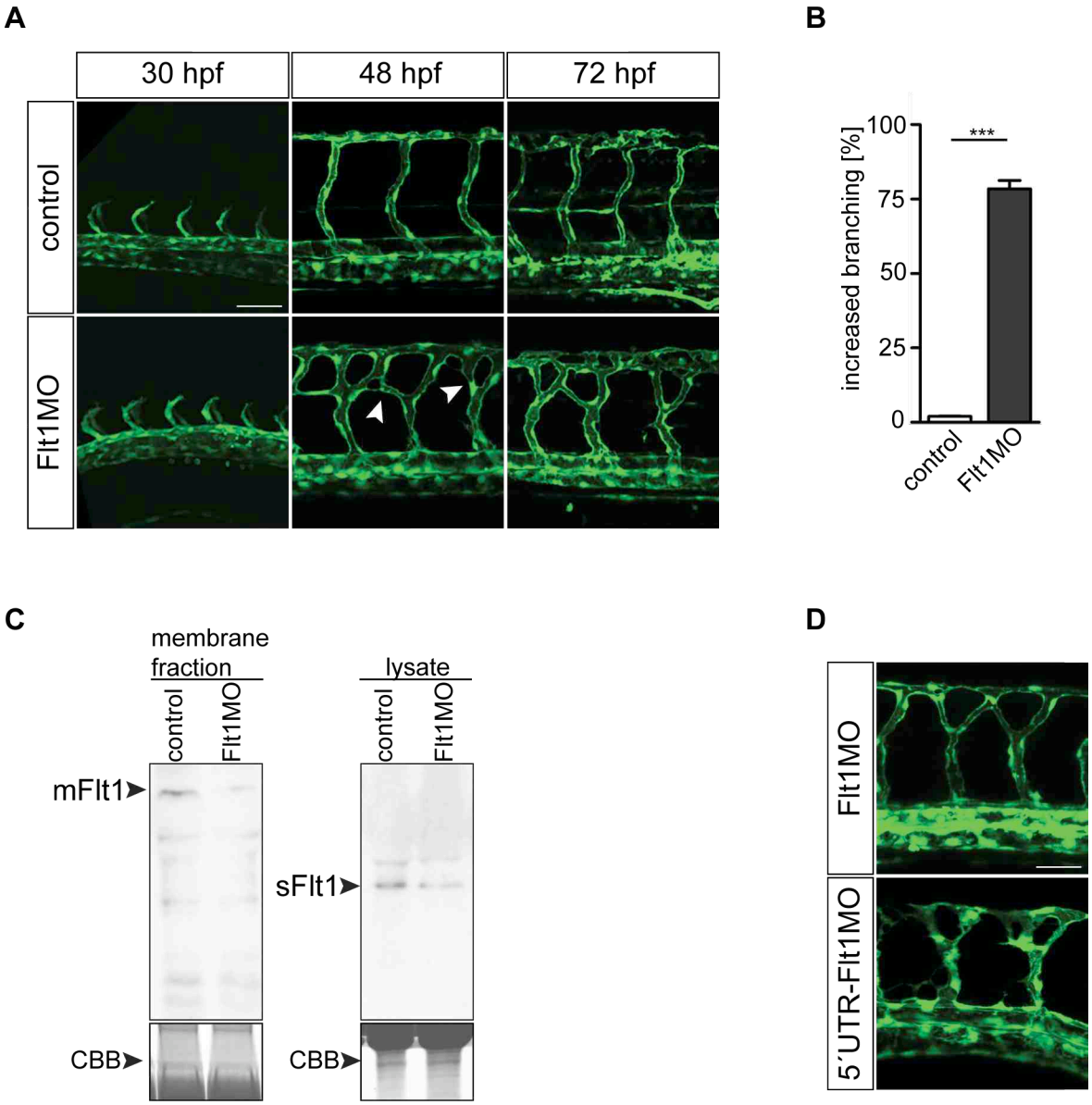

Figure 12. Flt1 loss-of-function results in hyperbranched segmental arteries. (A) Confocal images of the posterior region of Tg(*fli1a:egfp*)^{y1} embryos. In control morpholino injected zebrafish embryo (control) the stereotyped segmental arteries reached the horizontal myoseptum at 30 hpf, while the DLAV was formed at 48 hpf. Blood flow was observed at 72 hpf (top row). The segmental arteries of *flt1* morphants (Flt1MO) displayed no vascular defects during initial sprouting at 30 hpf, but showed aberrant segmental artery branches after 48 hpf (arrowheads). These lateral connections developed above the horizontal myoseptum and were perfused at 72 hpf (bottom row). (B) Statistical analysis of hyperbranched vessels revealed a significant increase in *flt1* morphants (78 ± 2%) compared to control (2 ± 0.1%) (n=4; 120 embryos/group). (C) Western blot analysis showed reduced protein levels of mFlt1 and sFlt1 in *flt1* morphants compared to control embryos and verified the functionality of the *flt1* morpholino. (D) Injection of the *flt1* ATG-blocking morpholino (Flt1MO) or of the *flt1* 5´ UTR targeting morpholino (5` UTR-Flt1MO) displayed similar vascular branching defects at 48 hpf. Scale bar 50 µm; CBB, Coomassie brilliant blue; Student's t-test; *** = p< 0.001; error bars represent SEM.

In summary, loss-of-function experiments using *flt1* morpholino resulted in hyperbranched segmental arteries.

To unravel Flt1's role during vascular development in more detail, we additionally performed Flt1 gain-of-function experiments.

5.2.2 Flt1 gain-of-function results in reduced segmental arteries

To obtain further information about Flt1 and its role within the process of branching morphogenesis overexpression experiments were performed. As loss of Flt1 was responsible for aberrant segmental artery branches, Flt1 gain-of-function would possibly reduce sprouting. Therefore we injected poly(A) capped *mflt1* or *sflt1* mRNA into embryos of the vascular reporter line Tg(*fli1a:egfp*)^{y1}. The injected *mflt1* and *sflt1* mRNA were generated by cloning the coding sequence into the pCS2+ vector. This vector contains a poly(A) signal downstream the cloning site and enabled a stable and ubiquitously expression of poly(A) capped *mflt1* and *sflt1* mRNA. Using confocal microscopy we imaged segmental arteries of the posterior region of mRNA injected embryos at 48 hpf (Figure 13A). The control embryo displayed segmental arteries in a stereotyped pattern that had formed the DLAV at 48 hpf. Consistent with a role for Flt1 in ISV branching, injection of *mflt1* (+mFlt1) or *sflt1* (+sFlt1) mRNA reduced sprouting of the segmental arteries (Figure 13A). Although the initial segmental sprout positioning was correct, sprout expansion stopped halfway towards the dorsal

roof. The tip cell of that sprout displayed no or short filopodia extensions (Figure 13A, bottom row). Statistical analysis demonstrated significantly more shortened sprouts in embryos overexpressing *mflt1* (75 ± 3%) or *sflt1* (81 ± 1%) compared to control embryos (2 ± 0.1%; Figure 13B). To confirm whether injected poly(A) capped *mflt1* and *sflt1* mRNA was stable in zebrafish embryos, we examined its expression level in *flt1* mRNA injected embryos at 48 hpf. Using quantitative real-time PCR we revealed a 4.6 fold in *mflt1* injected embryos and a 2.3 fold higher mRNA expression level in *sflt1* injected embryos compared to control embryos (Figure 13C). Our results verified the stability of poly(A) capped *flt1* mRNA in embryos at 48 hpf. In addition, Western blot analysis of *mflt1* and *sflt1* injected embryos at 48 hpf were performed. As expected, expression of mFlt1 and sFlt1 protein were increased in embryos that were injected with *in vitro* synthesised *mflt1* and *sflt1* mRNA (Figure 13D), confirming its proper translation and functionality in zebrafish embryos. Equally loaded protein samples were evaluated by Coomassie staining.

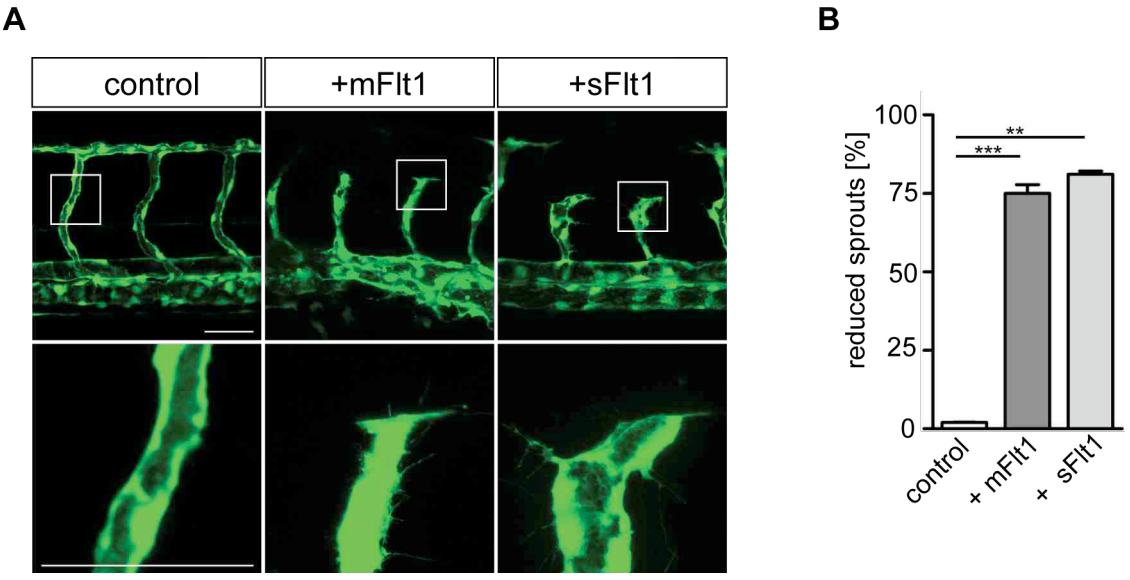

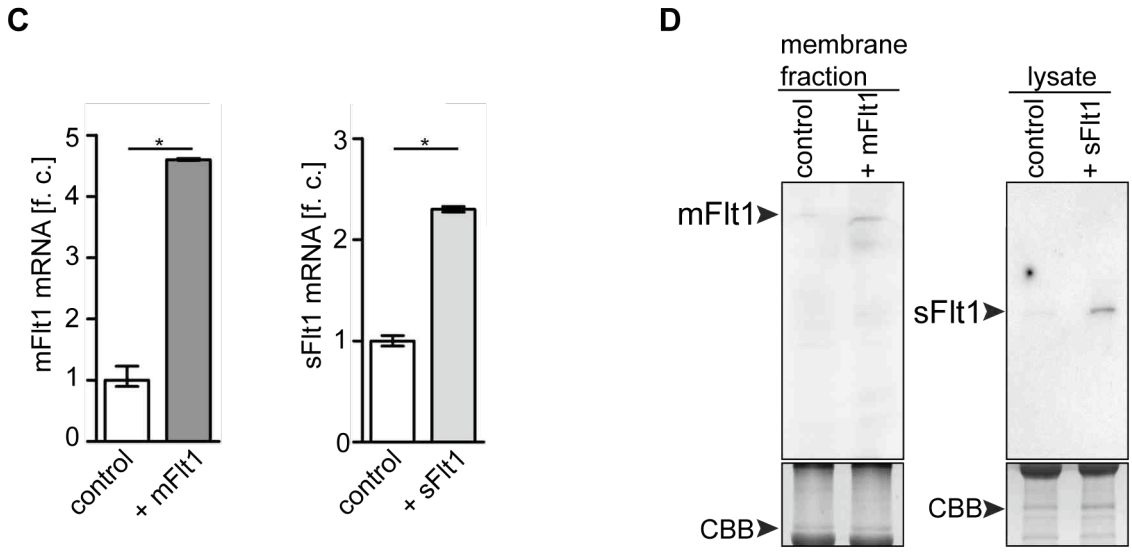

Figure 13. Flt1 *g*ain-of-function results in reduced segmental arteries. (A) Ubiquitous overexpression of *mflt1* (+mFlt1, middle panel) or *sflt1* (+sFlt1, right panel) resulted in reduced sprouts at 48 hpf compared to control embryos (left panel). High magnification of the boxed region shown on the bottom row highlights the short filopodia extensions of the sprout overexpressing *mflt1* or *sflt1*. (B) Quantification of reduced segmental arteries at 48 hpf revealed a significant increase of zebrafish embryos that were injected with *mflt1* (75 ± 2.8%) or *sflt1* (81 ± 1%) mRNA compared to control (2 ± 0.1%) (n=3; 360 embryos/group). (C) Quantitative real-time PCR of zebrafish embryos overexpressing *mflt1* or *sflt1* displayed increased *flt1* mRNA expression compared to control embryos at 48 hpf (n=3; 100 embryos/group). (D) Proper translation of the injected *mflt1* or *sflt1* mRNA was monitored using Western blot analysis of control and *mflt1* or *sflt1* mRNA injected embryos at 48 hpf. Scale bar 50 µm; CBB, Coomassie brilliant blue; Student's t-test; * = p< 0.05; ** = p< 0.01; *** = p< 0.001; error bars represent SEM.

Taken together, Flt1 gain-of-function resulted in reduced segmental arteries that remained at the horizontal myoseptum. This suggests a functional role for Flt1 during segmental artery formation, especially at the region above the horizontal myoseptum, called neural tube.

The specificity of the vascular phenotype caused by Flt1 knockdown and overexpression was evaluated by rescue experiments.

5.2.3 Vascular defects in *flt1* morphants are specific to reduced Flt1 levels

The specificity of the vascular phenotype observed in Flt1 loss- and gain-of-function experiments was analysed by rescue experiments (Figure 14A). Rescue experiments included co-injection of *flt1* ATG-blocking morpholino with either *mflt1* (Flt1MO+mFlt1) or *sflt1* (Flt1MO+sFlt1) mRNA in Tg(*fli1a:egfp*)^{y1} embryos. The same mRNA was employed for Flt1 gain-of-function experiments (5.2.2). Using confocal microscopy the manipulated embryos were examined at 48 hpf (Figure 14). Control morpholino injected embryos showed a stereotyped ISV pattern, whereas *flt1* morphants exhibited aberrant segmental arteries (Figure 14A, top row). *flt1* morphants that were injected with *sflt1* or *mflt1* mRNA revealed a segmental artery pattern reminiscent to that of control embryos (Figure 14A, bottom row). Hence, ubiquitous expression of *mflt1* or *sflt1* mRNA was able to restore the vascular branching defect in *flt1* morphants, confirming that the aberrant segmental arteries were caused by specific knockdown of Flt1. Furthermore, the extracellular VEGF-binding domain of mFlt1 and sFlt1 appeared sufficient to explain the vascular phenotype, as overexpression of each Flt1 isoform rescued the aberrant branching defect in *flt1* morphants.

Quantification of hyperbranched segmental arteries in *flt1* morphants revealed a significant decrease of the branching defect in embryos that were co-injected with Flt1MO and either *mflt1* or *sflt1* mRNA. This result confirmed a significant rescue of *flt1* morphants phenotype by *flt1* mRNA injection. (Figure 14B). Detailed analysis revealed 78 ± 2% of *flt1* morphants exhibiting increased sprouting and co-injection of Flt1MO with *mflt1* (19 ± 1%) or with *sflt1* (28 ± 2%) could reverse the vascular defect. Almost no branching defects were observed in control morpholino injected embryos (2 ± 0.1%).

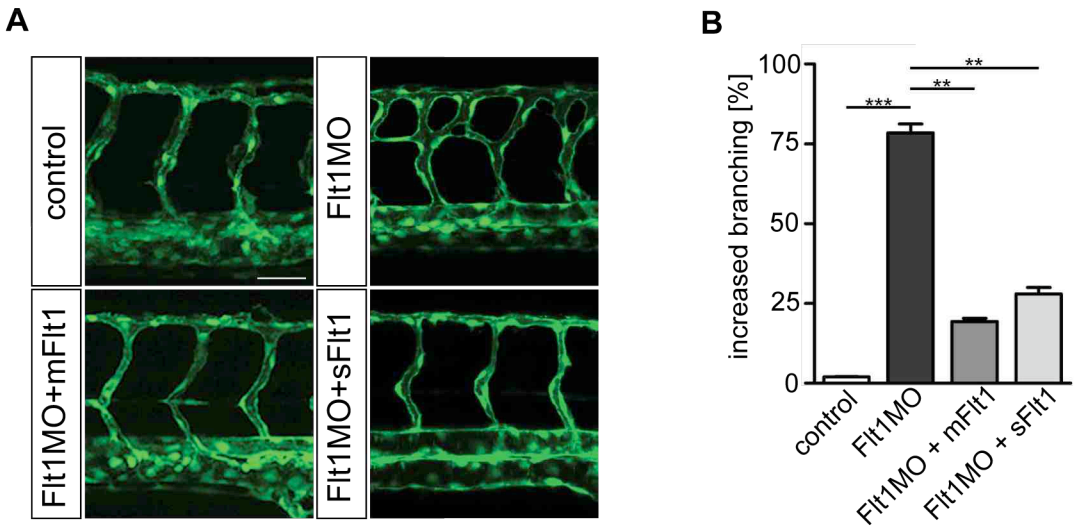

Figure 14. *flt1* mRNA injection can rescue the vascular phenotype of *flt1* morphants. (A) Confocal images of ISVs at 48 hpf demonstrates the stereotyped pattern of segmental arteries in control morpholino injected embryo (top row, left panel) and the hyperbranched segmental arteries in *flt1* deficient embryo (top row, right panel). Co-injection of Flt1MO and poly(A) capped mRNA for either *mflt1* (Flt1MO+mflt1) or *sflt1* (Flt1MO+sflt1) rescued aberrant segmental artery branches of *flt1* morphants (bottom row). (B) Statistical analysis of aberrant segmental artery branches as observed in *flt1* morphants (78 ± 2%) revealed a significant decrease of the branching defect in embryos that were co-injected with Flt1MO and either *mflt1* (19 ± 1%) or *sflt1* (28 ± 2%) mRNA. Control embryos displayed almost no branching defects (2 ± 0.1%) (n=4; 120 embryos/group). Scale bar 50 µm; Student's t-test; ** = p<0.01; *** = p< 0.001; error bars represent SEM.

Reduced Flt1 levels caused aberrant segmental artery branches of *flt1* morphants since injected *flt1* mRNA could rescue these defects.

The ability to rescue the *flt1* morphants' phenotype by injection of *flt1* mRNA validated the specificity of the *flt1* morpholino and excluded vascular non-target-related phenotypes. In order to assure entirely possible off-target effects caused by *flt1* morpholino injection, we examined the pigmentation pattern and cardiac contractility of morpholino injected embryos.

5.2.4 No toxic effects in *flt1* morphants using *flt1* morpholino

The use of morpholino antisense oligonucleotides is an effective method to knockdown genes in zebrafish. The dose of the morpholino required for a specifically gene knockdown without side effects, also called off-target effects, has to be chosen carefully. Up to 18% of morpholinos appear to have non-target-related phenotypes including for example developmental retardation (Ekker and Larson, 2001). Because pigmentation depends on the developmental stage of the embryo, retardation in development can be recognized easily. To exclude possible off-target effects caused by *flt1* morpholino injection, we analysed the pigmentation pattern of unbleached and *flt1* morpholino injected embryos. Using light microscopy, comparison of uninjected and *flt1* morpholino injected embryos at 48 hpf revealed a similar pigmentation pattern and body shape (Figure 15A), demonstrating that the used dosage of *flt1* morpholino did not affect unspecific transcripts.

Furthermore, Flt1 has been implicated in the regulation of heart rate. 2005, Rottbauer and co-workers demonstrated that injection of an *flt1* morpholino causes progressive reduction of ventricular contractility (Rottbauer et al., 2005). Therefore we analysed cardiac contractility and perfusion of the trunk vasculature in morpholino injected embryos using intravital microscopy. The measured heart rate was decreased in *flt1* morphants compared to control morpholino injected embryos (Figure 15B), but dorsal aorta, posterior cardinal vein and segmental vessels were perfused, indicating an established circulatory loop in *flt1* morphants. No progressive reduction of cardiac contractility was monitored in Flt1 deficient embryos.

Figure 15. No off-target effects of *flt1* morpholino and no progressive reduction of cardiac contractility in *flt1* morphants. (A) Using light microscopy the pigmentation pattern (arrows) and the body shape were monitored and displayed no differences between uninjected and with *flt1* morpholino injected embryos. Additionally, *flt1* morphants showed their characteristic aberrant segmental artery branches (arrowhead). (B) Quantification of the heart rate revealed a decrease in *flt1* morphants compared to control morpholino injected embryos (n=4; 10 embryos/group). Scale bar 200 µm; Student's t-test; * = p< 0.05; error bars represent SEM.

Our data demonstrated that *flt1* morpholino in the used dosage did not affect off-targets and reduced the cardiac contractility. These findings confirmed the specificity of hyperbranched segmental arteries caused by reduced Flt1 levels. Subsequent, the segmental artery formation was examined in detail by *in vivo* time-lapse imaging of morpholino injected embryos.

5.3 Flt1 acts as negative regulator for tip cell formation

5.3.1 *flt1* morphants display increased tip cell formation

To investigate cellular defects caused by loss of Flt1, we performed confocal time-lapse imaging in Tg(*fli1a:egfp*)^{y1} embryos and recorded in detail the dynamic progression of branching morphogenesis along with segmental artery formation. In general, the developing segmental artery uses three ECs with distinct positional fates and behaviours: a phalanx cell that is connected to the dorsal aorta, an adjacent stalk cell and a leading tip cell that uses filopodia protrusions to dictate the direction where the vascular plexus will expand (Lawson and Weinstein, 2002). Time-lapse imaging of Tg(*fli1a:egfp*)^{y1} embryos enabled the tracking of individual ECs in the sprout and allowed the determination of that position and behaviour. The phenotype of *flt1* morphants developed after 30 hpf (Figure 12A). Therefore we recorded segmental artery formation in control and *flt1* mopholino injected embryos from 32 hpf to 42 hpf. Snapshots of the time-lapse imaging are shown in Figure 16A. The individual ECs, recognized by strong eGFP signal, were designated in Figure 16A as number and its progeny as decimal number. At 32 hpf the sprout of the control morpholino injected embryo reached the horizontal myoseptum and consisted of one EC. During development two more ECs exited the dorsal aorta and migrated between somite

boundaries, while the first cell of the sprout continued to migrate dorsally in order to form the DLAV. The first EC of the sprout expanded filopodia protrusions and became a tip cell, whereas the following two ECs resembled the stalk and phalanx cells. By 42 hpf, segmental arteries in control morpholino injected embryos consisted of three ECs (Figure 16A, top row). Although the initial sprout formation in *flt1* morphants was similar as seen in control embryos, we observed in *flt1* morphants a different progression and behaviour of ECs during the segmental artery formation (Figure 16A, bottom row). Once the first EC, called tip cell, reached the horizontal myoseptum at 32 hpf, it underwent a single cell division after which two progeny tip cells spearheaded the sprout. Each tip cell expanded filopodia protrusions in order to navigate the growth direction of the sprout. Thus, the two tip cells led to the formation of aberrant segmental artery branches. Repeated EC proliferation finally caused hyperbranched, but lumenized segmental arteries. While the tip cell proliferated, two more ECs from the dorsal aorta entered the sprout and moved towards the leading edge of the segmental artery. These ECs were highly motile, some displayed filopodia extensions and attempted to make connections with adjacent segmental vessels. Based on their anatomical location, these cells might be assigned as stalk and phalanx cells. Based on their morphological features, they should be assigned as tip cells. By 42 hpf, the segmental arteries in *flt1* morphants were aberrantly branched and consisted of four cells. During segmental artery formation in *flt1* morphants we observed (1) segmental arteries spearheaded by two tip cells, (2) increased filopodia extensions throughout the sprout, (3) ECs at a position normally taken by stalk cells forming connections to adjacent vessels and (4) increased EC number in segmental arteries of *flt1* morphants compared to control embryos. Moreover, the dorsal extension of ISVs in *flt1* morphants appeared slower than in controls.

In order to confirm the increased EC number observed in *flt1* morphants, we quantified the proliferation of ECs during segmental artery formation on the basis of the recorded time-lapses. We observed more proliferating ECs in *flt1* morphants (1.8 EC/sprout) compared to control morpholino injected embryos (0.4 EC/sprout; Figure 16B). Detailed examination allowed the differentiation between tip or stalk cell proliferation (Figure 16C). We counted the leading cell as tip and the following cell as stalk cell. Comparisons of proliferating stalk cells in control morpholino injected embryos and *flt1* morphants revealed no differences, whereas proliferation of tip cells

in *flt1* morphants was significantly increased compared to control morpholino injected embryos (Figure 16C).

The monitored proliferation of the leading EC in *flt1* morphants at 32 hpf was verified by immunofluorescence staining with anti-phopho-histone H3 antibody. The proliferating ECs in the segmental arteries of *flt1* morphants were positive, in contrast to the control embryos with no staining in the segmental arteries (Figure 16D).

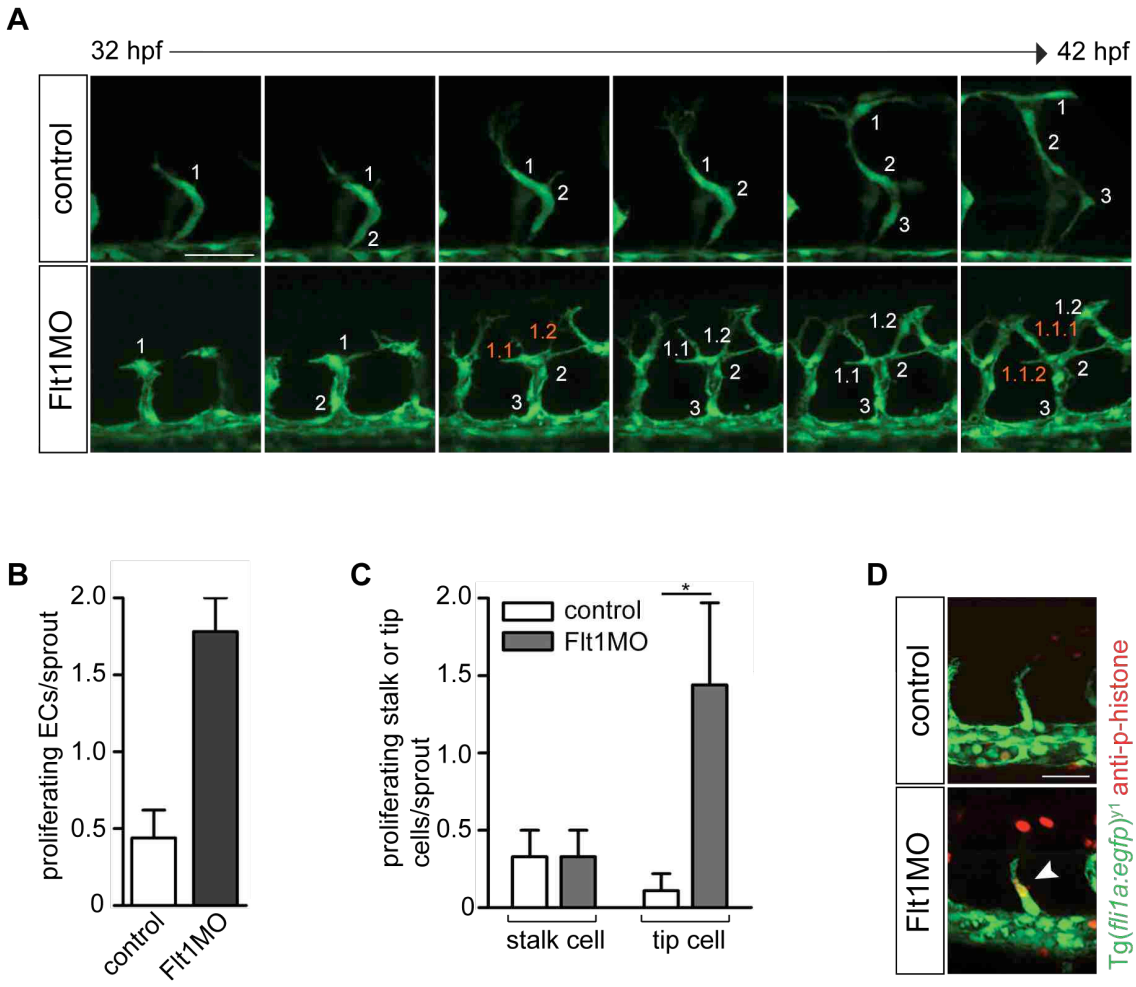

Figure 16. *flt1* morphants display increased tip cell formation in growing ISVs. (A) Snapshots of recorded ISV formation between 32 hpf and 42 hpf. In control embryo, segmental arteries developed using three migrating ECs, indicated as numbers (top row). In *flt1* morphant, ECs of the growing sprout proliferated, thereby forming two instead of one leading endothelial tip cell that consequently led to a branched segmental artery. Cells designed with decimal points indicate progeny cells (bottom row). (B) Quantification of proliferating segmental ECs during *in vivo* time-lapse imaging revealed a more frequent proliferation in *flt1* morphants compared to control embryos (n=3; 21 embryos/group). (C) Specification of proliferating ECs demonstrated an increased proliferation of tip cells in *flt1* morphants compared to control embryos. The stalk cell behaviour did not change (n=3; 21

embryos/group). (D) Anti-phospho-histone staining in zebrafish embryos confirmed proliferation of the leading segmental EC in *flt1* morphants at 32 hpf (arrowhead). Scale bar 50 µm; Student's t-test; * = p< 0.05; error bars represent SEM.

Due to the increased EC proliferation during ISV development in *flt1* morphants, we counted segmental ECs of four adjacent segmental arteries at 48 hpf and calculated the EC number of each sprout (Figure 17). The quantification of segmental ECs revealed a significant increase in *flt1* morphants. We counted one more EC per sprout in *flt1* morphants (4.9 EC/sprout) compared to control morpholino injected embryos at 48 hpf (3.8 EC/sprout).

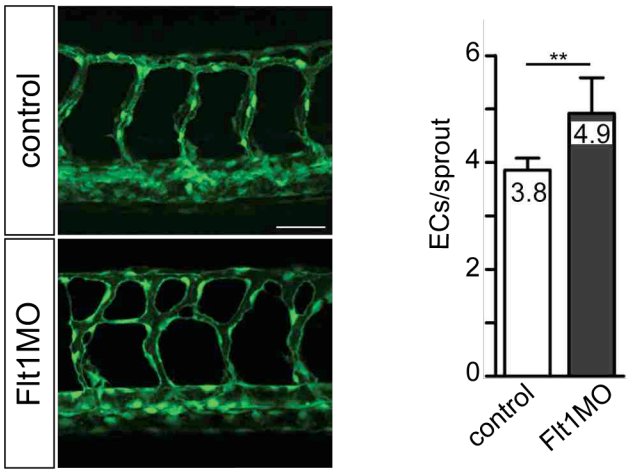

Figure 17. *flt1* morphants exhibit an increased EC number at 48 hpf. Segmental ECs were quantified by counting four pairs of adjacent segmental arteries at 48 hpf. Representative images for the quantification are depicted on the left side. Statistical analysis demonstrated an increase of one EC per sprout in *flt1* morphants compared to control embryos (n=3; 21 embryos/group). Scale bar 50 µm; Student's t-test; ** = p< 0.01; error bars represent SEM.

Using time-lapse imaging we recorded the segmental artery formation. In *flt1* morphants we observed an exceeded number of leading segmental ECs that displayed a migratory and proliferative behaviour. These results suggest that loss of Flt1 resulted in increased tip cell formation during ISV development.

To verify our observations, we performed WISH and quantitative real-time PCR of tip cell and stalk cell markers in morpholino injected embryos.

5.3.2 Altered tip and stalk cell marker expression in *flt1* morphants

Using time-lapse imaging we observed an increased tip cell formation in growing ISVs of *flt1* morphants compared to control morpholino injected embryos. In order to confirm this observation, we performed WISH of tip cell markers and compared the expression pattern in morpholino injected embryos at 30 hpf. Generally used tip cell markers are Kdra, the zebrafish orthologoues of VEGF receptor 2, Flt4, the zebrafish orthologoues of VEGF receptor 3 and the Notch ligand Dll4 (Thomson et al., 1998; Fouquet et al., 1997; Sumoy et al., 1997). These tip cell markers are not exclusively expressed in tip cells, but also prominent in arteries or veins as demonstrated in Figure 18A. *kdra* mRNA became preferentially expressed in the dorsal aorta and the developing segmental artery of control and *flt1* morpholino injected embryos. Detailed view of one segmental artery highlighted the increased *kdra* positive filopodia extensions of *flt1* morphants compared to control embryos (Figure 18A, arrowheads), suggesting excessive tip cell formation in Flt1 deficient embryos. Moreover, we found that expression of *flt4* was restricted to tip cells and the posterior cardinal vein in control morpholino injected embryos. In *flt1* morphants, we observed an additional ectopic *flt4* expression in the dorsal aorta, a feature previously associated with loss of Notch signalling (Siekmann and Lawson, 2007). Increased angiogenic cell behaviour is related to loss of Notch signalling and reminiscent to the ECs in developing segmental arteries of *flt1* morphants (Figure 17A). However, we found that expression of the Notch ligand *dll4* was maintained in the dorsal aorta and tip cells of control and *flt1* morpholino injected embryos (Figure 18A).

To directly compare the expression levels, we performed quantitative real-time PCR of tip and stalk cell markers in morpholino injected embryos at 30 hpf. As tip cell markers we used probes against the mRNA of *kdra*, *kdrb*, *flt4* and *dll4*. *kdrb* is a gene duplicate of *kdra* and because of its similar expression pattern in embryos at 30 hpf, it has not been investigated by WISH before (Bahary et al., 2007). Quantitative real-time PCR revealed increased expression levels of *kdra*, *kdrb* and *flt4* in *flt1* morphants, while the *dll4* expression level was not changed (Figure 18B). As stalk cell markers we used probes against *nrarpa* and *nrarpb* (Phng et al., 2009). The expression levels of the stalk cell markers *nrarpa* and *nrarpb* were slightly decreased in *flt1* morphants (Figure 18, C), suggesting a conversion of stalk cells into tip cells.

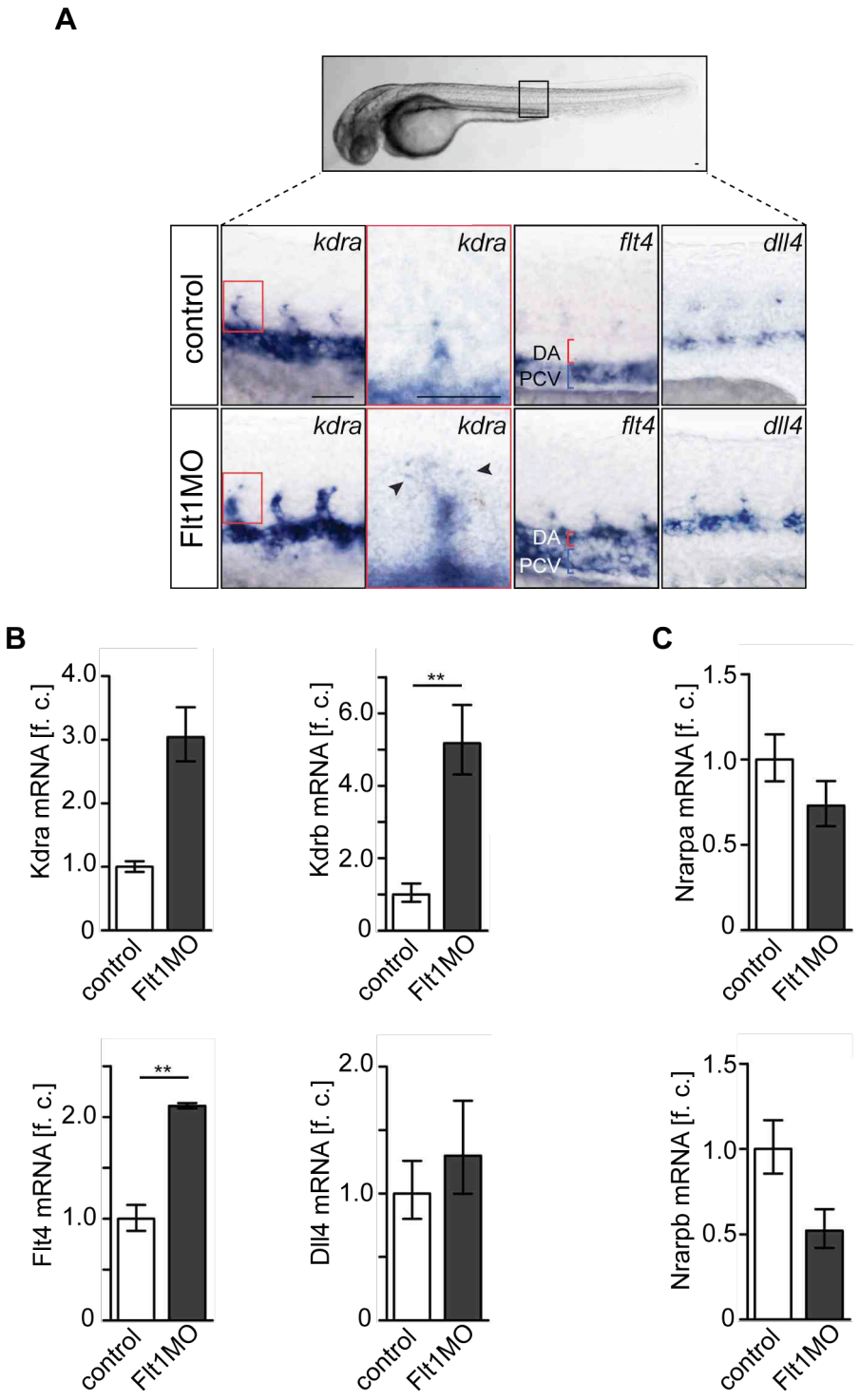

Figure 18. Altered tip and stalk cell marker expression in *flt1* morphants. (A) WISH for the tip cell marker *kdra*, *flt4* and *dll4* showed increased expression in *flt1* morphants compared to control embryos at 30 hpf. *kdra* expression was detected in segmental arteries, the dorsal aorta and the posterior cardinal vein. High magnification of the boxed region is represented in the second panel and highlights the *kdra* positive filopodia protrusions in *flt1* morphants (arrowheads). In control, *flt4* expression was apparent in the posterior cardinal vein, whereas in *flt1* morphants *flt4* was additionally expressed in the dorsal aorta. Expression of the Notch ligand *dll4* was maintained in the dorsal aorta

and tip cells of control and Flt1 deficient embryos. (B) Quantitative real-time PCR analysis confirmed increased expression of tip cell markers *kdra*, *kdrb*, *flt4*. *dll4* expression were unchanged (n=4; 120 embryos/group). (C) A slightly decreased expression of the stalk cell markers *nrarpa* and *nrarpb* were measured in *flt1* morphants compared to control embryos at 30 hpf (n=3; 100 embryos/group). Scale bar 50 µm; DA, dorsal aorta; PCV, posterior cardinal vein; ** = p<0.01; error bars represent SEM; f.c., fold change relative to the expression of age-matched control embryos.

Using WISH and quantitative real-time PCR we were able to evaluate the expression patterns and levels of tip and stalk cell markers in morpholino injected embryos. The analysis revealed an increased expression of the tip cell markers *kdra*, *kdrb* and *flt4*, while *dll4* expression was maintained. A slightly decreased expression of stalk cell markers was measured in *flt1* morphants compared to control, indicating that loss of Flt1 affected tip cell/stalk cell differentiation.

The tip cell/stalk cell differentiation is mediated through Notch signalling in zebrafish embryos (Siekmann and Lawson, 2007). Therefore we examined the Notch signalling pathway in morpholino injected embryos.

5.3.3 Decreased Notch signalling in *flt1* morphants

The evolutionary conserved Dll4-Notch signalling pathway has been implicated in the regulation of tip and stalk cell differentiation (Siekmann and Lawson, 2007; Gridley, 1997). To address the mechanism that regulates the cell fate decision in *flt1* morphants, we performed WISH for Notch receptors, Notch ligands and the Notch downstream target Ephrinb2a (Efnb2a). As loss of Flt1 resulted in increased tip cell formation, analysis of the responsible tip cell/stalk cell differentiation pathway would elucidate the postulated effect on branching morphogenesis caused by loss of Flt1.

In zebrafish exist four Notch receptors: Notch1a, Notch1b, Notch2, and Notch3 (Westin and Lardelli, 1997; van Eeden et al., 1996). Their expression pattern was examined by WISH in morpholino injected embryos at 30 hpf (Figure 19A). In control morpholino injected embryos, we found that transcripts of *notch1a*, *notch1b* and *notch3* were expressed within the dorsal aorta and neural tube, transcripts of *notch2* were detected in somites. Interestingly, in *flt1* morphants we found an abundant reduction in the expression pattern of all Notch receptors. Their transcripts were less

detectable in the neural tube. Moreover, expression in the dorsal aorta and somites were absent in *flt1* morphants (Figure 19A), indicating that the expression pattern of Notch was influenced by loss of Flt1.

It has been described that Notch receptors are activated by binding to their cognate ligands on neighbouring cells (Artavanis-Tsakonas et al., 1999). Hence, a putative effect of Flt1 on the expression pattern of the Notch ligands *jag1a*, *jag1b* and *jag2* were analysed using WISH (Figure 19A; Zecchin et al., 2005). In addition, the transcript level of the Notch downstream target *efnb2a* was examined. We found expression of the ligands *jag1a* and *jag2* in the neural tube, in particular, *jag1a* in spinal chord neurons of control morpholino injected embryos. Furthermore, *jag1b* and *efnb2a* transcripts were prominent within the dorsal aorta. In *flt1* morphants, the expression patterns of *jag* ligands were barely detectable. The Notch downstream target *efnb2a* showed decreased expression in *flt1* morphants (Figure 19A), demonstrating an indirect effect of Flt1 on *efnb2a* expression.

In order to evaluate the decreased expression pattern of the Notch signalling pathway in *flt1* morphants, we measured the expression levels of *notch1a*, *notch1b, notch3* and the Notch downstream target *efnb2a* using quantitative real-time PCR (Figure 19B). Indeed, the Notch receptors *notch1a*, *notch1b* and *notch3* exhibited reduced expression levels of approximately 50% in *flt1* morphants compared to control morpholino injected embryos. Furthermore, the Notch downstream target *efnb2a* revealed a decreased expression of approximately 25% in *flt1* morphants (Figure 19B).

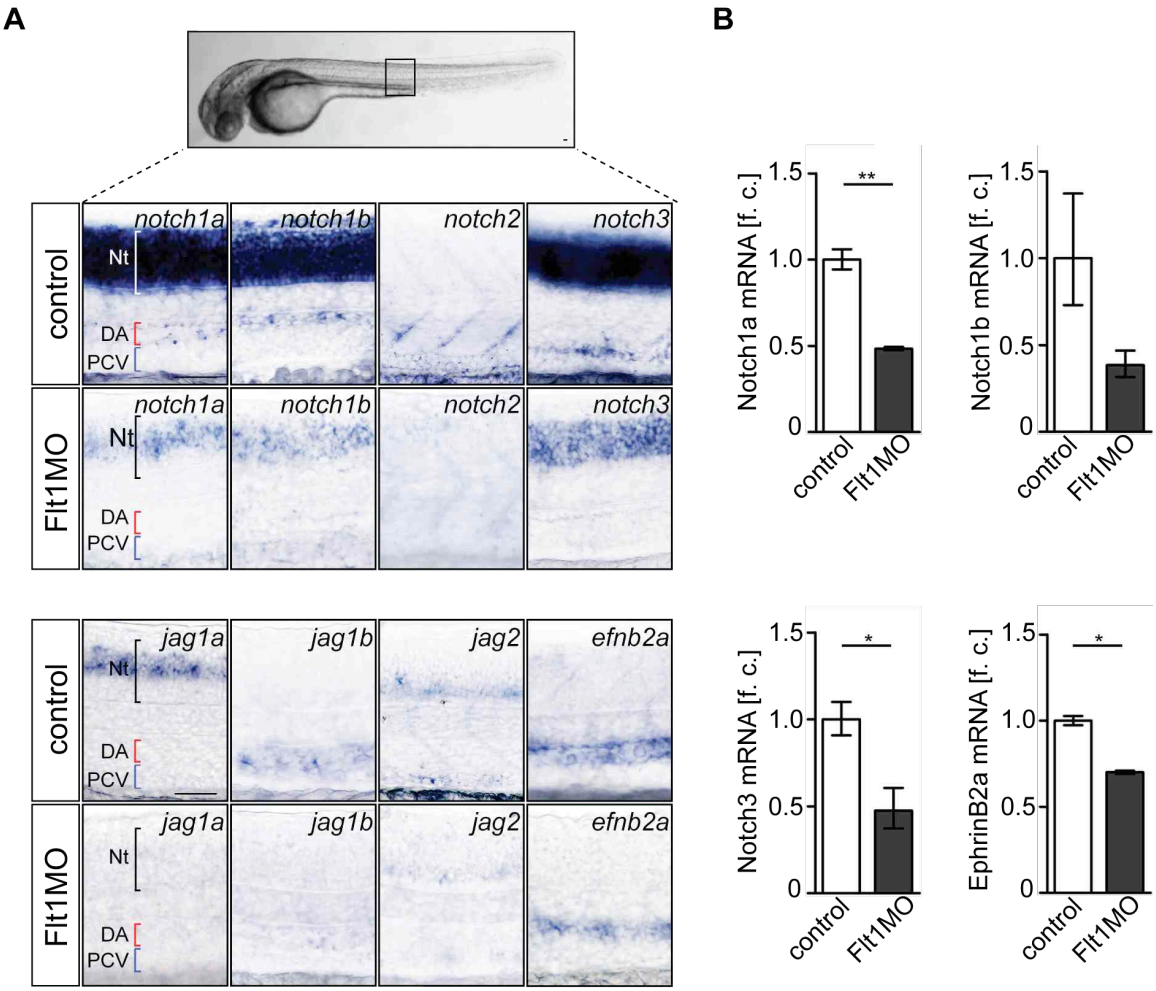

Figure 19. Decreased Notch signalling in *flt1* morphants. (A) WISH of all zebrafish Notch receptors (*notch1a*, *notch1b*, *notch2* and *notch3*), Notch ligands (*jag1a*, *jag1b* and *jag2*) and Notch downstream target *efnb2a* demonstrated a general decreased expression pattern in the dorsal aorta, the neural tube and somites in *flt1* morphants at 30 hpf. (B) Quantitative real-time PCR verified the reduced expression of *notch1a*, *notch1b*, *notch3* and *efnb2a* in *flt1* morphants compared to control embryos (n=3; 120 embryos/group). Scale bar 50 µm; DA, dorsal aorta; PCV, posterior cardinal vein; Nt, neural tube; Student's t-test; * = p< 0.05; ** = p<0.01; error bars represent SEM; f.c., fold change relative to the expression of age-matched control embryos.

To gain insight into the function of Flt1 during tip cell/stalk cell differentiation, we analysed the Notch signalling pathway and found a general reduction in the expression of Notch receptors, Notch ligands and Notch downstream target *efnb2a* in *flt1* morphants, indicating an influence of Flt1 deficiency on Notch signalling.

We subsequently analysed whether loss of Dll4-Notch signalling phenocopied the segmental artery defects associated with loss of Flt1.

5.3.4 Loss-of-function of Notch signalling does not phenocopy aberrant branches of *flt1* morphants

To determine whether loss of Dll4-Notch signalling is sufficient to explain the vascular branching pattern observed in *flt1* morphants, we studied vascular defects after inhibition of Notch signalling or knockdown of Dll4. Inhibition of Notch signalling was achieved by treating embryos with the Notch γ-secretase inhibitor DAPT. The membrane-spanning domain of Notch is not cleaved by the Notch γ-secretase, hence, the release of the Notch intracellular domain for further signalling is blocked (Geling et al., 2002). Knockdown of Dll4 was performed using a splice-blocking morpholino antisense oligonucleotide targeting *dll4* (Dll4MO) that prevents splicing of *dll4* pre mRNA (Leslie et al., 2007).

Using confocal microscopy the ISVs at 48 hpf were imaged (Figure 20). In control morpholino injected embryos, the segmental arteries and the DLAV were formed in a stereotyped pattern (Figure 20A, A`), whereas in *flt1* morphants the segmental arteries were aberrantly branched (Figure 20B, B`, yellow arrowhead). Embryos treated with DAPT exhibited filopodia extensions at the level of the DLAV (Figure 20C, C`, white arrowhead) and upon Dll4 knockdown the segmental arteries showed slight branches formed with the DLAV (Figure 20D, D`, red arrowhead). However, disruption of Dll4-Notch signalling by pharmacological inhibitor (Figure 20C, C`) or by blocking of *dll4* translation (Figure 20D, D`) resulted in milder vascular morphology defects and had no apparent effect on segmental artery formation compared with Flt1 deficient embryos (Figure 20B, B`). Thus, loss of Flt1 is associated with loss of Notch, but loss of Notch signalling did not phenocopy the vascular phenotype of *flt1* morphants.

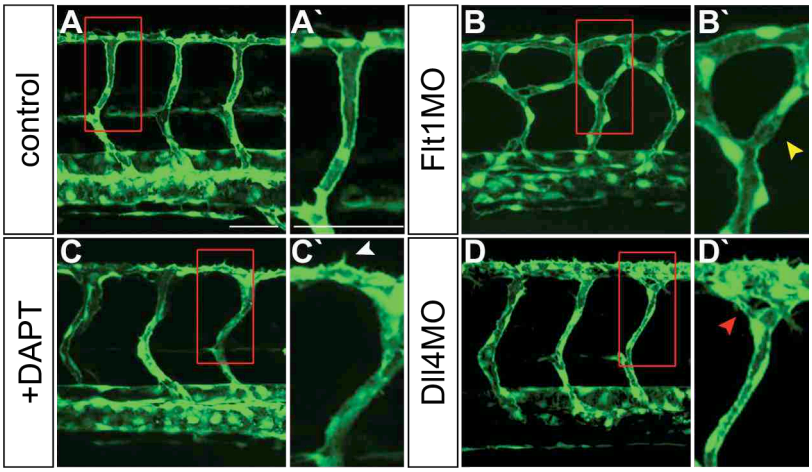

Figure 20. Loss-of-function of Notch signalling does not phenocopy the aberrant branches of *flt1* morphants. Confocal images of the zebrafish trunk of Tg(*fli1a:egfp*)^{y1} embryos at 48 hpf with high magnification of the boxed region in the respective right hand panel. (A/A`) Control morpholino injected embryo displayed the stereotyped pattern of segmental arteries, in contrast to (B/B`) the hyperbranched segmental arteries of *flt1* morphants (yellow arrowhead). (C/C`) Treatment with Notch γ-secretase inhibitor DAPT showed hyperactive ECs (white arrowhead) and (D/D`) knockdown of Dll4 aberrant branches at the dorsal roof (red arrowhead). Both treatments with DAPT or Dll4MO did not phenocopy the hyperbranched segmental arteries of *flt1* morphants. Scale bar 50 µm.

Loss of Dll4-Notch signalling was not able to phenocopy the aberrant segmental artery branches associated with Flt1 deficiency.

However, *flt1* morphants exhibited reduced Notch receptor expression and an EC behaviour related to loss of Notch. Therefore we addressed the question whether activation of Notch would ameliorate the branching defects of *flt1* morphants.

5.3.5 Notch activation restores vascular patterning defects caused by Flt1

To gain insight into the mechanism underlying the Flt1 phenotype, we analysed the impact of Notch activation in *flt1* morphants. A general downregulation of all Notch receptors and a hyperbranched phenotype with increased tip cell formation was observed in *flt1* morphants (Figure 19). Notch is required for tip cell/stalk cell differentiation and plays an essential role for EC migration and proliferation (Siekmann and Lawson, 2007). Therefore we analysed whether downregulation of Notch contributed to excessive tip cell formation associated with Flt1 deficiency. We used the double transgenic zebrafish line Tg(*uas:notch1aICD*) x Tg(*hsp70:gal4*) that enabled inducible activation of Notch1a intracellular cleaved domain (NICD) after heat shock (Lawson et al., 2001; Scheer et al., 1999). Using confocal microscopy the vasculature in the posterior region of embryos at 48 hpf was imaged (Figure 21A). Control morpholino injected embryos displayed a normal segmental artery patterning (Figure 21A, first panel), while *flt1* morphants showed excessive sprouting with laterally branched segmental arteries (Figure 21A, second panel). Induced overexpression of Notch in control embryos (+NICD) resulted in severely short segmental arteries that failed to migrate beyond the horizontal myoseptum (Figure 21A, third panel). In contrast, induced overexpression of Notch in *flt1* morphants (NICD+Flt1MO) inhibited excessive sprouting and restored the segmental artery patterning (Figure 21A, fourth panel), suggesting a partial rescue of *flt1* morphants' phenotype by Notch activation.

In order to verify our observations, we evaluated the efficiency of the partial rescue by counting the EC number per sprout, by measuring the length of the ISVs and the EC distribution within the segmental artery (Figure 21B-D). Additionally, the efficacy of the partial rescue was proven by quantification of aberrant segmental arteries in embryos at 48 hpf (Figure 21B). We found significant reduction of aberrant branches in Flt1 deficient embryos overexpressing Notch (11.8 ± 8.9%) compared to *flt1* morphants (68 ± 1.3%, Figure 21B), confirming a restoration of the segmental artery pattern by overexpression of Notch in *flt1* morphants. As expected, control morpholino injected embryos (2 ± 0.1%) or embryos with Notch overexpression (1 ± 0.1%) did not develop increased branching defects (Figure 21B). As shown in Figure 17, segmental arteries of *flt1* morphants contained more ECs per sprout compared to control embryos. We asked whether Notch activation in *flt1* morphants would affect the EC number. Indeed, Notch activation in *flt1* morphants showed a reduced EC

number (3.8 ± 0.1 EC/sprout) compared to *flt1* morphants (4.9 ± 0.3 EC/sprout) and was comparable to the amount of ECs observed in control morpholino injected embryos (3.9 ± 0.1 EC/sprout, Figure 21C). In line with previous studies, embryos overexpressing Notch revealed less ECs (2.5 ± 0.1 EC/sprout) compared to control embryos, *flt1* morphants or *flt1* morphants overexpressing Notch (Figure 21C; Siekmann and Lawson, 2007). Further validation of the partial rescue included the analysis of the segmental artery length (Figure 21D). Therefore we divided the ISVs in two groups: (1) with ISVs that ceased to migrate beyond the horizontal myoseptum and (2) that reached the DLAV. At 48 hpf, segmental arteries of control morpholino injected embryos, of *flt1* morphants and of *flt1* morphants overexpressing Notch were completely developed and reached the DLAV. In contrast, embryos overexpressing Notch exhibited reduced sprouts (Figure 21D). This indicates that Notch activation in Flt1 deficient embryos did not regulate the length of segmental arteries. Since Notch affects migration of ECs (Siekmann and Lawson, 2007), we evaluated the EC distribution within the segmental artery in embryos at 48 hpf (Figure 21E). Differentiation of ECs that (1) were located between the dorsal aorta and the horizontal myoseptum or (2) between the horizontal myoseptum and the DLAV enabled a detailed examination of their distribution. As expected, ECs in segmental arteries of control morpholino injected embryos were distributed equally. Similar observations were monitored in *flt1* morphants (Figure 21E). Related to reduced sprouts, ECs in embryos with Notch activation were mainly positioned ventrally of the horizontal myoseptum. Since the segmental artery pattern, the EC number and the segmental artery length in *flt1* morphants with Notch activation were comparable to that of control embryos, we questioned whether the migratory behaviour of ECs was affected. Interestingly, ECs in segmental arteries of *flt1* morphants overexpressing Notch were not equally distributed within the sprout. Approximately 75% of ECs were positioned in the ventral region of the sprout (Figure 21E), indicating that Notch activation decreases the EC migration in *flt1* morphants.

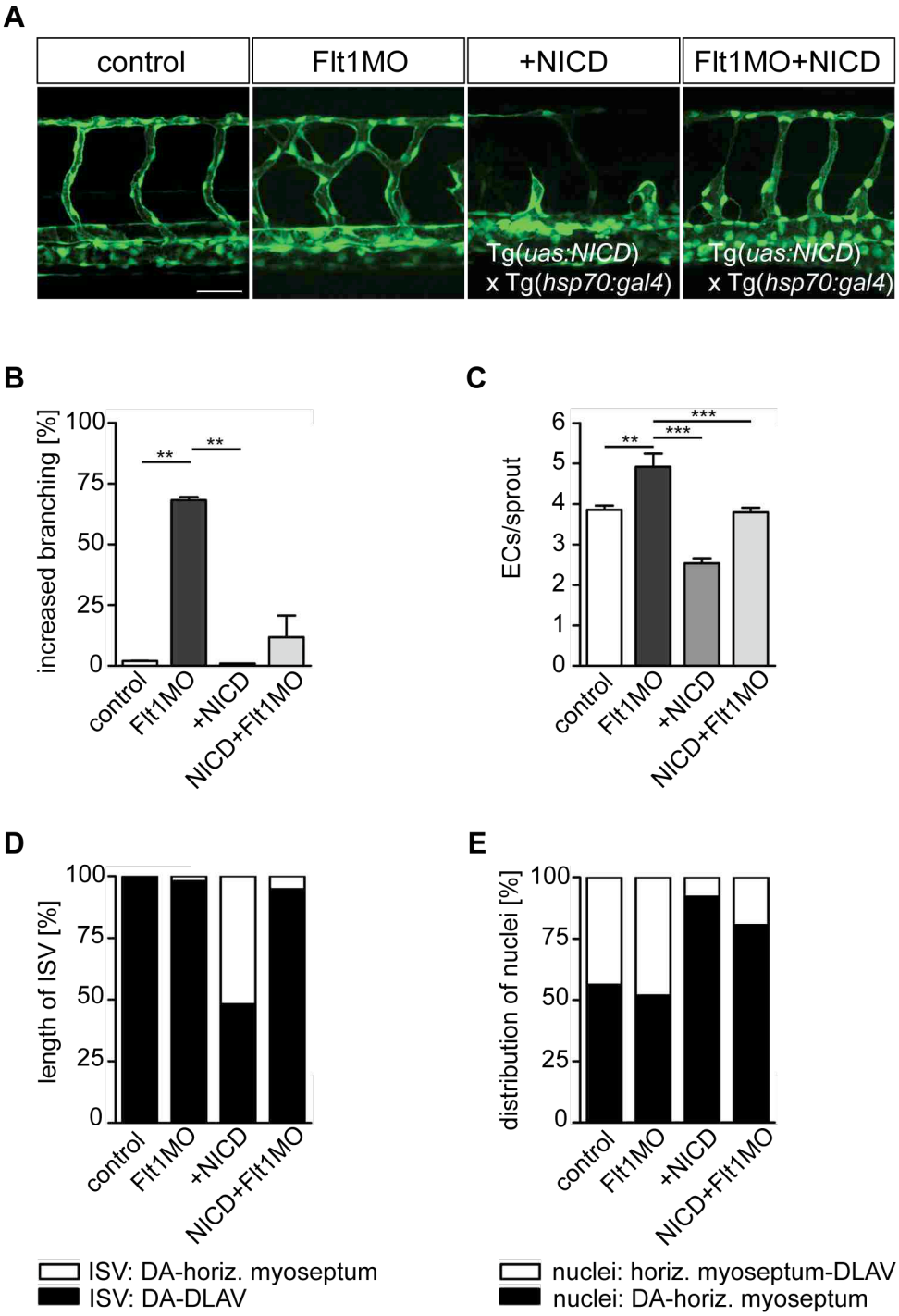

Figure 21. Activation of Notch restores aberrant branches of *flt1* morphants. (A) Confocal images displays the stereotyped ISVs in control embryos at 48 hpf (first panel). Vascular branching defects seen in *flt1* morphants (second panel) were restored by conditional overexpression of Notch intracellular cleaved domain (Flt1MO+NICD, fourth panel). Induced Notch activation led to reduced sprouts (+NICD, third panel). (B) Quantification of aberrant vessel branches revealed a significant restoration of vascular defects in *flt1* morphants with Notch activation (11.8 ± 8.9%) compared to *flt1* morphants (68.2 ± 1.3%). Control embryos (2 ± 0.1%) and embryos with Notch overexpression (1 ± 0.1%) displayed almost no branching defects (n=3; 90 embryos/group). (C) Notch activation in *flt1*

morphants resulted in a reduced EC number compared to *flt1* morphants and was comparable to control embryos (n=3; 90 embryos/group). (D) The length of ISVs was evaluated by differentiating ISVs that were grown to the horizontal myoseptum or to the DLAV at 48 hpf. Notch activation in *flt1* morphants did not affect the length of segmental arteries. Short ISVs were observed in Notch overexpressing embryos (n=3; 60 embryos/group). (E) The distribution of ECs within the sprout was examined. Nuclei between the dorsal aorta and the horizontal myoseptum or between the horizontal myoseptum and the DLAV were analysed and revealed an unequal distribution of ECs in *flt1* morphants overexpressing Notch (n=3; 60 embryos/group). Scale bar 50 µm; NICD, Notch intracellular cleaved domain; ISV, intersomitic vessel; DA, dorsal aorta; DLAV, dorsal longitudinal anastomotic vessel; Student's t-test; ***=p<0.01; *** = p< 0.001; error bars represent SEM.

In *flt1* morphants we observed a general downregulation of all Notch receptors and a hyperbranched phenotype (Figure 19). Since activation of Notch restored the branching pattern in *flt1* morphants, we concomitantly analysed the *flt1* mRNA expression in Notch overexpressing embryos. The expression of *mflt1* as well as for *sflt1* were slightly increased after conditional overexpression of NICD (Figure 22).

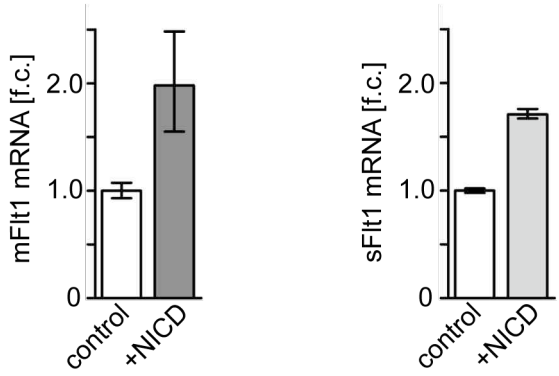

Figure 22. Activation of Notch enhances slightly *flt1* mRNA. Quantitative real-time PCR showed a slight increase of *mflt1* and *sflt1* expression after activation of NICD (n=3; 120 embryos/group). Error bars represent SEM.

Our data indicate that impaired Notch signalling was one molecular mechanism substantiating the vascular defects in *flt1* morphants. Inducible overexpression of Notch restored the aberrant branches observed in *flt1* morphants.

5.4 Macrophages do not contribute to aberrant segmental arteries in *flt1* morphants

Recent studies in mice showed that macrophages contribute to vessel anastomosis. Moreover, the VEGF-induced macrophage migration was strongly suppressed in *Flt1* tyrosine kinase-deficient homozygous mice (*Flt1*$^{TK-/-}$) (Hiratsuka et al., 1998). We hypothesised that the macrophage migration in Flt1 deficient zebrafish embryos is impaired, similar to the observations in mice. We performed WISH for the macrophage marker L-plastin in morpholino injected embryos at 30 hpf and 48 hpf (Figure 23A). L-plastin is primarily a pan-leucocyte marker, which initially detects the primary macrophages and remains expressed in differentiated, migrating macrophages (Herbomel et al., 1999). In control morpholino injected embryos *l-plastin* positive macrophages were mainly detected in the brain and the ventral trunk region at 30 hpf and 48 hpf (Figure 23A). In *flt1* morphants, we observed a general reduced *l-plastin* expression. Whereas the brain regions were colonized by macrophages in *flt1* morphants and control embryos, macrophages were less abundant in the trunk region of *flt1* morphants at 30 hpf and 48 hpf.

To evaluate the slight reduction in Flt1 deficient embryos at 48 hpf, we quantified the *l-plastin* positive macrophages in the posterior dorsal region, more precise, the region between the horizontal myoseptum and the DLAV of the trunk, where vessel anastomosis occurs. The analysis revealed a minor reduction of macrophages in the dorsal trunk region of *flt1* morphants compared to control embryos at 48 hpf (Figure 23B). Flt1 deficiency did not strongly affect the macrophage number in the trunk of zebrafish embryos.

However, recent studies supposed a major role for macrophages during vessel anastomosis. It has been hypothesised that macrophages act as bridge cells in order to arrange the correct position of two neighbouring tip cells for their further anastomosis (Fantin et al., 2010, Schmidt and Carmeliet, 2010). In zebrafish, the process of vessel anastomosis occurs when two endothelial tip cells of adjacent sprouts form the DLAV. Due to the aberrant branches of segmental arteries in *flt1* morphants, macrophages could possible contribute to the vascular phenotype. Therefore we inhibited the formation of macrophages and investigated their influence on the vasculature in Tg(*fli1a:egfp*)^{y1} embryos at 48 hpf (Figure 23C). The inhibition of macrophage formation was assessed using an antisense morpholino

oligonucleotide against *pu1* (Pu1MO), a transcription factor that is expressed in all cells of the myeloid lineage (Nerlov and Graf, 1998). We observed the stereotyped segmental artery pattern in control morpholino injected embryos, while hyperbranched segmental arteries were displayed in Flt1 deficient embryos (Figure 23C). Surprisingly, knockdown of Pu1 did not reveal any branching defects in the formation of segmental arteries or DLAV in zebrafish embryos at 48 hpf. Accordingly, co-injection of *pu1* and *flt1* morpholino showed the hyperbranched pattern as observed in Flt1 deficient embryos (Figure 23C). We propose that macrophages do not play an essential role in the vascular phenotype of *flt1* morphants.

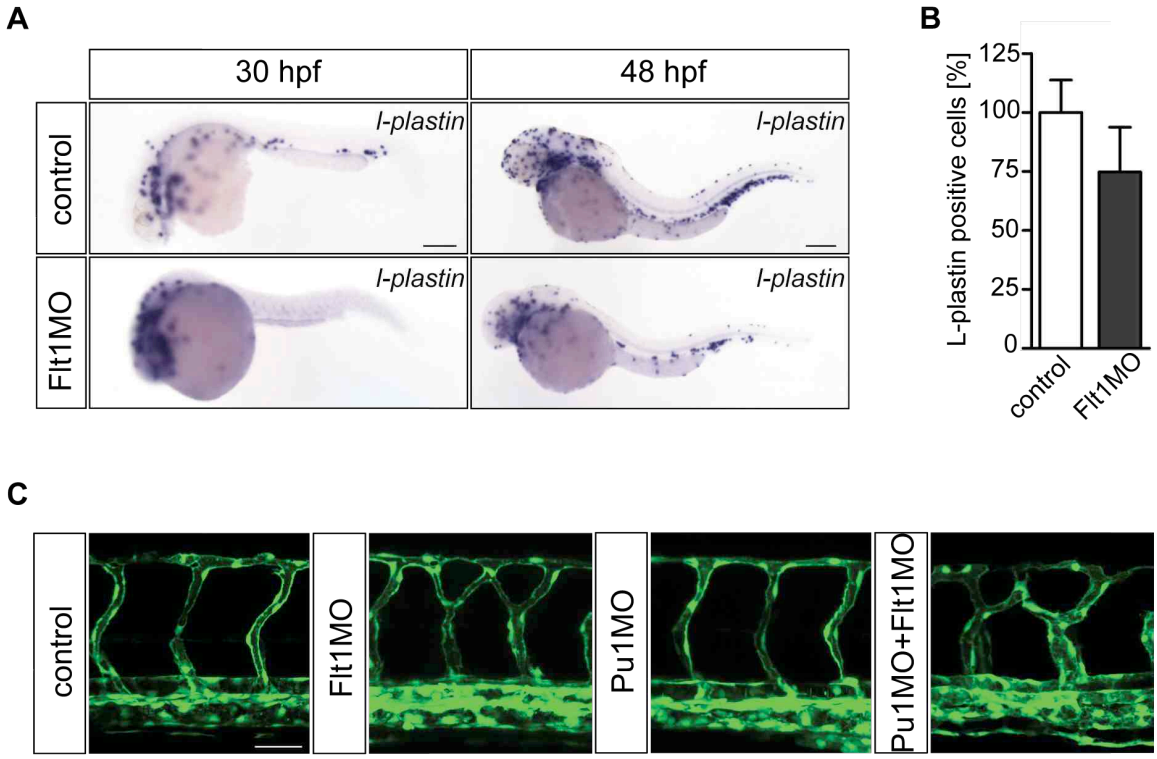

Figure 23. Macrophages do not contribute to aberrant segmental arteries in *flt1* morphants. (A) WISH for *l-plastin* demonstrated a slight reduction of *l-plastin* positive macrophages in *flt1* morphants compared to control embryos. (B) Quantification of *l-plastin* positive cells in the trunk at 48 hpf confirmed the decreased number of *l-plastin* positive macrophages in *flt1* morphants compared to control (n=3; 21 embryos/group). (C) Control embryo displayed a stereotyped pattern at 48 hpf (first panel), in contrast to the hyperbranched segmental arteries in *flt1* morphants (second panel). Injection of *pu1* morpholino did not affect segmental arteries (Pu1MO, third panel), while co-injection of *pu1* and *flt1* morpholino (Pu1MO + Flt1MO, fourth panel) displayed aberrant branches as observed in *flt1* morphants. Scale bar 50 µm; error bars represent SEM.

Based on WISH and knockdown experiments, we postulate that macrophages play a minor role during trunk vessel formation of zebrafish embryos at 48 hpf. We neither found a significant change in *l-plastin* positive cells of control and *flt1* morpholino injected embryos, nor knockdown of Pu1 displayed vascular defects.

5.5 Flt1 expression in the nervous system

5.5.1 *flt1* promoter is active in ECs and subset of neurons

Flt1 deficient embryos were characterized by hyperbranched segmental arteries. These segmental arteries formed lateral connections and developed above the horizontal myoseptum, on the level of the neural tube. A recent study demonstrated in mammals a prominent expression of Flt1 in dorsal root ganglia (Dhondt et al., 2011). We tested the hypothesis that Flt1 in zebrafish is also expressed in neurons, and thus, possibly contributes to the vascular defects of *flt1* morphants.

Therefore we analysed the Flt1 expression pattern using the double transgenic reporter line Tg(*flt1*^{BAC}*:yfp*) x Tg(*kdrl:ras-cherry*)^{s916}. Confocal microscopy of living 30 hpf embryos revealed *flt1*^{BAC}*:yfp* expression in vascular ECs, including the dorsal aorta, the segmental arteries and the posterior cardinal vein (Figure 11A). At 36 hpf, we observed a similar expression pattern in vascular ECs and an additional non-endothelial expression domain in a subpopulation of spinal cord neurons (Figure 24). The *flt1*^{BAC}*:yfp* positive spinal cord neurons were located between two adjacent segmental arteries. At 48 hpf, *flt1*^{BAC}*:yfp* was still prominently expressed in vascular ECs and abundant in a subset of spinal cord neurons (Figure 24).

The vascular specific promoter *kdrl* expressed Cherry in all ECs of embryos at 36 hpf and 48 hpf and was employed as vascular reference in order to confirm the endothelial expression of *flt1*^{BAC}*:yfp*.

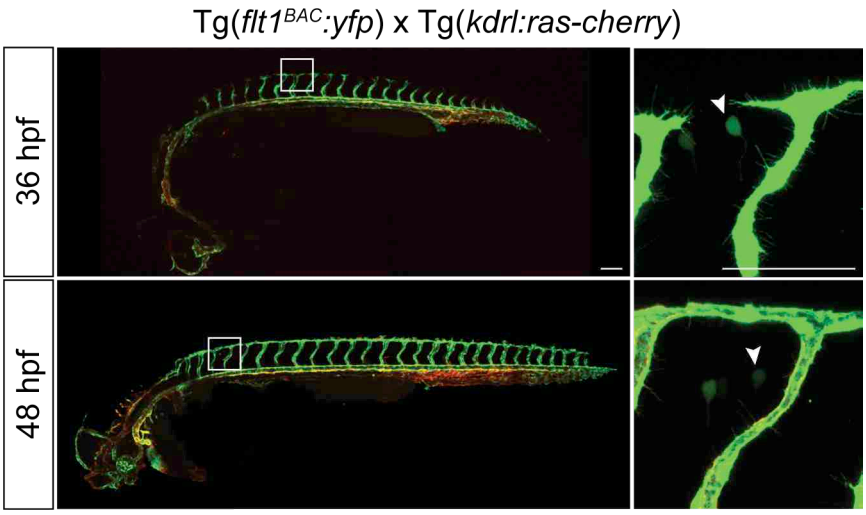

Figure 24. *flt1* promoter is active in ECs and subset of neurons. Overview of Tg(*flt1*^{BAC}*:yfp*) x Tg(*kdrl:ras-cherry*)^{s916} transgenic zebrafish embryos at 36 hpf and 48 hpf. Expression of *flt1*^{BAC}*:yfp* was detected in ECs and in a subpopulation of spinal cord neurons at 36 hpf and 48 hpf. The boxed area presented on the respective right panel highlights the *flt1*^{BAC}*:yfp* positive spinal chord neurons (arrowhead). Scale bar 100 µm.

Using Tg(*flt1*^{BAC}*:yfp*) x Tg(*kdrl:ras-cherry*)^{s916} embryos we found *flt1* promoter activity in ECs and in a subpopulation of spinal cord neurons at 36 hpf and 48 hpf.
To confirm our observations, we determined mRNA expression levels of *mflt1* and *sflt1* in isolated ECs and neurons.

5.5.2 *flt1* mRNA is expressed in ECs and neurons

During DLAV formation *flt1* promoter activity was observed in a subset of spinal cord neurons of Tg(*flt1*^{BAC}*:yfp*) x Tg(*kdrl:ras-cherry*)^{s916} embryos. To verify the unexpected *flt1* promoter activity in spinal cord neurons, we measured *flt1* mRNA expression in isolated ECs and neurons using quantitative real-time PCR.
Tg(*fli1a:egfp*)^{y1} embryos express eGFP under control of the endothelial *fli1a* promoter, and were utilized for ECs isolation (Figure 25A). Embryos of the transgenic line Tg(*huC:egfp*) express eGFP under the control of the neuronal promoter *huC* and were used for the isolation of neurons (Figure 25B). Proteolytic treatment of 30 hpf Tg(*fli1a:egfp*)^{y1} and Tg(*huC:egfp*) embryos dissociated cell populations for

subsequent FACS sorting (Figure 25). The cell populations were subdivided based on their fluorescence signal. The fluorescence intensity of isolated cell populations of Tg(*fli1a:egfp*)^{y1} embryos is illustrated in the histogram in Figure 25A and demonstrates the separation of ECs and non-ECs. In order to isolate neurons, we sorted cell populations of digested Tg(*huC:egfp*) embryos and attained separated eGFP+ and eGFP- cell populations, according to neuronal and non-neuronal cells (Figure 25B).

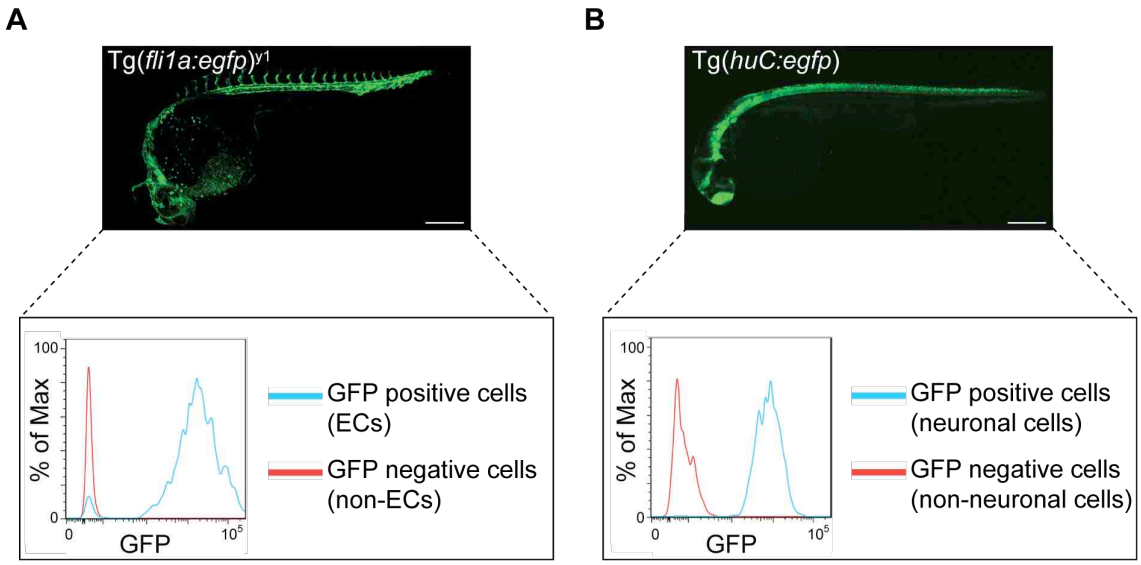

Figure 25. Isolation of ECs and neurons via FACS. (A) FACS sorting of GFP+ and GFP- cells of Tg(*fli1a:egfp*)^{y1} embryos at 30 hpf was used for isolation of ECs and non-ECs. (B) GFP+ and GFP- cells from the neuronal reporter line Tg(*huC:egfp*) were sorted by FACS. The histogram represents fluorescence intensity of separated neuronal and non-neuronal cells at 30 hpf. Scale bar 100 µm.

Since *flt1* promoter activity was observed in ECs and spinal chord neurons, we proved *flt1* mRNA expression by quantitative real-time PCR using isolated ECs and neurons as template. For quantitative real-time PCR the gene *dab2* was employed as endothelial marker. *islet2b* was used as neuronal reference, which is expressed in sensory Rohon-Beard neurons (Thisse et al., 2004; Tamme et al., 2002). Quantitative real-time PCR analysis revealed a significantly increased expression of the respective marker for the according cell population (Figure 26A) and verified the purity of the PCR template. We detected abundant *mflt1* expression in neurons compared to ECs (Figure 26B). Instead, *sflt1* were preferentially expressed in ECs

than in neurons (Figure 26B). Expression levels of both *flt1* isoforms in ECs demonstrated an elevated expression of *sflt1* compared to *mflt1* or to the endothelial marker *dab2* (Figure 26C). In neurons, we found a slightly enhanced expression of *mflt1*, but both *flt1* isoforms revealed a higher expression level than the neuronal marker *islet2b*, indicating that *mflt1* and *sflt1* are expressed in neurons (Figure 26D).

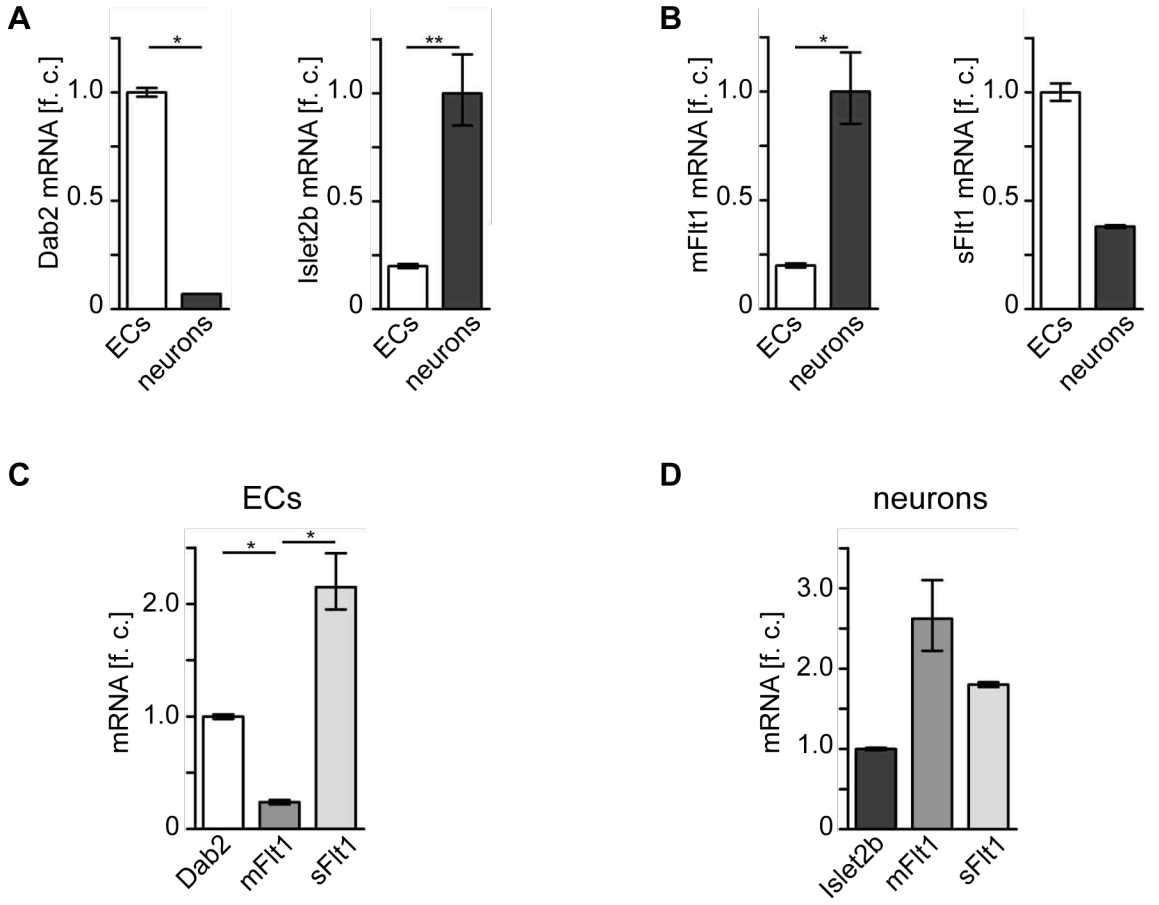

Figure 26. Expression of *mflt1* and *sflt1* mRNA in ECs and neurons. (A) Quantitative real-time PCR verified the purity of FACS isolated ECs using *dab2* as vascular marker and *islet2b* as neuronal marker (n=4; 120 embryos/group). (B) *mflt1* and *sflt1* expression in ECs and neurons were analysed via quantitative real-time PCR and revealed abundant expression of *mflt1* in neurons and prominent expression of *sflt1* in ECs (n=4; 120 embryos/group). (C) Analysis using quantitative real-time PCR showed an elevated expression level of *sflt1* compared to *mflt1* in ECs (n=4; 120 embryos/group). (D) In neurons, *mflt1* and *sflt1* expression levels were slightly increased compared to the neuronal marker *islet2b* and confirmed the expression of both *flt1* isoforms in neurons (n=4; 120 embryos/group). * = p< 0.05; ** = p<0.01.

Taken together, the quantified expression levels of *mflt1* and *sflt1* mRNA in isolated ECs and neurons verified the *flt1* promoter activity in Tg(*flt1*^{BAC}*:yfp*) x Tg(*kdrl:ras-cherry*)^{s916} embryos.
Subsequently, expression of mFlt1 and sFlt1 protein were examined by whole mount immunofluorescence staining.

5.5.3 Flt1 antibody confirms staining in vessels and neural tube

Due to the fact that *flt1* promoter activity and *flt1* mRNA expression were detected in ECs and in a subset of neurons in zebrafish embryos (Figure 24, Figure 26), we examined Flt1 protein location and distribution using whole mount immunofluorescence staining.
A custom made, affinity-purified antibody that detects both zebrafish Flt1 isoforms was generated (Figure 10, Figure 27). This antibody was also used for Western blot analysis (Figure 12C). Immunofluorescence staining using the Flt1 antibody in embryos of the neuronal reporter line Tg(*huC:egfp*) at 30 hpf showed a strong Flt1 expression throughout the neural tube (Figure 27A). Detailed view of the neural tube demonstrates eGFP+ neurons co-localized with Flt1 antibody. Two different focal planes illustrate Flt1 staining adjacent to mechanosensory Rohon-Beard neurons (Figure 27A`, arrowheads), spinal cord neurons, and motor neurons (Figure 27A``, arrowheads).
Surprisingly, the Flt1 antibody did not label vessels using the standard immunofluorescence technique. Therefore, we employed Tyramide Signal Amplification (TSA) to increase the Flt1 antibody signal and to attempt visualization of vascular Flt1. Indeed, we found Flt1 staining in vessels and throughout the somites in embryos of the vascular reporter line Tg(*fli1a:egfp*)^{y1} at 30 hpf (Figure 27B). High magnification of segmental arteries displays co-localization of Flt1 antibody and eGFP+ ECs at two different focal planes (Figure 27B`, B``, arrowheads).

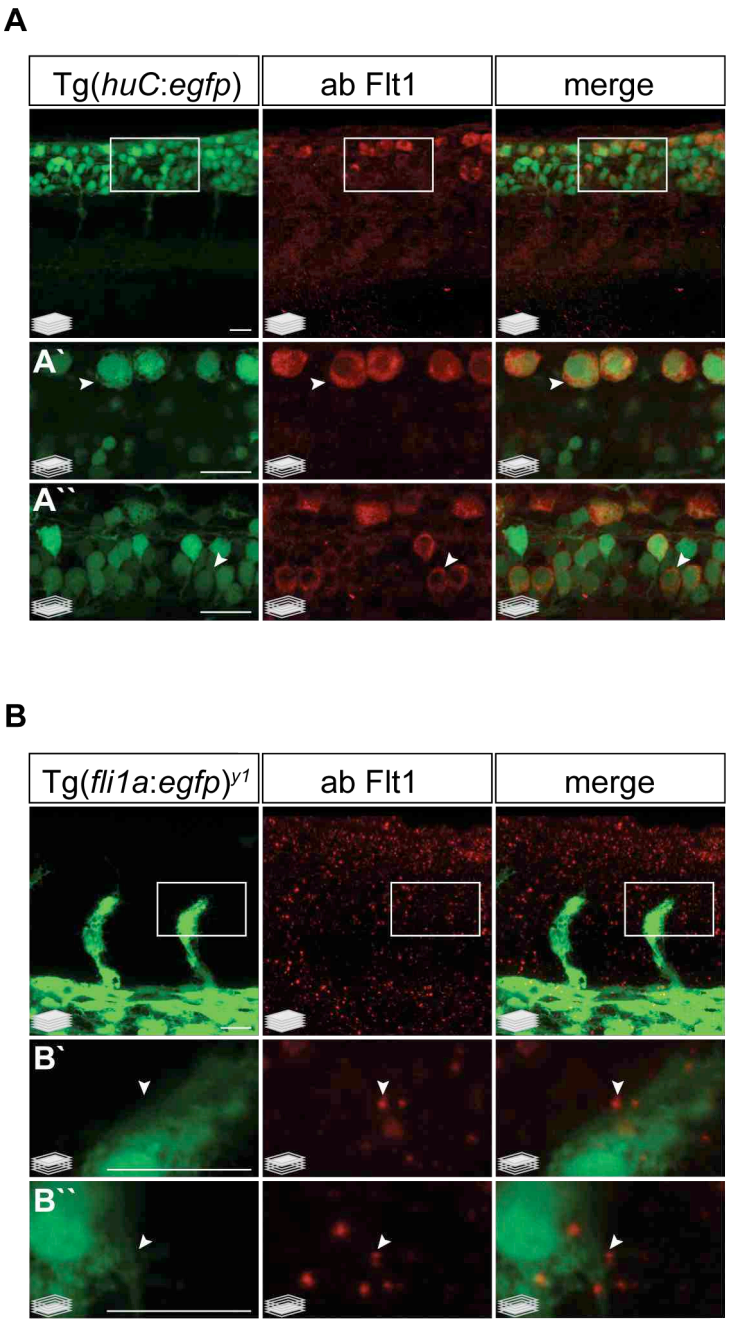

Figure 27. Immunofluorescence staining of Flt1. (A) Flt1 immunostaining of Tg(*huC:egfp*) neuronal reporter embryos showed Flt1 labelling throughout the neural tube at 30 hpf. The boxed areas at the top row are presented at higher magnification and in two different focal planes in A` and A``. Note, Flt1 antibody staining around eGFP+ neurons (arrowheads). (B) Flt1 protein expression in the vasculature and in the somites was detected by Flt1 antibody staining with tyramide signal amplification in Tg(*fli1a:egfp*)^{y1} embryos at 30 hpf. Detailed view and two different focal planes of the boxed region are shown in B` and B``. Arrowheads indicate Flt1 staining on segmental arteries. Scale bar 20 µm.

Using two different immunofluorescence techniques we found Flt1 positive labelled neurons, ECs and somites in whole mount zebrafish embryos at 30 hpf.
In order to specify Flt1 positive neurons, additional immunofluorescence stainings were applied.

5.5.4 Flt1 antibody recognizes subpopulations of neurons

Flt1 expression and distribution were detected in vessels and throughout the neural tube of zebrafish embryos using transgenic zebrafish lines (Figure 24), quantitative real-time PCR (Figure 26) and immunofluorescence staining (Figure 27). To obtain further information about the specification of Flt1 positive neurons, we performed additional immunofluorescence experiments.
In general, the zebrafish spinal cord includes all functional modalities, namely interneurons, sensory neurons and motor neurons (Lewis and Eisen, 2003). Interneurons are found throughout the spinal cord and connect afferent and efferent neurons, whereas sensory neurons convert external to internal stimuli (Bernhardt et al., 1990; Myers et al., 1985). Among the first sensory neurons develop mechanosensitive Rohon-Beard neurons that are located at the dorsal spinal cord (Rossi et al., 2009). Motor neurons are positioned at the level of the horizontal myoseptum and serve mainly for the innervations of muscle segments (Westerfield et al. 1986).
To specify whether interneurons are Flt1 positive, we performed immunofluorescence staining of Tg(*flt1*^{BAC}*:yfp*) embryos. This transgenic zebrafish line expresses *flt1*^{BAC}*:yfp* in vessels and in a subset of spinal cord neurons. These spinal cord neurons are classified as interneurons on the basis of soma size, position and axonal pattern. Confocal microscopy images in Figure 28A demonstrates the upper part of Tg(*flt1*^{BAC}*:yfp*) embryos showing YFP expression in segmental arteries, DLAV and interneurons. Immunofluorescence staining in Tg(*flt1*^{BAC}*:yfp*) embryos at 72 hpf using the custom made Flt1 antibody revealed co-localization of Flt1 labelling and *flt1*^{BAC}*:yfp* positive interneurons (Figure 28A, arrowhead), suggesting that at least a subset of interneurons is Flt1 positive in 72 hpf embryos.
Specification of possible Flt1 expression or distribution in/nearby sensory neurons and motor neurons was attained by immunofluorescence staining with the antibody

zn-12. Zn-12 is a neuron-specific surface antigen (Trevarrow et al., 1990), which recognizes motor neurons and mechanosensory Rohon-Beard neurons in zebrafish embryos. For immunofluorescence staining we used the Tg(*fli1a:egfp*)^{y1} transgenic line and imaged the posterior region including dorsal aorta and segmental arteries. Indeed, co-immunofluorescence staining using Flt1 antibody and zn-12 in 30 hpf Tg(*fli1a:egfp*)^{y1} embryos displayed a clear co-localization of their expression within Rohon-Beard neurons (Figure 28B, arrowhead) and motor neurons (Figure 28B, arrow). Interestingly, Rohon-Beard neurons in zebrafish are functional homologue to mammalian dorsal root ganglia, in which prominent Flt1 expression has been demonstrated recently (Dhondt et al., 2011), indicating a conserved role for Flt1 in Rohon-Beard neurons throughout vertebrates.

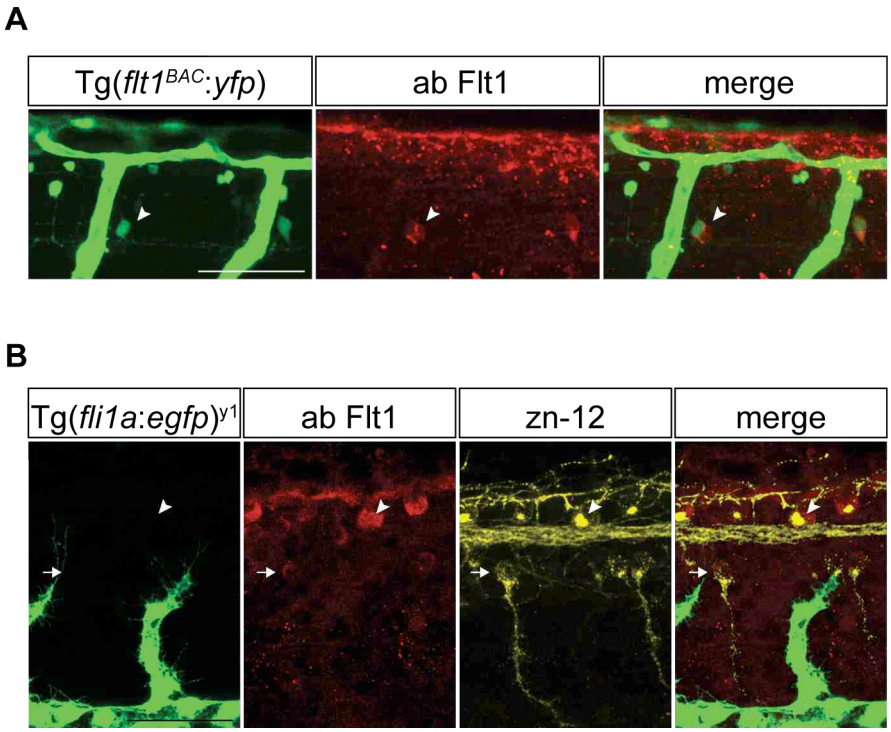

Figure 28. Flt1 antibody recognizes subpopulations of neurons. (A) Spinal cord neurons in Tg(*flt1*^{BAC}*:yfp*) embryos at 3 d were labelled by Flt1 antibody (arrowhead). (B) Co-staining with Flt1 and zn-12 antibody in 30 hpf Tg(*fli1a:egfp*)^{y1} embryos identified mechanosensory Rohon Beard neurons (arrowhead) and motor neurons (arrow) as Flt1 positive. Scale bar 50 µm.

Neuronal specification revealed co-localization of Flt1 protein in/nearby subpopulations of interneurons, Rohon-Beard neurons and motor neurons in zebrafish embryos.

To gain insight into neuronal Flt1 functions and its putative impact on vascular branching morphogenesis, Flt1 loss-of-function experiments were performed using double transgenic zebrafish lines expressing fluorescent proteins under control of endothelial and neuronal promoters.

5.6 Reduced Flt1 levels influence vascular and neuronal development

To address the question whether Flt1 influences neuronal development, Flt1 loss-of-function experiments were performed using endothelial and neuronal specific double transgenic zebrafish lines. Due to Flt1 expression in vessels and neurons, possibly a reduction of Flt1 affects not only the vascular branching morphogenesis (Figure 12A) but also the neuronal development.

In order to facilitate observations of vascular and neuronal dysfunctions in zebrafish, we mated two different transgenic zebrafish lines: (1) Tg(*flt1*^{BAC}*:yfp*) x Tg(*kdrl:ras-cherry*)^{s916} embryos and (2) Tg(*huC:egfp*) x Tg(*kdrl:ras-cherry*)^{s916} embryos, which include the neuronal promoter *huC* and the vascular promoter *kdrl* leading to eGFP expression in neurons and Cherry expression in vessels. For monitoring vascular and neuronal defects caused by Flt1 knockdown, we imaged the posterior region of the zebrafish trunk at 48 hpf.

As expected, morpholino mediated knockdown of Flt1 in both double transgenic zebrafish lines resulted in hyperbranched segmental arteries compared to the stereotyped pattern of ISVs of control embryos (Figure 29A). Interestingly, neuronal YFP expression in Tg(*flt1*^{BAC}*:yfp*) x Tg(*kdrl:ras-cherry*)^{s916} embryos was barely detectable in *flt1* morphants. Accordingly, neuronal eGFP expression in Tg(*huC:egfp*) x Tg(*kdrl:ras-cherry*)^{s916} embryos was decreased (Figure 29A, bottom panel).

The observed neuronal defect in Flt1 deficient embryos was evaluated by quantification of YFP positive interneurons of Tg(*flt1*^{BAC}*:yfp*) x Tg(*kdrl:ras-cherry*)^{s916} embryos at 48 hpf. Statistical analysis revealed a significantly reduced number of

interneurons in *flt1* morphants compared to control embryos (Figure 29B), suggesting a neuroprotective function for Flt1.

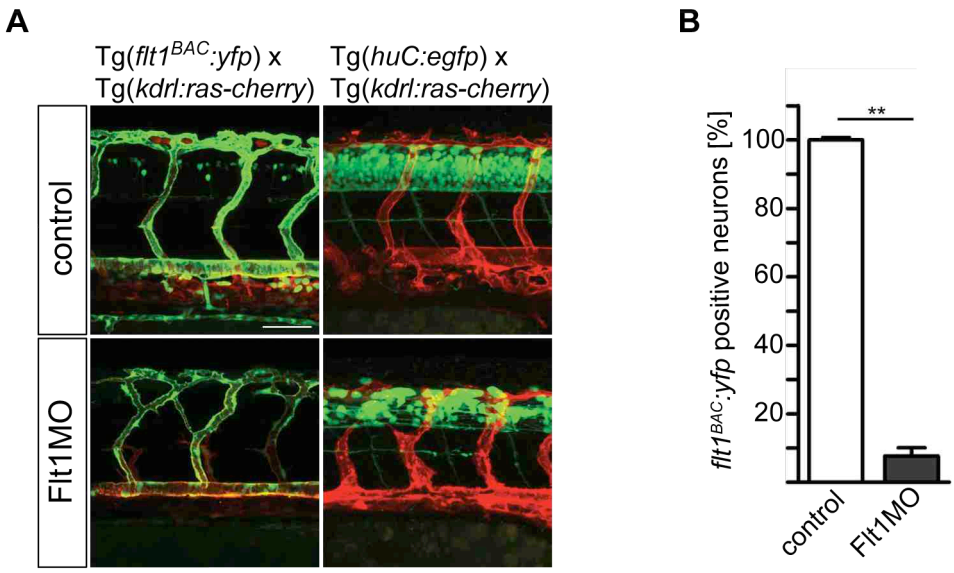

Figure 29. Reduced Flt1 levels disturb vascular and neuronal development. (A) Injection of *flt1* morpholino in Tg(*flt1*^{BAC}*:yfp*) x Tg(*kdrl:ras-cherry*)^{s916} embryos caused hyperbranching of segmental vessels and reduced *flt1:yfp*^{BAC} positive interneurons at 48 hpf compared to control embryo (left panel). Accordingly, knockdown of Flt1 using the transgenic zebrafish line Tg(*huC:egfp*) x Tg(*kdrl:ras-cherry*)^{s916} displayed aberrant segmental arteries and a decreased neuronal cell number (right panel), confirming that Flt1 affects vascular and neuronal development. (B) Quantification of *flt1:yfp*^{BAC} positive interneurons in Tg(*flt1*^{BAC}*:yfp*) x Tg(*kdrl:ras-cherry*)^{s916} embryos demonstrated a significant reduction of neurons in *flt1* morphants at 48 hpf (n=3; 60 embryos/group). Scale bar 50 µm; Student's t-test; ** = p<0.01; error bars represent SEM.

Taken together, knockdown of Flt1 caused hyperbranched segmental arteries at the level of the neural tube and reduced the neuronal cell number.

Therefore we addressed the question whether neurons contribute to the distribution of vascular specific sFlt1, and hence, possibly influence the segmental artery outgrowth.

5.7 sFlt1 distribution throughout the nervous system

5.7.1 sFlt1 originating from vessels distributes throughout the neural tube

To obtain further information about a possible contribution of the nervous system during vascular development, vascular specific overexpression of sFlt1 and its distribution were examined. Flt1 deficient embryos exhibited aberrant segmental arteries at the neural tube level and ubiquitous overexpression of mFlt1 or sFlt1 resulted in reduced segmental arteries that did not pass the neural tube. Thus, a fluorescent-labelled overexpression of vascular specific sFlt1 would potentially visualize a distribution of sFlt1 throughout the neural tube.

In order to enable vascular specific overexpression of sFlt1, Tol2 based expression constructs were used for Gateway cloning. The Tol2 cis elements facilitate the integration into the zebrafish genome and permit the expression of native or fusion proteins in zebrafish embryos (Villefranc et al., 2007). Our generated expression constructs contained the vascular specific promoter *fli1a* or *kdrl*, driving cherry or eGFP N-terminally fused sFlt1 expression and were named pTol*fliep:cherry-sflt1* and pminiTol*kdrl:egfp-sflt1*. The corresponding control constructs lacked *sflt1* coding sequence and were labelled with pTol*fliep:cherry* and pminiTol*kdrl:egfp*. Tg(*fli1a:egfp*)^{y1} and Tg(*kdrl:ras-cherry*)^{s916} embryos were injected with these constructs. Injection of the control construct pTol*fliep:cherry* in Tg(*fli1a:egfp*)^{y1} embryos revealed expected expression of Cherry in vessels that co-localized with vascular eGFP expression in dorsal aorta and segmental arteries (Figure 30A, upper panel). Injection of pTol*fliep:cherry-sflt1* resulted in Cherry-sFlt1 expression in vessels (arrow) and throughout the neural tube (Figure 30A, lower panel, arrowhead). To verify our observations, we repeated this experiment using a different vascular promoter, *kdrl*. Injection of the control construct pminiTol*kdrl:egfp* in Tg(*kdrl:ras-cherry*)^{s916} embryos demonstrated eGFP expression in segmental arteries, overlapping with the Cherry signal of the vascular specific transgenic zebrafish embryo (Figure 30B, upper panel). According to sFlt1 overexpression driven by *fli1a* promoter, injection of pminiTol*kdrl:egfp-sflt1* showed eGFP-sFlt1 expression in segmental arteries (arrow) and throughout the neural tube (Figure 30B, lower panel, arrowhead). This suggests that vascular specific overexpression of sFlt1 was produced in vessels and unexpectedly, distributed throughout the neural tube in zebrafish embryos at 30 hpf.

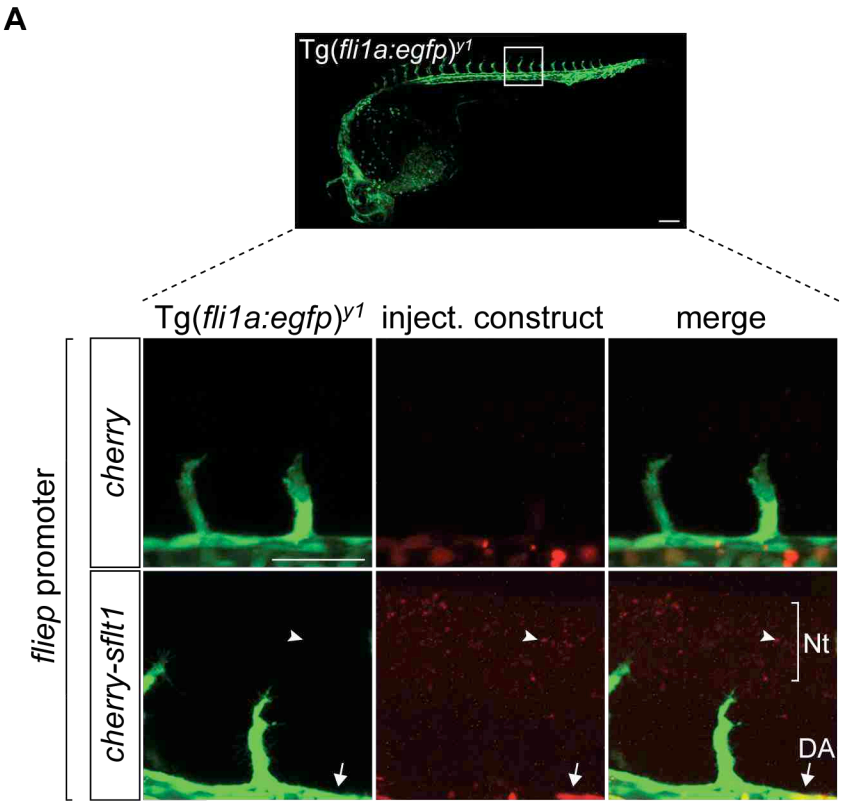
A
Tg(fli1a:egfp)y1
Tg(fli1a:egfp)y1
inject. construct
merge
fliep promoter
cherry
cherry-sflt1
Nt
DA
B
Tg(kdrl:ras-cherry)
Tg(kdrl:cherry)
inject. construct
merge
kdrl promoter
egfp
egfp-sflt1
Nt
Se

Figure 30. Distribution of vascular specific sFlt1 throughout the neural tube. (A) Vascular specific overexpression of sFlt1 by injection of pTol*fliep:cherry-sflt1* into Tg(*fli1a:egfp*)^{y1} embryos resulted in emergence of Cherry-sFlt1 protein in the vasculature (arrow) and throughout the neural tube at 30 hpf (arrowhead, bottom row). Injection of the control plasmid pTol*fliep:cherry* displayed the vascular specific *fliep* promoter expression in vessels (top row). (B) Overexpression of sFlt1 under the control of the vascular specific promoter *kdrl* (pminiTol*kdrl:egfp-sflt1*) showed eGFP-sFlt1 expression in segmental arteries (arrow) and neural tube (arrowhead) of Tg(*kdrl:ras-cherry*)^{s916} embryos at 30 hpf (bottom row), confirming sFlt1 distribution throughout the neural tube. The corresponding control pminiTol*kdrl:egfp* showed vascular eGFP expression similar to the expression of the vascular specific promoter *kdrl* (top row). Scale bar 50 µm; Nt, neural tube; Ao, dorsal aorta.

To corroborate the monitored distribution of sFlt1 into the neural tube, an additional study using the neuronal reporter line Tg(*huC:egfp*) was performed. High magnification images of the neural tube enabled a precise view of eGFP+ neurons (Figure 31). Injection of the control construct pTol*fliep:cherry* displayed no Cherry expression in the neural tube (Figure 31, first panel). In contrast, injection of pTol*fliep:cherry-sflt1* showed expression of the fusion protein Cherry-sFlt1 throughout the neural tube, which localized adjacent to eGFP+ neurons (Figure 31, second panel, arrowhead). Although the *fliep* promoter may be active in neural crest-derived neural tissue (Brown et al., 2000), we clearly observed Cherry-sFlt1 co-localizing with spinal cord neurons located in the ventral part of the neural tube. These neurons did not derive from neural crest. In order to exclude side effects of the *fliep* promoter, we cloned the coding sequence of *cherry-sflt1* downstream of the vascular *kdrl* promoter. Injection of the control construct pminiTol*kdrl:cherry* revealed no Cherry expression in the neural tube (Figure 31, third panel). In contrast, overexpression of Cherry-sFlt1 under the control of the *kdrl* promoter was noted throughout the neural tube (Figure 31, fourth panel). In addition, a diffuse Cherry-sFlt1 signal was observed between neurons.

These findings indicates that vascular specific overexpression of Cherry-sFlt1 results in clear distribution throughout the neural tube. We detected Cherry-sFlt1 adjacent to neurons.

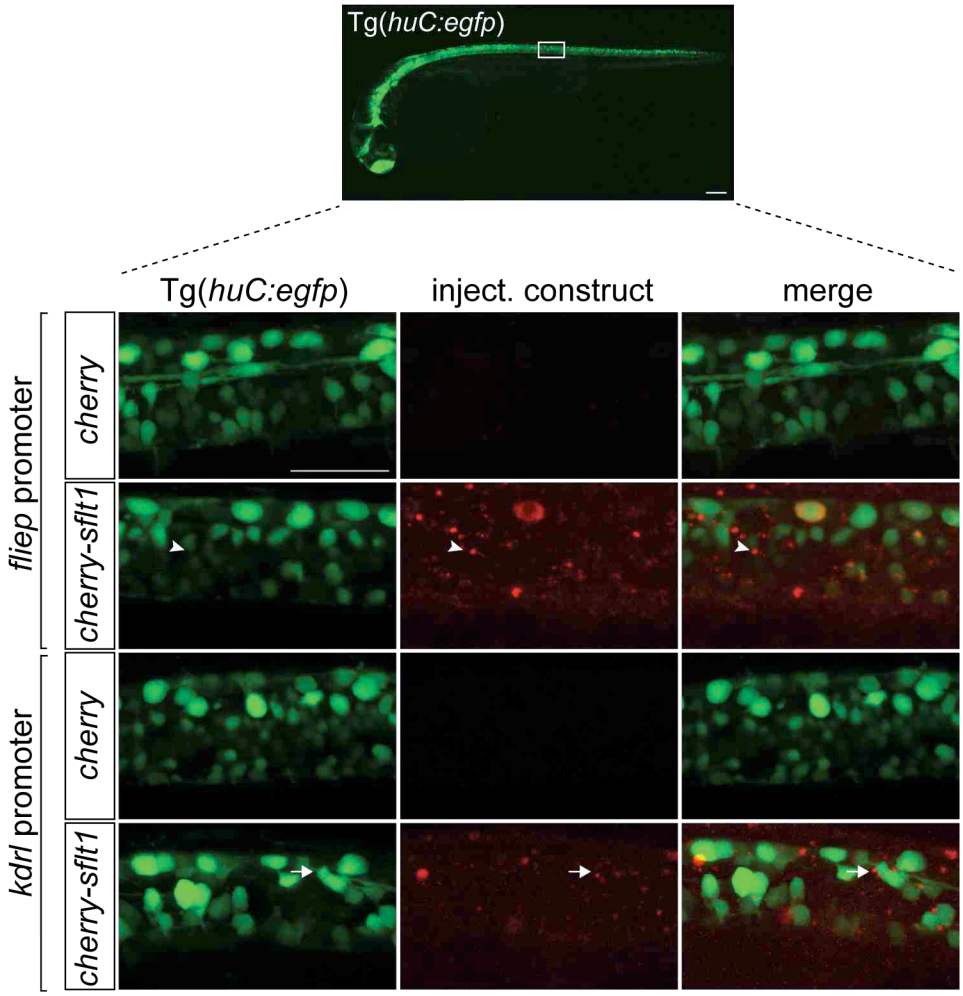

Figure 31. sFlt1 is located adjacent to neurons. High magnification of the neural tube of Tg(*huC:egfp*) embryos at 30 hpf. Overexpression of sFlt1 under the vascular specific promoter *fliep* demonstrated Cherry-sFlt1 expression next to eGFP+ neurons (arrowhead, second panel). Injection of the negative control pTol*fli:cherry* revealed no Cherry expression (first panel). A second approach using the vascular specific promoter *kdrl* obtained similar results. Injection of pminiTol*kdrl:cherry-sflt1* into the neuronal reporter line Tg(*huC:egfp*) displayed Cherry-sFlt1 distribution adjacent to neurons (arrow, fourth panel). Cherry expression of the equivalent negative control, *p*miniTol*kdrl:cherry*, was absent in the neural tube (third panel). Scale bar 50 µm.

Overexpression of Cherry-sFlt1 in a vascular specific manner led to subsequent distribution of Cherry-sFlt1 throughout the neural tube.

Thereupon arose the question, whether the distributional pattern of sFlt1 may influence segmental artery outgrowth.

5.7.2 sFlt1 distribution throughout the nervous system correlates with the outgrowth of segmental arteries *in vivo*

It has been shown that local availability and diffusion of VEGF-A is critical for vascular development (Stalmans et al., 2002). Accordingly, binding of VEGF-A to sFlt1 has been demonstrated to be essential for preventing corneal vascularisation in mice (Ambati et al., 2006), implicating the significance of sFlt1 function and distribution. Due to detection of secreted sFlt1 throughout the neural tube, we asked whether the distributional pattern of sFlt1 affects the outgrowth of segmental arteries in zebrafish embryos.

Therefore we performed confocal time-lapse imaging of Tg(*kdrl:ras-cherry*)^{s916} embryos injected with constructs that allow expression of eGFP or eGFP-sFlt1 under control of the *kdrl* promoter. Segmental artery formation in zebrafish embryos was recorded during the time period 32 hpf and 40 hpf. The corresponding snapshots are depicted in Figure 32. As control we used Tg(*kdrl:ras-cherry*)^{s916} embryos that were injected with the construct pminiTol*kdrl:egfp* for vascular specific eGFP expression. As expected, the eGFP signal co-localized mainly with the Cherry expression of the vascular transgenic zebrafish line (Figure 32, upper panel). Moreover, eGFP expression remained during segmental artery formation and did not affect the segmental artery outgrowth (Figure 32, upper panel). In contrast, injection of pminiTol*kdrl:egfp-sflt1* for vascular specific overexpression of eGFP-sFlt1 seemed to disturb the segmental artery formation. At 32 hpf the Cherry positive segmental arteries had reached the horizontal myoseptum (Figure 32, bottom panel, first row). Filopodia protrusions (arrow) sensed the environment in order to dictate the further outgrowth of the sprout. eGFP-sFlt1 expression was monitored at low abundance in the neural tube at 32 hpf (Figure 32, bottom panel, arrowhead). In a time dependent manner the eGFP-sFlt1 expression in the neural tube seemed to accumulate near segmental arteries (arrowheads). In parallel the filopodia extensions of the segmental arteries regressed (Figure 32, bottom panel, arrow).

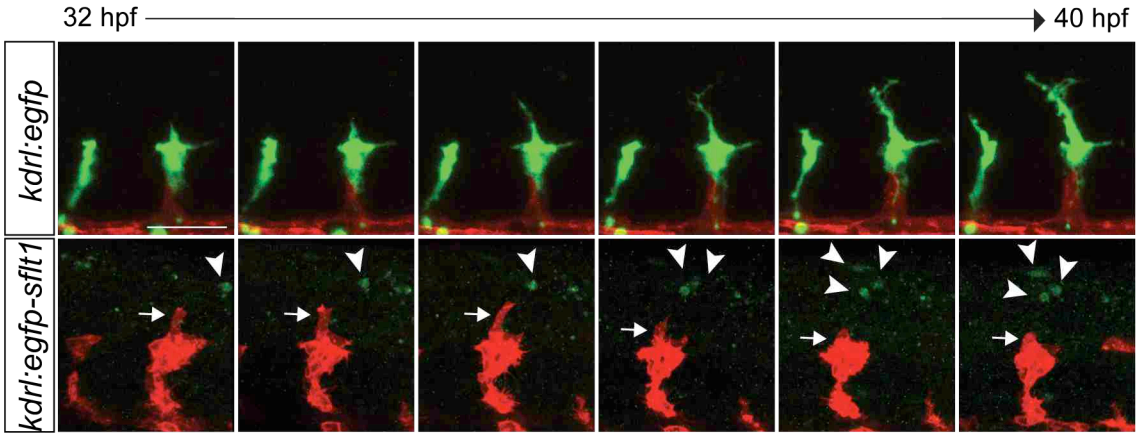

Figure 32. sFlt1 distribution throughout the neural tube correlates with the outgrowth of segmental arteries *in vivo.* Snapshots of recorded segmental artery formation of Tg(*kdrl:ras-cherry*)^{s916} embryos between 32 hpf and 40 hfp. Injection of the control construct pminiTol*kdrl:egfp* displayed eGFP expression in growing ISVs, but had no effect on its outgrowth (top panel). Vascular specific overexpression of sFlt1 by injection of pminiTol*kdrl:egfp-sflt1* resulted in eGFP-sFlt1 expression throughout the neural tube (bottom panel). In time response, neuronal eGFP-sFlt1 expression (arrowhead) accumulated nearby the growing segmental artery and, in parallel, sprout extensions (arrow) regressed, pointing towards a possible influence of sFlt1 that is located within the neural tube on segmental artery outgrowth.

Using confocal time-lapse imaging we observed a time dependent accumulation of eGFP-sFlt1 in the neural tube. Concomitantly, the segmental artery formation ceased to grow beyond the horizontal myoseptum. Taken together, these results indicate a potential communication of the developing vascular and the nervous system mediated by sFlt1.

6 Discussion

Being subject to numerous investigations, the VEGF receptors and their signalling pathway, crucial for vascular development have been identified (Fong et al., 1995; Kendall et al., 1993; Terman et al., 1992). It is known that VEGF receptors are essential for vessel growth and therefore acting as main players in medical conditions like stroke, heart infarct, and tumour growth (Carmeliet, 2005; Birnbaum, 1995). However, the precise role of VEGF receptor-1, termed Flt1, in mediating sprouting angiogenesis is undetermined.

The aim of this study was the examination of Flt1's function during sprouting angiogenesis *in vivo*. Due to embryonic lethality of *Flt1* homozygous knockout mice and the artificial settings for blood vessel development in *in vitro* experiments, we decided to investigate Flt1's function using transgenic zebrafish embryos (Geudens and Gerhardt, 2011; Fong et al., 1995). Based on the identification of two Flt1 isoforms in zebrafish, this model system allowed us to study the impact of Flt1 at physiological and molecular level. Using loss- and gain-of-function approaches, we elucidated Flt1 as negative regulator of tip cell formation during sprouting angiogenesis. *In vivo* time-lapse imaging of developing segmental arteries recorded an increased tip cell formation in Flt1 deficient embryos, a characteristic also observed in loss of Notch embryos (Siekmann and Lawson, 2007). Conditional overexpression of Notch restored the vascular defects of Flt1 deficient embryos. Interestingly, *flt1* promoter activity was observed not only in vessels, but also in the developing nervous system. Knockdown of Flt1 resulted in vascular hyperbranching and a reduced neuronal cell number. The importance of Flt1 at the neurovascular interface is furthermore highlighted by the observation that overexpression of sFlt1 under control of a vascular promoter resulted in distribution of sFlt1 protein in the nervous system. This suggests that sFlt1 maybe home to these domains, or alternatively is scavenged and transported there.

Taken together, Flt1 acts in a Notch dependent manner as negative regulator of tip cell formation. In addition, Flt1 affects the developing nervous system, pointing towards a potential cross-talk between the vascular and nervous system mediated by Flt1. The impact of these findings is discussed in more detail in the following chapters.

6.1 Flt1 expression in zebrafish embryos

So far Flt1 has been well described in mammals. In order to enable the investigation of Flt1's function in our study, we initially analysed the Flt1 encoding region in the zebrafish genome and its expression at the mRNA and protein levels in zebrafish embryos. In addition, we identified the temporal and spatial allocation of Flt1 during development.

6.1.1 Flt1 isoforms are widely conserved throughout vertebrates

Over the past years the *flt1* gene has been examined in different species. In humans it has been shown that *flt1* encodes one membrane-binding and four soluble variants of Flt1 (Heydarian et al., 2009; Thomas et al., 2007; Kendall et al., 1993). Similar findings were discovered in mice. Mice express one membrane-binding and three soluble Flt1 isoforms (Shibuya, 2001; Kendall and Thomas, 1993; Breier et al., 1992; de Vries et al., 1992). Additionally, Yamaguchi and colleagues described in 2002 the expression of mFlt1 and sFlt1 in chicken (Yamaguchi et al., 2002). Until now only one membrane-bound isoform of Flt1 has been annotated in zebrafish (Rottbauer et al., 2005). Based on the Flt1 variability in mammals and chicken, we suspected the existence of another, as yet unidentified Flt1 isoform in zebrafish. In order to enable the investigation of Flt1's function in zebrafish embryos, we determined its expression using RACE-PCR. For the first time, we identified a soluble isoform of Flt1 in zebrafish, termed sFlt1 (Figure 9). Homologous to other vertebrate species, the *flt1* gene in zebrafish encodes one membrane-bound and at least one soluble isoform of Flt1. Due to the location of the binding sites of GSP1/2 in exon 8 and 9 (Figure 9A), the detection of additional sFlt1 variants would be unlikely. We showed normal transcription of Flt1 isoforms and translation into protein by expression analysis on mRNA and protein levels (Figure 10, Figure 26, Figure 27). Comparison of the amino acid sequences of zebrafish and human sFlt1 revealed on average a 46% amino acid identity. Accordingly, zebrafish mFlt1 showed that 51% of amino acids were identical to the human mFlt1 (Rottbauer et al., 2005). Based on the known structure of mFlt1 in zebrafish, alignment of the amino acid sequences of both Flt1 isoforms enabled a structural organization of sFlt1. sFlt1 in zebrafish consists of four Ig-like domains that are necessary for high-affinity VEGF binding (Figure 10C,

ENSDARP00000106307). Similar to zebrafish sFlt1, one of the soluble Flt1 isoforms in human is also composed of four Ig-like domains (ENSP00000442630).
Taken together, these findings strongly suggest that mFlt1 and sFlt1 are widely conserved throughout vertebrates. In zebrafish as well as in other vertebrates one membrane-bound and at least one soluble isoform of Flt1 exist.

6.1.2 mFlt1 and sFlt1 expression is temporally regulated

The diversity of Flt1 isoforms throughout vertebrates results from posttranscriptional regulation, as they share a common transcription start site for each species. Posttranscriptional regulation may occur at the level of mRNA splicing, polyadenylation, cleavage, or degradation, or a combination of these processes (Lackner and Bahler, 2008). Our results show that the primary transcript of zebrafish *flt1* is alternatively spliced after exon 10 to produce two different transcripts (Figure 8C). The transcript *mflt1* is processed by exon skipping, whereas *sflt1* is formed by retention of exon 11a that carries a polyadenylation signal. In humans the posttranscriptional regulation of *flt1* is mainly mediated through intronic polyadenylation or alternative splicing (Thomas et al., 2010). Intronic poly(A) signals together with adjacent cis-elements reciprocally regulate polyadenylation and splicing of *flt1* in HUVECs (Thomas et al., 2007). For this reason, a detailed examination of intron 10 and 11 of zebrafish *flt1* would likely detect signals important for its posttranscriptional regulation.
Little is known about factors that influence upstream polyadenylation or splicing of *flt1*. On the basis of the suggested interaction of the splicing factor U2AF65 and Jumonji domain-containing protein 6 (Jmjd6), Boeckel and colleagues emphasized Jmjd6 as modulator of *flt1* splicing in HUVECs (Boeckel et al., 2011; Webby et al., 2009). They postulated Jmjd6 as sensor for oxygen levels that in response coordinates *flt1* splicing. Reduced oxygen levels, called hypoxia, have been implicated to induce preeclampsia, which is characterized by a disproportionate increase of sFlt1 (Thomas et al., 2010; Wu et al. 2010; Nagamatsu et al., 2004). Additionally, a differential stimulation of Flt1 isoforms was also described after treatment with dimethyloxalglycine (DMOG). DMOG inhibits the prolyl hydroxylase domain-containing protein, which finally leads to an upregulation of VEGF, as

observed during hypoxia (Thomas et al., 2010; Jaakkola et al., 2001). In our study we analysed the expression levels of *sflt1* and *mflt1* in zebrafish embryos using quantitative real-time PCR. During vascular development we found an increased expression of *sflt1* compared to *mflt1* (Figure 10A). These findings are similar to the observations after DMOG treatment or under hypoxia, and are in accordance with the potential function of Jmjd6. Further studies are needed to address the role of Jmjd6 for the splicing of *flt1* in zebrafish as well as possible other factors that are or are not influenced by VEGF. Recently, it has been shown that PlexinD1 can stimulate sFlt1 expression in zebrafish, but how this event is connected to Flt1's posttranscriptional regulation is still unclear (Zygmunt et al., 2011).

In addition to the regulation of Flt1 at posttranscriptional level, sFlt1 can also be regulated at the translational level. Using leukemic cancer cells Rahimi and colleagues demonstrated the proteolytic cleavage of mFlt1's ectodomain from the cell surface (Rahimi et al., 2009). The removal of the ectodomain requires metalloproteases, whereas γ-secretase activity is necessary for the release of the cytoplasmic domain. The ectodomain shedding contributes to the formation of sFlt1 in leukemic cancer cells. To what extend Flt1 isoforms in zebrafish are regulated at translational level is so far unknown, but has to be investigated by future experiments.

In summary, we showed a temporally differential expression of *mflt1* and *sflt1* on mRNA level during vascular development. Since mFlt1 and sFlt1 share the same transcription start site, selective overexpression is likely caused by posttranscriptional and translational regulation. Recent studies identified factors important for the regulation of Flt1 isoforms, at the same time the precise mechanisms are missing.

6.1.3 Flt1 isoforms are expressed by ECs

Angiogenesis requires a spatial coordination of angiogenic factors in a tissue-specific manner. The expression pattern of the angiogenic factors mFlt1 and sFlt1 in zebrafish was determined using Tg(*flt1*^{BAC}*:yfp*) x Tg(*kdrl:ras-cherry*)^{s916} embryos (Figure 11, Figure 24), real-time PCR (Figure 26) and immunofluorescence staining (Figure 27). Our findings showed a similar vascular expression pattern of Flt1 like in other vertebrates. Flt1 is expressed by vascular ECs of humans, by the embryonic

and adult endothelium of mice and by ECs of chicken (Yamaguchi et al., 2002; Ferrara and Davis-Smyth, 1997; Fong et al., 1996). Moreover, an active *flt1* gene has been described during EC differentiation in developing embryonic bodies derived from mouse ES cells (Quinn et al., 2000).

A detailed examination of the Flt1 expression in transgenic zebrafish embryos enabled the detection of *flt1* promoter activity in tip and stalk cells of developing segmental arteries (Figure 11A). Although the quantity of Flt1 in the tip and the stalk cell could not be determined, the expression itself in both cell types was debated before. Other studies supposed the expression of Flt1 in the stalk cell and therefore postulated a role for Flt1 in maintaining the identity of the stalk cell (Phng and Gerhardt, 2009). Based on our observations, we hypothesised a function for Flt1 in regulating the tip cell/stalk cell differentiation. This aspect is discussed in detail in chapter 6.3.

Using Tg(*flt1*^{BAC}*:yfp*) x Tg(*kdrl:ras-cherry*)^{s916} embryos as readout, *flt1* was mainly expressed in the arterial, but to a lesser extend in the venous domain. WISH showed arterial expression of *mflt1* and *sflt1* at mRNA level. Surprisingly, expression in the venous domain was restricted to *mflt1* (Figure 11B). Bussman and colleagues demonstrated *mflt1* expression in the dorsal aorta of zebrafish embryos, but did not explore any venous expression (Bussmann et al., 2007). This discrepancy is probably due to differences in the experimental procedure, like for instance, the staining time and the length of the WISH-probe. As we observed a diverged expression pattern of *flt1* isoforms, we postulate that mFlt1 and sFlt1 are not only temporally but also highly spatially regulated during angiogenesis in zebrafish embryos. Similar selective expression or independent regulation of mFlt1 and sFlt1 can be found in the mouse cornea, in spongiotrophoblasts of the murine placenta and in the human endometrium (Ambati et al., 2006; He et al., 1999; Krussel et al., 1999). Understanding how Flt1 isoforms are regulated in different tissues remains a challenging question. It has been shown that tandem poly(A) signal sequences can led to tissue-specific regulation of mRNA in the human transcriptome (Wang et al., 2008). Therefore Wang and colleagues hypothesised that tissue-specific expression of human sFlt1 is due to differences in the utilization of the proximal and distal intronic *sflt1* poly(A) signal sequences (Wang et al., 2008). Another explanation is based on the usage of tissue-specific expression of micro-RNAs (Lagos-Quintana et

al., 2002). Mirco-RNA-200 has been shown to negatively regulate the *flt1* 3´-UTR in metastasis-prone lung adenocarcinoma (Roybal et al., 2011).

The selective expression of *mflt1* in the venous domain implicates a specific role for the signalling domain herein. Supposing a putative function for mFlt1 during venous plexus formation, it has been described that inhibition of its ligand VEGF disrupts vessel segregation of the venous plexus in the zebrafish trunk (Herbert et al., 2009). The venous plexus of zebrafish embryos is partially formed by intussusceptive and by sprouting angiogenesis (Herbert et al., 2009). Intussusception can also be found in the chorioallantoic membrane of developing chicken (Patan et al., 1996). Recent studies emphasized a correlation of VEGF levels and an expansion of intussusception in chicken (Hlushchuk et al., 2011; Baum et al., 2010). Due to the demonstrated function of VEGF during intussusceptive angiogenesis by others, a putative involvement of its receptor mFlt1 would be likely.

We conclude that Flt1 is expressed by ECs of zebrafish embryos. Moreover, Flt1 isoforms are not only temporally, but also spatially regulated during vascular development.

6.1.4 Flt1 isoforms are expressed by neurons

In addition to Flt1 positive ECs, we observed Flt1 expression in a subset of neurons during vascular development. In Tg(*flt1*^{BAC}*:yfp*) x Tg(*kdrl:ras-cherry*)^{s916} embryos *flt1* promoter activity was visible in spinal cord neurons at 36 hpf (Figure 24). *flt1* mRNA could be detected in isolated neurons from zebrafish embryos at 30 hpf by real-time PCR (Figure 26C). Confirming these results, immunofluorescence staining using a custom made Flt1 antibody, revealed Flt1 labelling in interneurons, Rohon-Beard neurons and motor neurons (Figure 28). Additionally, a diffuse Flt1 staining was present throughout the neural tube of zebrafish embryos at 30 hpf (Figure 27A). The discrepancy of the detected *flt1* mRNA and Flt1 protein expression at 30 hpf and the absence of *flt1* promoter activity at this time-point (Figure 11A) is probably due to the generation of the transgenic zebrafish line Tg(*flt1*^{BAC}*:yfp*) x Tg(*kdrl:ras-cherry*)^{s916}. Most likely an enhancer element is missing in the BAC clone, as enhancers have a long-distance influence on promoters (Ong and Corces, 2011). Although we could not detect *flt1* promoter activity of Tg(*flt1*^{BAC}*:yfp*) x Tg(*kdrl:ras-cherry*)^{s916} embryos at

30 hpf, we conclude that Flt1 is expressed in a subset of neurons during vascular development. Supporting our results, Flt1 expression was also detected in embryonic and adult motor neurons of the mouse spinal cord (Poesen et al., 2008). Furthermore, Flt1 is prominently expressed in dorsal root ganglia of the mouse (Dhondt et al., 2011). Dorsal root ganglia in mammals are the functional homolog to sensory Rohon-Beard neurons in zebrafish, in which Flt1 staining was detected during our study (Figure 28B). Since not all neurons showed *flt1* promoter activity, some neuronal population might actually bind or sequester sFlt1 protein produced by other cells. Postulating this idea, we overexpressed sFlt1 under control of a vascular specific promoter and found sFlt1 protein throughout the neural tube (Figure 30, Figure 31). One possibility would be that sFlt1 gets to neurons by diffusion, as sFlt1 is secreted by ECs and neurons. Another option would be an uptake and transport of sFlt1 by developing axons, since some axons develop in close proximity to segmental arteries. The latter has been shown in rates, where VEGF and its receptor VEGFR-2 are retrogradely and anterogradely transported in axons (Storkebaum et al., 2005). Understanding how sFlt1 can distribute to the neural tube will be one goal of future studies.

Not only the transport but also the potential binding of sFlt1 in neurons is still unclear. sFlt1 lacks the membrane-spanning domain, although it can form non-signalling heterodimers with the membrane-binding receptor VEGFR-2, which is also expressed by neurons (Almodovar et al., 2011; Bellon et al., 2010; Gomes and Rockwell, 2008; Sondell et al., 2000; Kendall et al., 1996). Furthermore, the accessory receptor heparin sulphate proteoglycan is expressed at the extracellular matrix and could bind sFlt1, as its fourth Ig-like domain consists of a heparin-binding site (Wu et al., 2010; Park and Lee, 1999). Presupposing a spatial regulation of putative sFlt1 binding partners, a controlled binding of sFlt1 would modify the pre-existing gradient of VEGF that guides vascular outgrowth. Alternatively, diffusion of sFlt1 could modulate the VEGF gradient, whereby the generation of sFlt1 by ECs and neurons has to be precisely regulated.

In summary, Flt1 is present in a subset of neurons in zebrafish embryos. The suggested major role of Flt1 during vascular and neuronal development requires a temporally and spatially highly regulated expression.

6.2 Flt1 is relevant for vascular and neuronal development

Over the past years, VEGF has been highlighted as angiogenic growth factor, while recent studies emphasized a role for VEGF during neurogenesis (Ruiz de Almodovar et al., 2011; Ogunshola et al., 2002; Carmeliet et al., 1996; Fong et al., 1995; Shalaby et al., 1995). To unravel the function of Flt1 during vascular and neuronal development, we performed a combination of experiments using transgenic zebrafish embryos.

6.2.1 Flt1 is required for branching morphogenesis

To gain insight into a potential impact of Flt1 during vascular development, we performed Flt1 loss- and gain-of-function experiments in Tg(*fli1a:egfp*)^{y1} embryos. Flt1 deficient embryos displayed normal ISV formation during the initial sprouting, while aberrant connections between segmental arteries were formed at later time-points (Figure 12). Those connections carried blood flow and developed into functional vessels.

Studies in the past tried to elucidate Flt1's function using several mouse models. The homozygous *Flt1* deficient mice were embryonic lethal due to an increased and disorganized blood vessel network (Fong et al., 1995). These aberrant blood vessels were caused by an increased commitment of mesodermal progenitors to become hemangioblasts (Fong et al., 1999). In our study knockdown of Flt1 also revealed aberrant vessel branches, but did not result in embryonic lethality. We speculate that the survival of *flt1* morphants is due to an incomplete loss of Flt1 that has been demonstrated by Western blot analysis (Figure 12C). We emphasize that the quantity of Flt1 and consequently the local availability of VEGF are highly critical for vascular patterning. Moreover, the small size of zebrafish embryos facilitates their survival since nutrient distribution does not require a normally formed vasculature. In order to reveal the significance of specific Flt1 domains, mice that lack the tyrosine kinase domain of *Flt1* (*Flt1*$^{TK-/-}$) were generated. These mice developed a normal vasculature, suggesting that the extracellular VEGF-binding domain of Flt1 is essential for vascular development (Hiratsuka et al, 1998). Recently, mice that lack the tyrosine kinase and the transmembrane-spanning domain of *Flt1* (*Flt1*$^{TM-/-TK-/-}$) were examined (Hiratsuka et al., 2005). High endogenous VEGFR-2 levels led to

embryonic lethality in *Flt1*$^{TM-/-TK-/-}$ mice due to an uncompleted circulatory system. The VEGFR-2 activity was reduced in these mice, as VEGF was not recruited efficiently to the plasma membrane. This indicates that mFlt1 is required for the recruitment of VEGF to stimulate VEGFR-2. The *Flt1*$^{TM-/-TK-/-}$ mice with low endogenous VEGFR-2 activity survived, which indicates that sFlt1 is able to full fill some functions encoded by mFlt1. We highlighted in our study the requirement of sFlt1 during vascular development, too. The aberrant branches of *flt1* morphants were largely rescued by either *mflt1* or *sflt1* mRNA (Figure 14). We speculate that the extracellular domain is essential for segmental artery formation and that sFlt1 can adopt some functions of mFlt1. The rescue after *mflt1* injection implicates therefore the contribution of mFlt1 to form sFlt1, as it is discussed in chapter 6.1.2. Consistent with our observations, it has been shown that Flt1 deletion in ES cells derived from *Flt1* deficient mice led to dysmorphogenesis of vessels and sFlt1 was sufficient to rescue the vessel branching (Kappas et al., 2008). Other studies of Flt1 have yielded contrasting results, as for instance Kearney and colleagues demonstrated a less branched vascular network *in vitro* due to deletion of Flt1 (Kearny et al., 2004). Nevertheless, the significance of sFlt1 during blood vessel formation has been highlighted in several independent studies. One model proposes a spatially regulated secretion of sFlt1 in areas adjacent to emerging blood vessels and therefore generating a VEGF-rich path for the developing sprout (Chappell et al., 2009). In our experiments we did neither detect an accumulated Flt1 staining in these areas (Figure 27), nor did Flt1 knockdown affect the initial sprouting (Figure 12A). The developing segmental arteries of *flt1* morphants reached in a stereotyped pattern the horizontal myoseptum. If sFlt1 would be secreted as supposed by Chappell, knockdown of Flt1 would affect the sprout at its origin. We observed aberrant vessel branches above the horizontal myoseptum at the level of the neural tube. We speculate that Flt1's function during vascular development is more complex than believed at the present. An interdependence of vessels and neurons might be rather obvious since Flt1 expression has been detected in ECs and neurons. This issue is discussed precisely in chapter 6.5.

However, it is known that vascular patterning requires a highly regulated local availability of VEGF (Stalmans et al., 2002). In our work overexpression with either *mflt1* or *sflt1* mRNA resulted in short segmental arteries with short filopodia protrusions (Figure 13). This was consistent with a recent study that showed

overexpression of sFlt1 as suppressor of segmental artery sprouting (Zygmunt et al., 2011). Consistent with our rescue experiments, these findings emphasize the requirement of the extracellular VEGF-binding domain that is present in mFlt1 and sFlt1. Consequently, sFlt1 appears to be sufficient for reducing VEGF levels by scavenging VEGF and additionally, by forming inactive heterodimers with VEGFR-2. Although the heterodimers sFlt1/VEGFR-2 can bind VEGF, the general function of VEGFR-2 as activator for EC migration and proliferation are disturbed (Cross et al., 2003; Gerber et al., 1998). Similar findings have been demonstrated by *in vitro* studies. Overexpression of sFlt1 inhibited the VEGF-induced migration of ECs by generating a non-signalling complex with VEGF and VEGFR-2 (Roeckl et al. 1998; Kendall et al., 1993). Studying the effect of reduced VEGF concentration, Ruhrberg and colleagues demonstrated impaired extensions of EC filopodia (Ruhrberg et al., 2002). Concomitantly, disrupted ISV sprouting in *Vegf* deficient embryos emphasizes the relevance of a VEGF gradient for segmental artery formation (Herbert et al., 2009). In our study segmental arteries overexpressing *mflt1* and *sflt1* mRNA stopped to grow beyond the horizontal myoseptum and did not pass through the neural tube (Figure 13). As mFlt1 or sFlt1 are expressed by neurons (Figure 26) and distributed throughout the neural tube (Figure 27), we assume a putative contribution of the nervous system in modulating the VEGF gradient (see chapter 6.5). Based on these results, we conclude that the ability of sFlt1 to sequester VEGF and to generate inactive heterodimers with VEGFR-2 is essential for proper vessel branching. In addition, a putative contribution of Flt1 expressing neurons during segmental artery formation cannot be excluded.

Understanding the role of mFlt1 during ISV formation remains a challenging question. Over the past years, it has been reported that mFlt1 has no direct proliferative, migratory or cytoskeletal effect due to its weak tyrosine kinase activity (Seetharam et al., 1995; Park et al., 1994; Waltenberger et al., 1994). Supporting these findings, the blood vasculature of *Flt1*$^{TK-/-}$ mice was not affected. Intriguingly, half of *Flt1*$^{TK-/-TM-/-}$ mice were embryonic lethal (Fong et al, 1995; Hiratsuka et al, 2005) due to an uncompleted circulatory system. A reduced VEGFR-2 activity has been found and Hiratsuka postulated that mFlt1, especially its transmembrane-spanning domain, is required for the recruitment of VEGF to VEGFR-2. In general, Flt1 has a greater binding affinity for VEGF than VEGFR-2, but this ability can be reversed by heparin (Robinson and Stringer, 2001; Ito and Claesson-Welsh, 1999; Terman et al., 1994).

A potential impact of heparin for the mFlt1 dependent recruitment of VEGF to VEGFR-2 will be investigated by future studies. Another work demonstrated ectodomain shedding of mFlt1 followed by release of its cytoplasmic domain (Rahimi et al., 2009). The molecular interactions and responses generated by the cytoplasmic and the transmembrane-spanning domain in the EC remain to be determined.

Some evidences have been indicated that mFlt1 regulates angiogenesis by transmitting intracellular signals. Kanno and colleagues demonstrated *in vitro* mFlt1 mediated activation of p38 MAP kinase in response to VEGF (Kanno et al., 2000). The mFlt1 mediated signal modulates the actin reorganization and thereby the EC migration. The remodelling of the actin cytoskeleton and its connection with the extracellular matrix by integrins are essential for EC migration (Senger et al., 1996). It has been demonstrated that mFlt1 activates an RB4A-dependent pathway that leads to transport of integrins to the plasma membrane (Jones et al., 2009). Furthermore, a recent study postulated that Flt1 regulates the EC migration via the protein tyrosine kinase-7-(PTK7)-dependent pathway (Lee et al., 2011). Under normal conditions phosphorylation of Flt1 activates the downstream signals Akt and focal adhesion kinase, while inhibition of PTK7 results in downregulation of these signals (Lee et al., 2011; Nishi et al., 2008; Maru et al., 2001). The EC migration is essential for the lumen formation of segmental arteries. Integrins and the Notch signalling pathway have been identified as potential players for lumen formation (Tung et al., 2012; Sainson et al., 2005). In our study we observed aberrant, but functional segmental arteries that had formed lumen (Figure 12A). Moreover, we showed a general decrease of the Notch signalling pathway in *flt1* morphants (Figure 19), implicating an influence of Flt1 on Notch and consequently on the lumen formation. Other studies emphasized an Flt1 mediated EC proliferation. It has been reported that Flt1 activates phospholipase C and phosphoinositol 3 phosphate kinase, which subsequently influences cell proliferation and the angiogenic response to VEGF (Banerjee et al., 2008; Ito and Claesson-Welsh, 2001). Several studies described mFlt1 as critical factor for EC migration, lumen formation and proliferation. Moreover, the signalling properties of mFlt1 seem to depend on physiological conditions, since several disease models of *Flt1*$^{TK-/-}$ mice exhibit impaired inflammation and angiogenesis (Kami et al., 2008; Murakami et al., 2006; Hiratsuka et al., 2002; Hiratsuka et al., 2001).

Taken together, Flt1 is required for proper branching morphogenesis during vascular development. By regulating the VEGF gradient, sFlt1 might be more efficient than mFlt1 at shaping vessel branching. mFlt1 appears to be involved in several other aspects, as for instance lumen formation.

6.2.2 Flt1 may act as neuroprotective receptor

Although VEGF was originally discovered as angiogenic factor, some studies revealed an impact of VEGF on neurons. It has been shown *in vivo* that VEGF exerts direct neuroprotective effects on motor neurons and dorsal root ganglia (Storkebaum et al., 2005; Sondell et al., 2000). Additionally, VEGF enhances the survival of neurons in a dose-dependent manner and regulates the release of proteins important for the neuronal viability *in vitro* (Sanchez et al., 2010). A reduced expression of VEGF is associated with neurodegenerative diseases (Ruiz de Almodovar et al., 2009; Poesen et al., 2008; Storkebaum et al., 2005; Azzouz et al., 2004). Given evidence that VEGF affects vessels and neurons and that its receptor Flt1 is expressed in both tissues (Chapter 6.1), we performed knockdown experiments using double transgenic zebrafish embryos. Knockdown of Flt1 showed simultaneously aberrant segmental artery branches and a significant reduction of the neuronal cell number (Figure 29), suggesting that Flt1 is required for branching morphogenesis and the maintenance or growth of neurons. Recent *in vitro* and *in vivo* studies demonstrated that the Flt1 specific ligand VEGF-B protects primary motor neurons against degeneration (Poesen et al., 2008). Intriguingly, these effects depend on the tyrosine kinase activity of Flt1, suggesting that Flt1 is a neuroprotective receptor (Poesen et al., 2008). Consistent with these results, we observed a reduced neuronal cell number in *flt1* morphants. In addition, *mflt1* mRNA is prominently expressed in neurons of control embryos (Figure 26C), hypothesising mFlt1 and its signalling pathway as a relevant factor for neuronal development. Under pathologic conditions *Flt1* deficient mice displayed degenerated sensory neurons (Dhondt et al., 2011). Accordingly, delivery of VEGF-B improves the disease outcome by protecting the degeneration of motor and sensory neurons (Dhondt et al., 2011; Poesen et al., 2008). VEGF-B exerts its function through Flt1 and activates its signalling cascade directing the neuroprotective effects (Poesen et al., 2008).

Although knockdown of Flt1 predicts increased VEGF-A and VEGF-B levels, we speculate that the loss of neurons in our setting is not mainly caused by enhanced Flt1 ligands, but by reduced mFlt1 expression and signalling. Supporting this hypothesis, it has been shown that VEGF-A exerts its neuroprotective effect primarily through VEGFR-2, whereas VEGF-B acts via mFlt1 and its tyrosine kinase (Dhondt et al., 2011; Ruiz de Almodovar et al., 2011). An indirect function of sFlt1 cannot be excluded, as sFlt1 scavenges VEGF and regulates thereby the signalling ability of VEGFR-2.

In addition to VEGF, the Notch signalling pathway has been determined as another critical mechanism for neuronal development. The neuronal cell diversity and cell fate decisions are regulated by cell-cell interactions of Notch receptors and its ligands (Louvi and Artavanis-Tsakonas, 2006; Yoon and Gaiano, 2005). We observed a general reduction of Notch receptors (*notch1a*, *notch1b* and *notch3*) and Jagged ligands (*jag1a* and *jag2*) throughout the neural tube of *flt1* morphants (Figure 19). Additionally, Flt1 deficient zebrafish embryos revealed a reduced neuronal cell number (Figure 29). We speculate that Flt1 affects the Notch signalling pathway in neurons and consequently the neuronal cell diversity and cell fate. Earlier studies showed that reduced Notch activity caused by pharmacological inhibitor or by genetic ablation resulted in increased formation of primary motor neurons and a deficit of interneurons, confirming Notch as regulator for cell diversity (Batista et al., 2008; Shin et al., 2007). Moreover, Notch activation has been found to promote proliferation, as Notch defected *mind bomb* (*mib*) mutants exhibited fewer cells than wild-type zebrafish embryos (Aguirre et al., 2010; Androutsellis-Theotokis et al., 2006; Itoh et al., 2003). Thus, Notch signalling maintains cells in proliferative state and serves to expand neuronal cell numbers. Since *flt1* morphants showed reduced Notch signalling throughout the neural tube, an impact of Flt1 on Notch signalling would potentially affect the proliferation of neurons and consequently the neuronal cell number as seen in *flt1* morphants. We speculate that Flt1 regulates the neuronal survival via VEGF-B induced signalling and modulates the proliferation of neurons by modulating the Notch signalling pathway. Flt1 might act as neuroprotective receptor.

Overall, we found aberrant branches and a reduced neuronal cell number in *flt1* morphants, thus suggesting that Flt1's activity exerts dual effects on ECs and neurons. The ability of sFlt1 to sequester VEGF and the signalling capacities of mFlt1

in neurons are important for proper vessel branching and neuronal survival. Concomitantly, ECs and neurons provide critical input for their own development.

6.3 Regulation of tip cell formation by Flt1

The formation of blood vessels requires a tight coordination of ECs displaying distinct phenotypes within the sprout. Endothelial heterogeneity is controlled by the Dll4-Notch signalling pathway. We analysed the function of Flt1 on cellular and molecular level during segmental artery formation.

6.3.1 Flt1 negatively coordinates the tip cell formation

In our study the blood vessel network of Flt1 deficient embryos displayed aberrant segmental artery branches (Figure 12). To determine the underlying mechanism, we performed *in vivo* time-lapse imaging and recorded the segmental artery outgrowth of control and Flt1 deficient embryos. In control embryos, we noticed a precise order of three migrating ECs, including one tip cell and one stalk cell, which moved dorsally to form the DLAV (Figure 16A). In contrast, in *flt1* morphants we observed segmental ECs proliferating at the horizontal myoseptum that gave rise to two leading ECs displaying tip cell characteristics (Figure 16A). Such increased tip cell differentiation has been described in Dll4-Notch loss-of-function models (Hellstrom et al., 2007; Lobov et al., 2007; Siekmann and Lawson, 2007; Suchting et al., 2007). Using mouse retina, inhibition of Notch by γ-secretase inhibitor resulted in increased vascular density and tip cell marker expression, suggesting that inhibition of Notch revealed more tip cells (Hellstrom et al., 2007). Supporting this finding, Notch signalling defective zebrafish mutants like *deadly-seven* (*des*) or *mib* showed ectopic numbers of filopodia on segmental arteries, a feature normally observed in tip cells (Therapontos and Vargesson, 2010; Lawson et al., 2001). Loss of Notch signalling was additionally revealed by morpholino-mediated knockdown of Recombining protein suppressor of hairless (Rbpsuh). Reminiscent to the segmental artery formation of *flt1* morphants, Rbpsuh deficient embryos exhibited excessive ECs displaying tip cell behaviour, enhanced EC migration and excessive sprouting (Siekmann and Lawson, 2007). Additionally, *flt1* morphants showed an increased

proliferative behaviour of ECs, resulting in an augmented EC number within segmental arteries, a feature that is also shared by Rbpsuh deficient embryos (Figure 17, Kappas et al., 2008; Kearney et al., 2008; Siekmann and Lawson, 2007). Indeed, *flt1* morphants displayed reduced expression of Notch receptors and the Notch downstream target *efnb2a* (Figure 19), demonstrating decreased Notch signalling in *flt1* morphants. Moreover, Flt1 deficient embryos displayed an ectopic expression of *flt4* in the arterial endothelium; normally associated with loss of Notch signalling (Figure 18A, Siekmann and Lawson, 2007). Since reduced Notch signalling is accompanied with more tip cells, we observed a significantly increased expression of the tip cell markers *flt4* and *kdra/b* in *flt1* morphants (Figure 18). Conversely, it has been shown that Notch activation represses *flt4* and *kdra/b* expression (Taylor et al., 2002; Lawson et al., 2001). Therefore the enhanced expression of the VEGF receptors *flt4* and *kdra/b* might not only be due to a presumed increase of VEGF in *flt1* morphants, but also to a reduced Notch signalling. We propose that Flt1 regulates factors that influence the transcription of *kdra/b* since *flt1* morphants showed a high in increase of *kdra/b* expression (Figure 18B).

In contrast to *flt4* and *kdra/b*, the generally known tip cell marker and Notch ligand *dll4* was only slightly augmented in *flt1* morphants (Figure 18B). Intriguingly, *Dll4* heterozygous mice (*dll4*$^{+/-}$) revealed a decreased expression of Flt1; on the contrary, activation of Dll4 *in vitro* elevated Flt1 expression (Harrington et al., 2008; Suchting et al., 2007). We conclude that Flt1 is regulated by Dll4, while Dll4 is not largely modulated by Flt1. Several studies demonstrated in *Dll4* heterozygous mice and *dll4* morphants enhanced angiogenic sprouting, although the effect on ISV formation was milder than in Rbpsuh deficient embryos (Leslie et al., 2007; Suchting et al., 2007). This implicates that other Notch substrates in addition to Dll4 are involved in segmental artery formation. Moreover, absence of Dll4 and inhibition of VEGF prevented the aberrant sprouting, indicating that VEGF promotes the aberrant sprouting of tip cells (Leslie et al., 2007). Since *dll4* was expressed in *flt1* morphants, we suggest an intact VEGF receptor signalling and the loss of Notch signalling in *flt1* morphants is due to a reduction in Notch expression. A recent study demonstrated that Notch activation stimulated Flt1, while inhibition of Notch decreases Flt1 expression *in vitro* (Funahashi et al., 2010). Based on our results in which we found a general reduction of Notch expression in *flt1* morphants, we propose that not only Notch controls Flt1, but also Flt1 regulates Notch expression and consequently the

tip cell/stalk cell differentiation. We highlighted an essential role for the VEGF decoy receptor sFlt1 during sprouting angiogenesis. sFlt1 modulates the VEGF bioavailability and may adopt functions of mFlt1. Our data indicate a functional role for the extracellular domain of Flt1 in regulating vascular branching (Chapter 6.2), but it remains to be determined how loss of Flt1 causes loss of Notch signalling.

Due to a general reduced expression of all Notch receptors in Flt1 deficient embryos, Flt1 might modulate an upstream factor that is involved in the regulation of all Notch receptors. One of those factors could be the Fringe family of glycosyltransferases. Fringe glycosylates the extracellular domain of Notch (Moloney et al., 2000). This results in an enhanced Notch signalling via Dll4 and a repressed Notch signalling via Jagged 1 (Benedito et al., 2009). Flt1 probably modulates the Fringe activity and therefore the ligand mediated activation of Notch. The Notch ligand Jagged 1 acts as an antagonist of the Dll4-Notch signalling and was downregulated in *flt1* morphants (Figure 19, Benedito et al., 2009). Another possibility as putative factor for Flt1 mediated Notch regulation would be the NAD^+-dependent deacetylase sirtuin 1 (SIRT1). SIRT1 deacetylates NICD in ECs and functions as an intrinsic negative modulator of Notch signalling (Guarani et al., 2011). Inactivation of SIRT1 *in vivo* caused reduced vascular branching and enhanced Notch signalling (Guarani et al., 2011). SIRT1 has been defined as a potential regulator of Notch. Flt1 might negatively regulate SIRT1 and consequently influence the expression of Notch.

Understanding the Flt1 mediated mechanism that regulates the expression of Notch is important to elucidate, since Dll4-Notch signalling in suppressing tip cell formation is not only critical for physiological blood vessel formation, but also for tumour angiogenesis (Kuhnert et al., 2011; Segarra et al., 2008). Beside the central role for Notch signalling during tip cell/stalk cell differentiation, the Notch pathway has been implicated to regulate the arterial-venous differentiation. As the expression of Notch, the arterial marker *efnB2a* as well as the venous marker *flt4* were changed in *flt1* morphants, it would have been anticipated that Flt1 might affect the arterial-venous differentiation. Performing intra vital microscopy of 72 hpf Flt1 deficient embryos revealed no defect of the vessel identity, suggesting that the significance of Notch signalling during arterial-venous differentiation and during sprouting angiogenesis is dose dependent.

Taken together, segmental arteries of *flt1* morphants exhibited ECs with a high degree of migratory and proliferative behaviour. The developing sprout of *flt1*

morphants displayed more tip cells when compared with wild-type embryos. We postulate that these features, combined with a presumed increase of VEGF and the observed reduction of Notch, account for the hyperbranching of segmental arteries in Flt1 deficient embryos. Consistent with this concept, Flt1 may act as a negative regulator of tip cell formation by functioning as a decoy receptor for VEGF and by modulating the Notch expression.

6.3.2 Flt1 mediated branching morphogenesis is Notch dependent

The Dll4-Notch signalling pathway coordinates tip cell/stalk cell differentiation that in turn leads to a controlled formation of segmental arteries. In our study *flt1* morphants displayed hypersprouting of segmental arteries with an increased number of tip cells, features that have been associated with deficient Dll4-Notch signalling (Hellstrom et al., 2007; Siekmann and Lawson et al., 2007; Suchting et al., 2007). Due to the compatible functional and molecular characteristics, we compared the vascular defects of *flt1* morphants with embryos that were treated with *dll4* morpholino or with a Notch inhibitor.

Both *flt1* and *dll4* morphants showed ISV branching defects, but several differences existed including the onset of the hypersprouting and the functionality of the additional sprouts. While aberrant branches in *flt1* morphants emerged at the horizontal myoseptum, the abnormal sprouts in Dll4 deficient embryos arose in close proximity to the DLAV (Figure 20B, B´, D, D´; Leslie et al., 2007). This discrepancy is likely due to a different Flt1 expression and distribution in both morphants, resulting in a fine-tuned VEGF bioavailability that guides the sprout expansion. Moreover, the lumen diameter of aberrant segmental arteries from *flt1* morphants was sufficiently large to allow blood flow, whereas the additional sprouts of *dll4* morphants were unperfused (Figure 20B, D, B´, D´; Leslie et al., 2007). These differences might involve differential effects on stalk cell differentiation as these cells are thought to contribute to lumen formation in developing segmental arteries. Expression of the arterial markers *notch1a* and *efnb2a* were reduced in *flt1* morphants, in contrast to the unaltered expression of arterial and venous markers in Dll4 deficient embryos (Figure 19; Leslie et al., 2007). We conclude that Flt1 functions at a different level

than Dll4 during sprouting angiogenesis. Supporting these findings, the *dll4* expression was only slightly increased in *flt1* morphants (Figure 18).

The vascular branching pattern of *flt1* morphants was not comparable to DAPT treated embryos. DAPT is a γ-secretase inhibitor that blocks Notch signalling (Geling et al., 2002). The vascular phenotype of *flt1* morphants was more severe than that of DAPT treated embryos, in which ECs of the ISVs displayed increased filopodia activity instead of aberrant segmental artery branches (Figure 20B, B´, C, C´). It has been reported that inhibition of Notch resulted in reduced Flt1 expression; conversely, we detected a general reduction of Notch in Flt1 deficient embryos (Figure 19; Funahashi et al., 2010). The discrepancy of the vascular branching pattern of both modified embryos might exist in the extent of Flt1 reduction or distribution induced by DAPT or by Flt1 knockdown. In addition, Flt1 might exert a functional role beyond the level of the tip cell/stalk cell interface, independent of Notch. We showed expression and distribution of sFlt1 throughout the neural tube (Figure 24, Figure 26, Figure 27). Loss of Flt1 reduced the neuronal cell number and caused aberrant segmental artery branches at the level of the neural tube (Figure 29). Although both loss of Notch and Flt1 are associated with decreased Flt1 expression, it is likely that differences exist concerning Flt1 distribution or function that might contribute to differences in the vascular phenotypes. To what extent Flt1 might be regulated by Notch in the neural tube has to be determined by future studies. We conclude that loss of Dll4-Notch signalling does not phenocopy the aberrant segmental artery branches of Flt1 deficient embryos.

During the segmental artery formation of *flt1* morphants we observed a decreased expression of Notch receptors and the downstream target *efnb2a*, an ectopic *flt4* expression in the arterial domain, increased migratory and proliferative behaviour of segmental ECs and an increased tip cell number (Figure 16, Figure 18, Figure 19). Although loss of Dll4-Notch signalling did not phenocopy the aberrant vessel branches of *flt1* morphants, all the observed features suggest a general reduction of Notch signalling in *flt1* morphants and indicate its involvement on the vascular phenotype. Recent studies highlighted Notch in regulating the angiogenic cell behaviour and tip cell differentiation of segmental arteries (Jakobsson et al., 2010; Siekmann and Lawson, 2007). During development, activated Notch restricts the shuffling of segmental ECs from the tip to the stalk cell position and *vice versa* (Jakobsson et al., 2010). Conversely, loss of Notch facilitates shuffling and allows

integration of ECs to the leading edge, reminiscent of the EC behaviour in *flt1* morphants (Figure 16A; Jakobsson et al., 2010). The segmental ECs of Flt1 deficient embryos displayed an increased filopodia activity, a characteristic normally restricted to the tip cells of segmental arteries of wild-type embryos. Conditional overexpression of Notch rescued segmental vessel patterning defects in *flt1* morphants (Figure 21A, B). In this setting, segmental sprouts reached the dorsal roof and formed a DLAV, although the EC movements in the sprout appeared to be limited (Figure 21D). The ECs were more frequently localized at the base of the segmental vessel, instead of being distributed evenly along its length (Figure 21E). A similar accumulation of ECs in the lower part of the sprout was observed in wild-type embryos with activated Notch; nevertheless, these sprouts failed to migrate beyond the horizontal myoseptum (Figure 21A, D, E; Siekmann and Lawson et al., 2007).

We propose a model in which activation of Notch in Flt1 deficient embryos limits the EC migration within the sprout. A reduction in shuffling of ECs displaying tip cell characteristics from the stalk cell towards the leading edge of the segmental sprout might prevent the formation of additional aberrant segmental artery branches. Furthermore, activation of Notch reduced the increased EC number within the segmental arteries of *flt1* morphants (Figure 21C). Consistent with activated Notch signalling, *flt1* mRNA expression increased after Notch activation (Figure 22). An increase in Flt1 levels might contribute to the reduced EC number as well as to the restoration of ISV patterning defects in *flt1* morphants, since Flt1 regulates the VEGF bioavailability and therefore reduces the tip cell formation. These results suggest that Flt1 activation normally enhances Notch signalling and modulates the VEGF bioactivity to limit angiogenic cell behaviour in developing segmental arteries.

6.4 Macrophages are not required for Flt1 mediated ISV formation

Several studies implied a critical role for macrophages during formation of blood vessel networks (Rymo et al., 2011; Stefater et al., 2011; Fantin et al., 2010; Fong et al., 1999). Since Flt1 is not only expressed by vascular ECs but also by hematopetic stem cells (HSCs) of developing blood islands, we analysed an involvement of macrophages in the vascular patterning defects of *flt1* morphants (Heil et al., 2000; Clauss et al., 1996). Using WISH we observed a reduced expression of *l-plastin*, a

macrophage marker, in *flt1* morphants (Figure 23B). While the brain regions were colonized by macrophages, the trunk region of *flt1* morphants displayed fewer macrophages compared to control embryos (Figure 23A, B). We propose that Flt1 deficiency causes an impaired macrophage migration in zebrafish embryos, comparable to the findings in *Flt1*$^{TK-/-}$ mice. The *Flt1*$^{TK-/-}$ mice showed an apparent defect in the migration of macrophages towards VEGF, suggesting that Flt1 conveys signals that regulate the VEGF mediated macrophage migration (Hiratsuka et al., 2001; Hiratsuka et al., 1998). Furthermore, *Flt1*$^{-/-}$ mice exhibited an increased commitment of mesodermal progenitors to become hemangioblasts (Fong et al., 1999). The abnormal increase of hemangioblasts caused disorganized blood vessels that led to embryonic lethality of *Flt1*$^{-/-}$ mice (Fong et al., 1999). These studies emphasised Flt1 as regulator of hemangioblast growth and differentiation and implicated a function for macrophages during blood vessel formation.

A two-way communication between blood vessels and macrophages has been shown in aortic ring assays, where blood vessels attract macrophages, which in turn secrete pro-angiogenic factors (Rymo et al., 2011). In contrast, another study in mice retina demonstrated macrophages as negative regulator of vessel density by producing sFlt1 (Stefater et al., 2011). However, since macrophages, in particular type M2 macrophages, promote angiogenesis by releasing pro-angiogenic factors, it has been hypothesised that macrophages can serve as bridge cells. Facilitating the fusion of two tip cells, macrophages might contribute to the formation of new circuits in the vascular network (Rymo et al., 2011; Carmeliet et al., 2010; Fantin et al., 2010; Tammela et al., 2008; Checchin et al., 2006). This process is called vessel anastomosis and can be observed in zebrafish embryos, when developing sprouts reach the dorsal roof and connect with each other to build the DLAV. A complete absence of macrophages does not affect anastomosis, albeit it occurs less frequent (Rymo et al., 2011; Fantin et al., 2010; Kubota et al., 2009; Checchin et al., 2006). Consequently, macrophages are mainly involved in refining the connecting process. Recently, it has been shown that Notch expression by macrophages is critical for their localization and interaction with tip cells (Outtz et al., 2011). During sprouting angiogenesis the location of macrophages between two anastomosing tip cells was less frequent in *Notch1* mutant mice compared with wild-type (Outtz et al., 2011). In *flt1* morphants we observed an impaired migration of macrophages (Figure 23A, B) and a general reduction of Notch signalling (Figure 19). To gain insight into a putative

contribution of macrophages during vessel anastomosis in *flt1* morphants, we performed knockdown of Pu1, a transcription factor that is expressed in all cells of the myeloid lineage. The vessel pattern of Pu1 deficient embryos revealed no obvious defects, indicating that vessel anastomosis in zebrafish is mainly EC-autonomous (Figure 23C). Accordingly, simultaneous knockdown of Flt1 and Pu1 resulted in aberrant segmental artery branches that were comparable to the vascular patterning defects in *flt1* morphants (Figure 23C). Although Flt1 deficiency caused an impaired migration of macrophages, these results suggest that absence of macrophages does not influence the aberrant branches of *flt1* morphants (Figure 23A, B; Figure 19). We conclude that macrophages are not required for Flt1 mediated branching morphogenesis.

6.5 Flt1 may mediate a cross-talk between neurons and vessels during development

VEGF has initially been characterized as EC-specific growth factor, but recent studies indicated that VEGF is also important for neuronal function (Ruiz de Almodovar et al., 2011; Ogunshola et al., 2002; Carmeliet et al., 1996; Fong et al., 1995; Shalaby et al., 1995). Due to the bidirectional function, VEGF has been described as neurovascular link. During our study we detected expression of its cognate receptor Flt1 in vessels and spinal cord neurons (discussed in Chapter 6.1). Concomitantly, knockdown of Flt1 showed aberrant segmental artery branches and a reduced neuronal cell number (discussed in Chapter 6.2). Our results indicate that Flt1 is involved in the regulation of the vascular and nervous system and might possibly mediate a potential cross-talk between neurons and vessels. Latest evidence proposed an influence of vascular guidance cues on neuronal development. While VEGFR-3 is known to modulate lymphangiogenesis and angiogenesis, a recent study emphasized VEGFR-3 as controller for neurogenesis through VEGF-C in mice (Calvo et al., 2011; Tammela et al., 2008). Furthermore, VEGFR-2 has been characterized to be essential for vascular development and in addition, to act as mediator for axonal outgrowth of neurons in response to semaphorin (Bellon et al., 2010; Olsson et al., 2006).

As noted above, there is strong evidence for the coordination between neurons and vessels; both share similar pathways and grow in close anatomical position to another. Vessels can often be found alongside to neurons and *vice versa*. For instance, the patterning of vessels and nerves is interdependent in the mouse embryo skin and certain embryonic arteries are associated with sensory nerves (Zacchigna et al., 2008; Mukouyama et al., 2002). In our study, vascular specific overexpression of sFlt1 led to a distribution throughout the neural tube (Figure 30, Figure 31). In addition, untreated embryos displayed a diffuse Flt1 staining throughout the neural tube (Figure 27A). These observations indicate that sFlt1 is secreted by ECs and in part can reach the neural tube. How sFt1 reaches the neural tube can possibly be explained by diffusion or by retrograde transport via axons since axons of motor neurons develop in close proximity to segmental arteries in zebrafish embryos. Supporting this hypothesis, we found Flt1 staining in motor neurons of untreated embryos (Figure 28B) and a retrograde transport has been demonstrated for VEGF and VEGFR-2 in rats (Storkebaum et al., 2005; Chapter 6.2.2). To gain insight into a potential influence of distributed sFlt1 and the segmental artery outgrowth, we recorded the segmental artery formation in embryos that overexpressed vascular sFlt1. Indeed, we observed an accumulation of sFlt1 in the neural tube and reduced sprouts that ceased to growth beyond the horizontal myoseptum (Figure 32). Whether the increase of sFlt1 in the neural tube correlates directly with defected vessel sprouting has to be addressed by future studies. It seems likely that sFlt1 secreted by ECs modulates the pre-existing VEGF gradient and therefore the guidance of ISVs. As VEGF is known to affect vessels and neurons, the spatial allocation of sFlt1 in the neural tube might also be required for neuronal survival (Ruiz de Almodovar et al., 2011). In addition to the sFlt1 distribution, we detected Flt1 expression in neurons (Figure 26). Neuronal Flt1 is possibly not only required for neuronal development, but also for the outgrowth of segmental arteries, since Flt1 deficient embryos displayed aberrant vessel branches at the level of the neural tube. We propose that sFlt1 might act cell autonomously as well as non-cell autonomously during development in zebrafish embryos. Earlier studies hypothesised that the function of sFlt1 is context dependent. In the trunk arterial tree of zebrafish embryos sFlt1 appears cell autonomous despite its diffusible nature, while in the mice retina sFlt1 can act non-cell autonomously (Zygmunt et al., 2011; Ambati et al., 2006).

Like the common signal VEGF, Notch has been identified to determine cell fate decisions in the nervous and vascular system. Notch controls the neurogenic commitment of neural stem cells, the endothelial tip cell/stalk cell differentiation and the endothelial arterial-venous cell fate specification (Pierfelice et al., 2011; Swift and Weinstein, 2009; Siekmann and Lawson, 2007). In our study *flt1* morphants exhibited a significantly decreased expression of Notch receptors in arteries and the neural tube (Figure 19), indicating that Flt1 affects Notch expression. As Notch has been characterized to determine cell fate decisions of the vascular and the nervous system, the Flt1 mediated regulation of Notch may has an impact on neuronal survival and vessel outgrowth.

Several studies emphasized a functional interdependence between neurons and vessels. It has been shown that local blood flow influences neuronal activity and that the extent of cerebral perfusion after stroke is associated with the survival of neuronal tissue (Melani and Weinstein, 2010; Krupinski et al., 1994). Furthermore, motor neurons are required for vascular pathfinding in zebrafish embryos (Lim et al., 2011). VEGF and Notch are common signals that are involved in processes of the nervous and vascular system. Since Flt1 can modulate the distribution of VEGF and the expression of Notch in vessels and neurons, we postulate that Flt1 mediates a potential cross-talk between neurons and vessels. The spatial and temporal pattern of Flt1 indicates a role in coordinating segmental artery formation and neuronal cell survival. The open questions for future research are, whether Flt1 plays a functional role at the neurovascular interface by fine-tuning VEGF levels and Notch expression to determine ISV patterning events and neuronal cell survival.

6.6 Conclusions and perspectives

In the last two decades several studies provided insight into the complex mechanism of blood vessel formation, in which VEGF and Notch are important common components. VEGF can act through different receptors, including Flt1. In this work we have studied the function of Flt1 during sprouting angiogenesis in zebrafish embryos. As mammals express different Flt1 isoforms, we initially proved the variability of Flt1 in zebrafish and identified a new soluble isoform of Flt1, termed

sFlt1. Examination of segmental arteries revealed Flt1 expression in stalk and tip cells (Figure 33). Loss- and gain-of-function experiments highlighted a role for Flt1 during branching morphogenesis. Notably, the extracellular VEGF-binding domain appears to be essential in this process, as both Flt1 isoforms could rescue the aberrant vessel branches of *flt1* morphants. Furthermore, we identified Flt1 as a negative regulator of the tip cell formation on physiological and molecular levels. *In vivo* time-lapse imaging revealed an increased number of tip cells during segmental artery formation as well as an upregulation of tip cell markers like *kdra/b* of Flt1 deficient embryos. In addition to heterodimerization, we suggest that Flt1 indirectly regulates *kdra/b* expression (Figure 33). The required Notch signalling activity for tip cell formation was significantly decreased, while surprisingly, the expression of the main Notch ligand *dll4* was unchanged in *flt1* morphants. Therefore we suggest that Flt1 affects Notch signalling and consequently the tip cell formation independently of Dll4 (Figure 33). In general, it has been shown that Notch regulates Flt1 expression, but there is strong evidence that Flt1 can also affect Notch expression (Funahashi et al., 2010; Phng and Gerhardt, 2009). The dynamic behaviour of segmental ECs is controlled by Notch (Jakobsson et al., 2010). Since we observed increased tip cell behaviour and a decreased Notch expression in *flt1* morphants, conditional activation of Notch restored the elevated EC movements and hence the patterning defects caused by Flt1 deficiency. We propose a model in which Flt1 negatively regulates the tip cell formation by influencing Notch expression and the VEGF gradient. To gain insight into the modulation of the VEGF gradient mediated by Flt1, we performed vascular specific overexpression of sFlt1 and observed a distribution throughout the neural tube. In addition, we detected Flt1 expression in spinal cord neurons (Figure 33). This indicates that Flt1 produced by vessels and neurons can modulate the VEGF gradient, which is required for segmental artery outgrowth. Furthermore, we emphasize Flt1 as potential neuroprotective receptor, as Flt1 deficiency resulted in a reduced neuronal cell number. Flt1 plays a critical role during vascular and nervous development. Recently, several studies demonstrated an interdependence of the vascular and the nervous system that in particular is mediated by VEGF and Notch. Since Flt1 affects Notch expression and VEGF distribution, a potential role at the neurovascular interface is suggested for Flt1.

Outstanding questions for future studies are whether Flt1 acts as functional mediator for vessel and neuronal development, how Flt1 can regulate Notch expression and which factors influence Flt1 splicing.

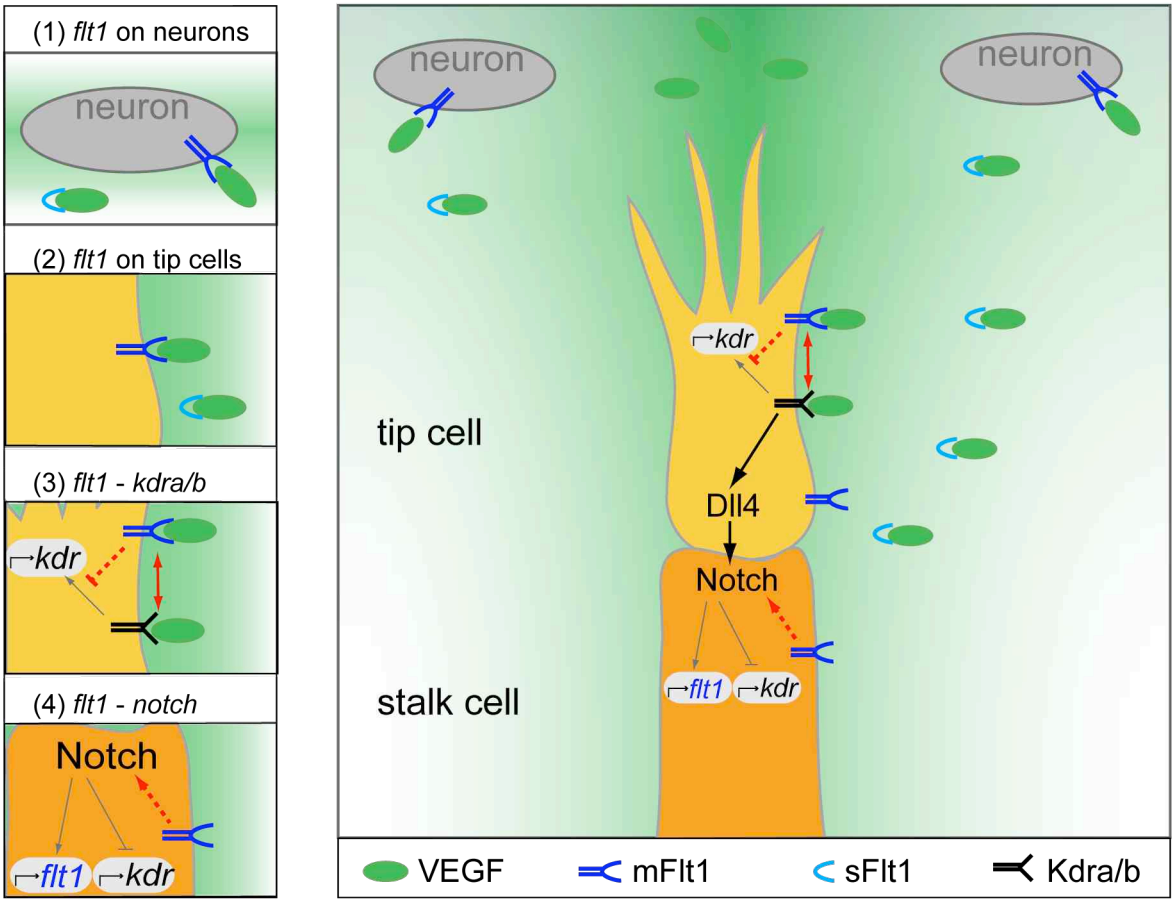

Figure 33. Involvement of Flt1 during segmental artery formation. Blood vessel formation requires a coordinated tip cell/stalk cell differentiation. The leading tip cell of the growing segmental artery is guided by the VEGF gradient. The cognate receptors mFlt1 and sFlt1 are expressed by (1) neurons, (2) tip and stalk cells. In addition, sFlt1 produced by ECs, can distribute to the neural tube. Flt1's spatial allocation modulates the pre-existing VEGF gradient important for segmental artery outgrowth. The tip cell/stalk cell differentiation is controlled by the Dll4-Notch signalling pathway. Flt1 negatively influences (3) *kdra/b* expression and competes with Kdra/b for VEGF binding. While Notch activates *flt1* expression, (4) Flt1 can in return positively regulate the *notch* expression, independently from Dll4.

Blood vessels are required for the transport of oxygen and nutrients to the demanding tissue. Insufficient vessel growth is associated with disorders like myocardial infarction, stroke and neurodegeneration, while an uncontrolled vessel

growth contributes to tumorigenesis and eye diseases (Carmeliet, 2003; Folkman, 1995). Understanding the molecular mechanisms that control the formation of an adequate vessel network will allow us to design new drugs for therapeutic applications. Flt1 has been considered to play a key role in several pathologic conditions since an increased expression is linked to cancer, ocular disorders, and preeclampsia (Herz et al., 2012; Fischer et al., 2008). Flt1 is an important player and regulator for physiological and pathological formation of new blood vessels, thus making it a promising target for potential therapeutics. Combinational therapies with inhibitors against Flt1 and VEGF or VEGFR-2 are used to target anti-angiogenesis in cancers (Chung and Ferrara, 2010; Fischer et al., 2008). In this study we elucidated the involvement of Flt1 during sprouting angiogenesis. Flt1 acts in a Notch dependent manner as negative regulator of tip cell formation. In addition, we revealed insight into Flt1's dual function during the vascular and the neuronal development, which might be interdependent. Towards a therapeutic approach, new insights into the mechanisms of Flt1 during blood vessel formation offer new possibilities. The demonstrated function of Flt1 on vessels and neurons implicate a careful consideration regarding the application of drugs against Flt1 and its side effects. Thus, it is important to further determine the detailed functions of Flt1, that potentially modulate the development of the nervous and the vascular system.

7 Bibliography

AASE, K., VON EULER, G., LI, X., PONTEN, A., THOREN, P., CAO, R., CAO, Y., OLOFSSON, B., GEBRE-MEDHIN, S., PEKNY, M., ALITALO, K., BETSHOLTZ, C. & ERIKSSON, U. (2001) Vascular endothelial growth factor-B-deficient mice display an atrial conduction defect. *Circulation,* 104**,** 358-64.

ADAMS, R. H. & ALITALO, K. (2007) Molecular regulation of angiogenesis and lymphangiogenesis. *Nat Rev Mol Cell Biol,* 8**,** 464-78.

ADAMS, R. H. & EICHMANN, A. (2010) Axon guidance molecules in vascular patterning. *Cold Spring Harb Perspect Biol,* 2**,** a001875.

AGUIRRE, A., RUBIO, M. E. & GALLO, V. (2010) Notch and EGFR pathway interaction regulates neural stem cell number and self-renewal. *Nature,* 467**,** 323-7.

AMBATI, B. K., NOZAKI, M., SINGH, N., TAKEDA, A., JANI, P. D., SUTHAR, T., ALBUQUERQUE, R. J., RICHTER, E., SAKURAI, E., NEWCOMB, M. T., KLEINMAN, M. E., CALDWELL, R. B., LIN, Q., OGURA, Y., ORECCHIA, A., SAMUELSON, D. A., AGNEW, D. W., ST LEGER, J., GREEN, W. R., MAHASRESHTI, P. J., CURIEL, D. T., KWAN, D., MARSH, H., IKEDA, S., LEIPER, L. J., COLLINSON, J. M., BOGDANOVICH, S., KHURANA, T. S., SHIBUYA, M., BALDWIN, M. E., FERRARA, N., GERBER, H. P., DE FALCO, S., WITTA, J., BAFFI, J. Z., RAISLER, B. J. & AMBATI, J. (2006) Corneal avascularity is due to soluble VEGF receptor-1. *Nature,* 443**,** 993-7.

AMBATI, B. K., PATTERSON, E., JANI, P., JENKINS, C., HIGGINS, E., SINGH, N., SUTHAR, T., VIRA, N., SMITH, K. & CALDWELL, R. (2007) Soluble vascular endothelial growth factor receptor-1 contributes to the corneal antiangiogenic barrier. *Br J Ophthalmol,* 91**,** 505-8.

ANDRÉ, T., KOTELEVETS, L., VAILLANT, J. C., COUDRAY, A. M., WEBER, L., PREVOT, S., PARC, R., GESPACH, C. & CHASTRE, E. (2000) Vegf, Vegf-B, Vegf-C and their receptors KDR, FLT-1 and FLT-4 during the neoplastic progression of human colonic mucosa. *Int J Cancer,* 86**,** 174-81.

ANDROUTSELLIS-THEOTOKIS, A., LEKER, R. R., SOLDNER, F., HOEPPNER, D. J., RAVIN, R., POSER, S. W., RUEGER, M. A., BAE, S. K., KITTAPPA, R. & MCKAY, R. D. (2006) Notch signalling regulates stem cell numbers in vitro and in vivo. *Nature,* 442**,** 823-6.

ARTAVANIS-TSAKONAS, S., RAND, M. D. & LAKE, R. J. (1999) Notch signaling: cell fate control and signal integration in development. *Science,* 284**,** 770-6.

AUTIERO, M., WALTENBERGER, J., COMMUNI, D., KRANZ, A., MOONS, L., LAMBRECHTS, D., KROLL, J., PLAISANCE, S., DE MOL, M., BONO, F., KLICHE, S., FELLBRICH, G., BALLMER-HOFER, K., MAGLIONE, D., MAYR-BEYRLE, U., DEWERCHIN, M., DOMBROWSKI, S., STANIMIROVIC, D., VAN HUMMELEN, P., DEHIO, C., HICKLIN, D. J., PERSICO, G., HERBERT, J. M., SHIBUYA, M., COLLEN, D., CONWAY, E. M. & CARMELIET, P. (2003) Role of PlGF in the intra- and intermolecular cross talk between the VEGF receptors Flt1 and Flk1. *Nat Med,* 9**,** 936-43.

AZZOUZ, M., RALPH, G. S., STORKEBAUM, E., WALMSLEY, L. E., MITROPHANOUS, K. A., KINGSMAN, S. M., CARMELIET, P. & MAZARAKIS, N. D. (2004) VEGF delivery with retrogradely transported lentivector prolongs survival in a mouse ALS model. *Nature,* 429**,** 413-7.

BAHARY, N., GOISHI, K., STUCKENHOLZ, C., WEBER, G., LEBLANC, J., SCHAFER, C. A., BERMAN, S. S., KLAGSBRUN, M. & ZON, L. I. (2007) Duplicate VegfA genes and orthologues of the KDR receptor tyrosine kinase family mediate vascular development in the zebrafish. *Blood,* 110**,** 3627-36.

BALDWIN, M. E., HALFORD, M. M., ROUFAIL, S., WILLIAMS, R. A., HIBBS, M. L., GRAIL, D., KUBO, H., STACKER, S. A. & ACHEN, M. G. (2005) Vascular endothelial growth factor D is dispensable for development of the lymphatic system. *Mol Cell Biol,* 25**,** 2441-9.

BANERJEE, S., MEHTA, S., HAQUE, I., SENGUPTA, K., DHAR, K., KAMBHAMPATI, S., VAN VELDHUIZEN, P. J. & BANERJEE, S. K. (2008) VEGF-A165 induces human aortic smooth muscle cell migration by activating neuropilin-1-VEGFR1-PI3K axis. *Biochemistry,* 47**,** 3345-51.

BARLEON, B., SIEMEISTER, G., MARTINY-BARON, G., WEINDEL, K., HERZOG, C. & MARME, D. (1997) Vascular endothelial growth factor up-regulates its receptor fms-like tyrosine kinase 1 (FLT-1) and a soluble variant of FLT-1 in human vascular endothelial cells. *Cancer Res,* 57**,** 5421-5.

BATISTA, M. F., JACOBSTEIN, J. & LEWIS, K. E. (2008) Zebrafish V2 cells develop into excitatory CiD and Notch signalling dependent inhibitory VeLD interneurons. *Dev Biol,* 322**,** 263-75.

BAUM, O., SUTER, F., GERBER, B., TSCHANZ, S. A., BUERGY, R., BLANK, F., HLUSHCHUK, R. & DJONOV, V. (2010) VEGF-A promotes intussusceptive angiogenesis in the developing chicken chorioallantoic membrane. *Microcirculation,* 17**,** 447-57.

BELLAMY, W. T., RICHTER, L., SIRJANI, D., ROXAS, C., GLINSMANN-GIBSON, B., FRUTIGER, Y., GROGAN, T. M. & LIST, A. F. (2001) Vascular endothelial cell growth factor is an autocrine promoter of abnormal localized immature myeloid precursors and leukemia progenitor formation in myelodysplastic syndromes. *Blood,* 97**,** 1427-34.

BELLON, A., LUCHINO, J., HAIGH, K., ROUGON, G., HAIGH, J., CHAUVET, S. & MANN, F. (2010) VEGFR2 (KDR/Flk1) signaling mediates axon growth in response to semaphorin 3E in the developing brain. *Neuron,* 66**,** 205-19.

BENEDITO, R., ROCA, C., SORENSEN, I., ADAMS, S., GOSSLER, A., FRUTTIGER, M. & ADAMS, R. H. (2009) The notch ligands Dll4 and Jagged1 have opposing effects on angiogenesis. *Cell,* 137**,** 1124-35.

BENEDITO, R., ROCHA, S. F., WOESTE, M., ZAMYKAL, M., RADTKE, F., CASANOVAS, O., DUARTE, A., PYTOWSKI, B. & ADAMS, R. H. (2012) Notch-dependent VEGFR3 upregulation allows angiogenesis without VEGF-VEGFR2 signalling. *Nature,* 484**,** 110-4.

BENTLEY, K., GERHARDT, H. & BATES, P. A. (2008) Agent-based simulation of notch-mediated tip cell selection in angiogenic sprout initialisation. *J Theor Biol,* 250**,** 25-36.

BERNHARDT, R. R., CHITNIS, A. B., LINDAMER, L. & KUWADA, J. Y. (1990) Identification of spinal neurons in the embryonic and larval zebrafish. *J Comp Neurol,* 302**,** 603-16.

BIRNBAUM, D. (1995) VEGF-FLT1 receptor system: a new ligand-receptor system involved in normal and tumor angiogenesis. *Jpn J Cancer Res,* 86**,** inside cover.

BLUM, Y., BELTING, H. G., ELLERTSDOTTIR, E., HERWIG, L., LUDERS, F. & AFFOLTER, M. (2008) Complex cell rearrangements during intersegmental vessel sprouting and vessel fusion in the zebrafish embryo. *Dev Biol,* 316**,** 312-22.

BOECKEL, J. N., GUARANI, V., KOYANAGI, M., ROEXE, T., LENGELING, A., SCHERMULY, R. T., GELLERT, P., BRAUN, T., ZEIHER, A. & DIMMELER,

S. (2011) Jumonji domain-containing protein 6 (Jmjd6) is required for angiogenic sprouting and regulates splicing of VEGF-receptor 1. *Proc Natl Acad Sci U S A,* 108**,** 3276-81.

BREIER, G., ALBRECHT, U., STERRER, S. & RISAU, W. (1992) Expression of vascular endothelial growth factor during embryonic angiogenesis and endothelial cell differentiation. *Development,* 114**,** 521-32.

BROWN, L. A., RODAWAY, A. R., SCHILLING, T. F., JOWETT, T., INGHAM, P. W., PATIENT, R. K. & SHARROCKS, A. D. (2000) Insights into early vasculogenesis revealed by expression of the ETS-domain transcription factor Fli-1 in wild-type and mutant zebrafish embryos. *Mech Dev,* 90**,** 237-52.

BURRI, P. H., HLUSHCHUK, R. & DJONOV, V. (2004) Intussusceptive angiogenesis: its emergence, its characteristics, and its significance. *Dev Dyn,* 231**,** 474-88.

BUSSMANN, J., BAKKERS, J. & SCHULTE-MERKER, S. (2007) Early endocardial morphogenesis requires Scl/Tal1. *PLoS Genet,* 3**,** e140.

CALVO, C. F., FONTAINE, R. H., SOUEID, J., TAMMELA, T., MAKINEN, T., ALFARO-CERVELLO, C., BONNAUD, F., MIGUEZ, A., BENHAIM, L., XU, Y., BARALLOBRE, M. J., MOUTKINE, I., LYYTIKKA, J., TATLISUMAK, T., PYTOWSKI, B., ZALC, B., RICHARDSON, W., KESSARIS, N., GARCIA-VERDUGO, J. M., ALITALO, K., EICHMANN, A. & THOMAS, J. L. (2011) Vascular endothelial growth factor receptor 3 directly regulates murine neurogenesis. *Genes Dev,* 25**,** 831-44.

CARMELIET, P. (2003) Angiogenesis in health and disease. *Nat Med,* 9**,** 653-60.

CARMELIET, P. & JAIN, R. K. (2000) Angiogenesis in cancer and other diseases. *Nature,* 407**,** 249-57.

CARMELIET, P., MACKMAN, N., MOONS, L., LUTHER, T., GRESSENS, P., VAN VLAENDEREN, I., DEMUNCK, H., KASPER, M., BREIER, G., EVRARD, P., MULLER, M., RISAU, W., EDGINGTON, T. & COLLEN, D. (1996) Role of tissue factor in embryonic blood vessel development. *Nature,* 383**,** 73-5.

CARMELIET, P. & TESSIER-LAVIGNE, M. (2005) Common mechanisms of nerve and blood vessel wiring. *Nature,* 436**,** 193-200.

CHAPPELL, J. C., TAYLOR, S. M., FERRARA, N. & BAUTCH, V. L. (2009) Local guidance of emerging vessel sprouts requires soluble Flt-1. *Dev Cell,* 17**,** 377-86.

CHECCHIN, D., SENNLAUB, F., LEVAVASSEUR, E., LEDUC, M. & CHEMTOB, S. (2006) Potential role of microglia in retinal blood vessel formation. *Invest Ophthalmol Vis Sci,* 47**,** 3595-602.

CHI, N. C., SHAW, R. M., JUNGBLUT, B., HUISKEN, J., FERRER, T., ARNAOUT, R., SCOTT, I., BEIS, D., XIAO, T., BAIER, H., JAN, L. Y., TRISTANI-FIROUZI, M. & STAINIER, D. Y. (2008) Genetic and physiologic dissection of the vertebrate cardiac conduction system. *PLoS Biol,* 6**,** e109.

CHILDS, S., CHEN, J. N., GARRITY, D. M. & FISHMAN, M. C. (2002) Patterning of angiogenesis in the zebrafish embryo. *Development,* 129**,** 973-82.

CHITNIS, A. B. (1995) The role of Notch in lateral inhibition and cell fate specification. *Mol Cell Neurosci,* 6**,** 311-21.

CHUNG, A. S. & FERRARA, N. (2010) Targeting the tumor microenvironment with SRC kinase inhibition. *Clin Cancer Res,* 16**,** 775-7.

CLAUSS, M., WEICH, H., BREIER, G., KNIES, U., ROCKL, W., WALTENBERGER, J. & RISAU, W. (1996) The vascular endothelial growth factor receptor Flt-1 mediates biological activities. Implications for a functional role of placenta growth factor in monocyte activation and chemotaxis. *J Biol Chem,* 271**,** 17629-34.

COREY, D. R. & ABRAMS, J. M. (2001) Morpholino antisense oligonucleotides: tools for investigating vertebrate development. *Genome Biol,* 2**,** REVIEWS1015.

COULTAS, L., CHAWENGSAKSOPHAK, K. & ROSSANT, J. (2005) Endothelial cells and VEGF in vascular development. *Nature,* 438**,** 937-45.

CROSS, M. J., DIXELIUS, J., MATSUMOTO, T. & CLAESSON-WELSH, L. (2003) VEGF-receptor signal transduction. *Trends Biochem Sci,* 28**,** 488-94.

DAVIS-SMYTH, T., CHEN, H., PARK, J., PRESTA, L. G. & FERRARA, N. (1996) The second immunoglobulin-like domain of the VEGF tyrosine kinase receptor Flt-1 determines ligand binding and may initiate a signal transduction cascade. *EMBO J,* 15**,** 4919-27.

DE JONG, J. S., VAN DIEST, P. J., VAN DER VALK, P. & BAAK, J. P. (1998) Expression of growth factors, growth-inhibiting factors, and their receptors in invasive breast cancer. II: Correlations with proliferation and angiogenesis. *J Pathol,* 184**,** 53-7.

DE SMET, F., SEGURA, I., DE BOCK, K., HOHENSINNER, P. J. & CARMELIET, P. (2009) Mechanisms of vessel branching: filopodia on endothelial tip cells lead the way. *Arterioscler Thromb Vasc Biol,* 29**,** 639-49.

DE VRIES, C., ESCOBEDO, J. A., UENO, H., HOUCK, K., FERRARA, N. & WILLIAMS, L. T. (1992) The fms-like tyrosine kinase, a receptor for vascular endothelial growth factor. *Science,* 255**,** 989-91.

DECAUSSIN, M., SARTELET, H., ROBERT, C., MORO, D., CLARAZ, C., BRAMBILLA, C. & BRAMBILLA, E. (1999) Expression of vascular endothelial growth factor (VEGF) and its two receptors (VEGF-R1-Flt1 and VEGF-R2-Flk1/KDR) in non-small cell lung carcinomas (NSCLCs): correlation with angiogenesis and survival. *J Pathol,* 188**,** 369-77.

DHONDT, J., PEERAER, E., VERHEYEN, A., NUYDENS, R., BUYSSCHAERT, I., POESEN, K., VAN GEYTE, K., BEERENS, M., SHIBUYA, M., HAIGH, J. J., MEERT, T., CARMELIET, P. & LAMBRECHTS, D. (2011) Neuronal FLT1 receptor and its selective ligand VEGF-B protect against retrograde degeneration of sensory neurons. *FASEB J,* 25**,** 1461-73.

DICKSON, B. J. (2002) Molecular mechanisms of axon guidance. *Science,* 298**,** 1959-64.

DJONOV, V., BAUM, O. & BURRI, P. H. (2003) Vascular remodeling by intussusceptive angiogenesis. *Cell Tissue Res,* 314**,** 107-17.

DUARTE, A., HIRASHIMA, M., BENEDITO, R., TRINDADE, A., DINIZ, P., BEKMAN, E., COSTA, L., HENRIQUE, D. & ROSSANT, J. (2004) Dosage-sensitive requirement for mouse Dll4 in artery development. *Genes Dev,* 18**,** 2474-8.

DUMONT, D. J., JUSSILA, L., TAIPALE, J., LYMBOUSSAKI, A., MUSTONEN, T., PAJUSOLA, K., BREITMAN, M. & ALITALO, K. (1998) Cardiovascular failure in mouse embryos deficient in VEGF receptor-3. *Science,* 282**,** 946-9.

EICHMANN, A., LE NOBLE, F., AUTIERO, M. & CARMELIET, P. (2005) Guidance of vascular and neural network formation. *Curr Opin Neurobiol,* 15**,** 108-15.

EKKER, S. C. & LARSON, J. D. (2001) Morphant technology in model developmental systems. *Genesis,* 30**,** 89-93.

FAN, F., WEY, J. S., MCCARTY, M. F., BELCHEVA, A., LIU, W., BAUER, T. W., SOMCIO, R. J., WU, Y., HOOPER, A., HICKLIN, D. J. & ELLIS, L. M. (2005) Expression and function of vascular endothelial growth factor receptor-1 on human colorectal cancer cells. *Oncogene,* 24**,** 2647-53.

FANTIN, A., VIEIRA, J. M., GESTRI, G., DENTI, L., SCHWARZ, Q., PRYKHOZHIJ, S., PERI, F., WILSON, S. W. & RUHRBERG, C. (2010) Tissue macrophages act as cellular chaperones for vascular anastomosis downstream of VEGF-mediated endothelial tip cell induction. *Blood,* 116**,** 829-40.

FERRARA, N., CARVER-MOORE, K., CHEN, H., DOWD, M., LU, L., O'SHEA, K. S., POWELL-BRAXTON, L., HILLAN, K. J. & MOORE, M. W. (1996) Heterozygous embryonic lethality induced by targeted inactivation of the VEGF gene. *Nature,* 380**,** 439-42.

FERRARA, N. & DAVIS-SMYTH, T. (1997) The biology of vascular endothelial growth factor. *Endocr Rev,* 18**,** 4-25.

FERRARA, N., GERBER, H. P. & LECOUTER, J. (2003) The biology of VEGF and its receptors. *Nat Med,* 9**,** 669-76.

FIEDLER, W., GRAEVEN, U., ERGUN, S., VERAGO, S., KILIC, N., STOCKSCHLADER, M. & HOSSFELD, D. K. (1997) Vascular endothelial growth factor, a possible paracrine growth factor in human acute myeloid leukemia. *Blood,* 89**,** 1870-5.

FLAMME, I., FROLICH, T. & RISAU, W. (1997) Molecular mechanisms of vasculogenesis and embryonic angiogenesis. *J Cell Physiol,* 173**,** 206-10.

FLAMME, I., VON REUTERN, M., DREXLER, H. C., SYED-ALI, S. & RISAU, W. (1995) Overexpression of vascular endothelial growth factor in the avian embryo induces hypervascularization and increased vascular permeability without alterations of embryonic pattern formation. *Dev Biol,* 171**,** 399-414.

FOLKMAN, J. (1995) Angiogenesis in cancer, vascular, rheumatoid and other disease. *Nat Med,* 1**,** 27-31.

FOLKMAN, J. & D'AMORE, P. A. (1996) Blood vessel formation: what is its molecular basis? *Cell,* 87**,** 1153-5.

FOLKMAN, J. & SHING, Y. (1992) Angiogenesis. *J Biol Chem,* 267**,** 10931-4.

FONG, G. H., KLINGENSMITH, J., WOOD, C. R., ROSSANT, J. & BREITMAN, M. L. (1996) Regulation of flt-1 expression during mouse embryogenesis suggests a role in the establishment of vascular endothelium. *Dev Dyn,* 207**,** 1-10.

FONG, G. H., ROSSANT, J., GERTSENSTEIN, M. & BREITMAN, M. L. (1995) Role of the Flt-1 receptor tyrosine kinase in regulating the assembly of vascular endothelium. *Nature,* 376**,** 66-70.

FONG, G. H., ZHANG, L., BRYCE, D. M. & PENG, J. (1999) Increased hemangioblast commitment, not vascular disorganization, is the primary defect in flt-1 knock-out mice. *Development,* 126**,** 3015-25.

FOUQUET, B., WEINSTEIN, B. M., SERLUCA, F. C. & FISHMAN, M. C. (1997) Vessel patterning in the embryo of the zebrafish: guidance by notochord. *Dev Biol,* 183**,** 37-48.

FUNAHASHI, Y., SHAWBER, C. J., VORONTCHIKHINA, M., SHARMA, A., OUTTZ, H. H. & KITAJEWSKI, J. (2010) Notch regulates the angiogenic response via induction of VEGFR-1. *J Angiogenes Res,* 2**,** 3.

GAZAVE, E., LAPEBIE, P., RICHARDS, G. S., BRUNET, F., ERESKOVSKY, A. V., DEGNAN, B. M., BORCHIELLINI, C., VERVOORT, M. & RENARD, E. (2009) Origin and evolution of the Notch signalling pathway: an overview from eukaryotic genomes. *BMC Evol Biol,* 9**,** 249.

GELING, A., STEINER, H., WILLEM, M., BALLY-CUIF, L. & HAASS, C. (2002) A gamma-secretase inhibitor blocks Notch signaling in vivo and causes a severe neurogenic phenotype in zebrafish. *EMBO Rep,* 3**,** 688-94.

GERBER, H. P., MCMURTREY, A., KOWALSKI, J., YAN, M., KEYT, B. A., DIXIT, V. & FERRARA, N. (1998) Vascular endothelial growth factor regulates endothelial cell survival through the phosphatidylinositol 3'-kinase/Akt signal transduction pathway. Requirement for Flk-1/KDR activation. *J Biol Chem,* 273**,** 30336-43.

GERHARDT, H., GOLDING, M., FRUTTIGER, M., RUHRBERG, C., LUNDKVIST, A., ABRAMSSON, A., JELTSCH, M., MITCHELL, C., ALITALO, K., SHIMA, D. & BETSHOLTZ, C. (2003) VEGF guides angiogenic sprouting utilizing endothelial tip cell filopodia. *J Cell Biol,* 161**,** 1163-77.

GEUDENS, I. & GERHARDT, H. (2011) Coordinating cell behaviour during blood vessel formation. *Development,* 138**,** 4569-83.

GHANEM, M. A., VAN STEENBRUGGE, G. J., SUDARYO, M. K., MATHOERA, R. B., NIJMAN, J. M. & VAN DER KWAST, T. H. (2003) Expression and prognostic relevance of vascular endothelial growth factor (VEGF) and its receptor (FLT-1) in nephroblastoma. *J Clin Pathol,* 56**,** 107-13.

GOMES, E. & ROCKWELL, P. (2008) p38 MAPK as a negative regulator of VEGF/VEGFR2 signaling pathway in serum deprived human SK-N-SH neuroblastoma cells. *Neurosci Lett,* 431**,** 95-100.

GRIDLEY, T. (1997) Notch signaling in vertebrate development and disease. *Mol Cell Neurosci,* 9**,** 103-8.

GUARANI, V., DEFLORIAN, G., FRANCO, C. A., KRUGER, M., PHNG, L. K., BENTLEY, K., TOUSSAINT, L., DEQUIEDT, F., MOSTOSLAVSKY, R., SCHMIDT, M. H., ZIMMERMANN, B., BRANDES, R. P., MIONE, M., WESTPHAL, C. H., BRAUN, T., ZEIHER, A. M., GERHARDT, H., DIMMELER, S. & POTENTE, M. (2011) Acetylation-dependent regulation of endothelial Notch signalling by the SIRT1 deacetylase. *Nature,* 473**,** 234-8.

HANAHAN, D. & WEINBERG, R. A. (2000) The hallmarks of cancer. *Cell,* 100**,** 57-70.

HARRINGTON, L. S., SAINSON, R. C., WILLIAMS, C. K., TAYLOR, J. M., SHI, W., LI, J. L. & HARRIS, A. L. (2008) Regulation of multiple angiogenic pathways by Dll4 and Notch in human umbilical vein endothelial cells. *Microvasc Res,* 75**,** 144-54.

HE, Y., SMITH, S. K., DAY, K. A., CLARK, D. E., LICENCE, D. R. & CHARNOCK-JONES, D. S. (1999) Alternative splicing of vascular endothelial growth factor (VEGF)-R1 (FLT-1) pre-mRNA is important for the regulation of VEGF activity. *Mol Endocrinol,* 13**,** 537-45.

HEIL, M., CLAUSS, M., SUZUKI, K., BUSCHMANN, I. R., WILLUWEIT, A., FISCHER, S. & SCHAPER, W. (2000) Vascular endothelial growth factor (VEGF) stimulates monocyte migration through endothelial monolayers via increased integrin expression. *Eur J Cell Biol,* 79**,** 850-7.

HELLSTROM, M., PHNG, L. K., HOFMANN, J. J., WALLGARD, E., COULTAS, L., LINDBLOM, P., ALVA, J., NILSSON, A. K., KARLSSON, L., GAIANO, N., YOON, K., ROSSANT, J., IRUELA-ARISPE, M. L., KALEN, M., GERHARDT, H. & BETSHOLTZ, C. (2007) Dll4 signalling through Notch1 regulates formation of tip cells during angiogenesis. *Nature,* 445**,** 776-80.

HERBERT, S. P., HUISKEN, J., KIM, T. N., FELDMAN, M. E., HOUSEMAN, B. T., WANG, R. A., SHOKAT, K. M. & STAINIER, D. Y. (2009) Arterial-venous segregation by selective cell sprouting: an alternative mode of blood vessel formation. *Science,* 326**,** 294-8.

HERBERT, S. P. & STAINIER, D. Y. (2011) Molecular control of endothelial cell behaviour during blood vessel morphogenesis. *Nat Rev Mol Cell Biol,* 12**,** 551-64.

HERBOMEL, P., THISSE, B. & THISSE, C. (1999) Ontogeny and behaviour of early macrophages in the zebrafish embryo. *Development,* 126**,** 3735-45.

HERZ, K., HEINEMANN, J. C., HESSE, M., OTTERSBACH, A., GEISEN, C., FUEGEMANN, C. J., ROLL, W., FLEISCHMANN, B. K. & WENZEL, D. (2012) Live monitoring of small vessels during development and disease using the flt-1 promoter element. *Basic Res Cardiol,* 107**,** 257.

HEYDARIAN, M., MCCAFFREY, T., FLOREA, L., YANG, Z., ROSS, M. M., ZHOU, W. & MAYNARD, S. E. (2009) Novel splice variants of sFlt1 are upregulated in preeclampsia. *Placenta,* 30**,** 250-5.

HIRASHIMA, M., LU, Y., BYERS, L. & ROSSANT, J. (2003) Trophoblast expression of fms-like tyrosine kinase 1 is not required for the establishment of the maternal-fetal interface in the mouse placenta. *Proc Natl Acad Sci U S A,* 100**,** 15637-42.

HIRATSUKA, S., MARU, Y., OKADA, A., SEIKI, M., NODA, T. & SHIBUYA, M. (2001) Involvement of Flt-1 tyrosine kinase (vascular endothelial growth factor receptor-1) in pathological angiogenesis. *Cancer Res,* 61**,** 1207-13.

HIRATSUKA, S., MINOWA, O., KUNO, J., NODA, T. & SHIBUYA, M. (1998) Flt-1 lacking the tyrosine kinase domain is sufficient for normal development and angiogenesis in mice. *Proc Natl Acad Sci U S A,* 95**,** 9349-54.

HIRATSUKA, S., NAKAMURA, K., IWAI, S., MURAKAMI, M., ITOH, T., KIJIMA, H., SHIPLEY, J. M., SENIOR, R. M. & SHIBUYA, M. (2002) MMP9 induction by vascular endothelial growth factor receptor-1 is involved in lung-specific metastasis. *Cancer Cell,* 2**,** 289-300.

HIRATSUKA, S., NAKAO, K., NAKAMURA, K., KATSUKI, M., MARU, Y. & SHIBUYA, M. (2005) Membrane fixation of vascular endothelial growth factor receptor 1 ligand-binding domain is important for vasculogenesis and angiogenesis in mice. *Mol Cell Biol,* 25**,** 346-54.

HLUSHCHUK, R., EHRBAR, M., REICHMUTH, P., HEINIMANN, N., STYP-REKOWSKA, B., ESCHER, R., BAUM, O., LIENEMANN, P., MAKANYA, A., KESHET, E. & DJONOV, V. (2011) Decrease in VEGF expression induces intussusceptive vascular pruning. *Arterioscler Thromb Vasc Biol,* 31**,** 2836-44.

HOGAN, B. M., BOS, F. L., BUSSMANN, J., WITTE, M., CHI, N. C., DUCKERS, H. J. & SCHULTE-MERKER, S. (2009) Ccbe1 is required for embryonic lymphangiogenesis and venous sprouting. *Nat Genet,* 41**,** 396-8.

HOUCK, K. A., FERRARA, N., WINER, J., CACHIANES, G., LI, B. & LEUNG, D. W. (1991) The vascular endothelial growth factor family: identification of a fourth molecular species and characterization of alternative splicing of RNA. *Mol Endocrinol,* 5**,** 1806-14.

ISOGAI, S., LAWSON, N. D., TORREALDAY, S., HORIGUCHI, M. & WEINSTEIN, B. M. (2003) Angiogenic network formation in the developing vertebrate trunk. *Development,* 130**,** 5281-90.

ITO, N. & CLAESSON-WELSH, L. (1999) Dual effects of heparin on VEGF binding to VEGF receptor-1 and transduction of biological responses. *Angiogenesis,* 3**,** 159-66.

ITO, N., HUANG, K. & CLAESSON-WELSH, L. (2001) Signal transduction by VEGF receptor-1 wild type and mutant proteins. *Cell Signal,* 13**,** 849-54.

ITOH, M., KIM, C. H., PALARDY, G., ODA, T., JIANG, Y. J., MAUST, D., YEO, S. Y., LORICK, K., WRIGHT, G. J., ARIZA-MCNAUGHTON, L., WEISSMAN, A. M., LEWIS, J., CHANDRASEKHARAPPA, S. C. & CHITNIS, A. B. (2003) Mind bomb is a ubiquitin ligase that is essential for efficient activation of Notch signaling by Delta. *Dev Cell,* 4**,** 67-82.

JAAKKOLA, P., MOLE, D. R., TIAN, Y. M., WILSON, M. I., GIELBERT, J., GASKELL, S. J., KRIEGSHEIM, A., HEBESTREIT, H. F., MUKHERJI, M., SCHOFIELD, C. J., MAXWELL, P. H., PUGH, C. W. & RATCLIFFE, P. J. (2001) Targeting of HIF-alpha to the von Hippel-Lindau ubiquitylation complex by O2-regulated prolyl hydroxylation. *Science,* 292**,** 468-72.

JAKOBSSON, L., FRANCO, C. A., BENTLEY, K., COLLINS, R. T., PONSIOEN, B., ASPALTER, I. M., ROSEWELL, I., BUSSE, M., THURSTON, G., MEDVINSKY, A., SCHULTE-MERKER, S. & GERHARDT, H. (2010) Endothelial cells dynamically compete for the tip cell position during angiogenic sprouting. *Nat Cell Biol,* 12**,** 943-53.

JEBBINK, J., KEIJSER, R., VEENBOER, G., VAN DER POST, J., RIS-STALPERS, C. & AFINK, G. (2011) Expression of placental FLT1 transcript variants relates to both gestational hypertensive disease and fetal growth. *Hypertension,* 58**,** 70-6.

JELTSCH, M., KAIPAINEN, A., JOUKOV, V., MENG, X., LAKSO, M., RAUVALA, H., SWARTZ, M., FUKUMURA, D., JAIN, R. K. & ALITALO, K. (1997) Hyperplasia of lymphatic vessels in VEGF-C transgenic mice. *Science,* 276**,** 1423-5.

JONES, E. A., LE NOBLE, F. & EICHMANN, A. (2006) What determines blood vessel structure? Genetic prespecification vs. hemodynamics. *Physiology (Bethesda),* 21**,** 388-95.

JONES, M. C., CASWELL, P. T., MORAN-JONES, K., ROBERTS, M., BARRY, S. T., GAMPEL, A., MELLOR, H. & NORMAN, J. C. (2009) VEGFR1 (Flt1) regulates Rab4 recycling to control fibronectin polymerization and endothelial vessel branching. *Traffic,* 10**,** 754-66.

KAIPAINEN, A., KORHONEN, J., MUSTONEN, T., VAN HINSBERGH, V. W., FANG, G. H., DUMONT, D., BREITMAN, M. & ALITALO, K. (1995) Expression of the fms-like tyrosine kinase 4 gene becomes restricted to lymphatic endothelium during development. *Proc Natl Acad Sci U S A,* 92**,** 3566-70.

KAMI, J., MURANAKA, K., YANAGI, Y., OBATA, R., TAMAKI, Y. & SHIBUYA, M. (2008) Inhibition of choroidal neovascularization by blocking vascular endothelial growth factor receptor tyrosine kinase. *Jpn J Ophthalmol,* 52**,** 91-8.

KANNO, S., ODA, N., ABE, M., TERAI, Y., ITO, M., SHITARA, K., TABAYASHI, K., SHIBUYA, M. & SATO, Y. (2000) Roles of two VEGF receptors, Flt-1 and KDR, in the signal transduction of VEGF effects in human vascular endothelial cells. *Oncogene,* 19**,** 2138-46.

KAPLAN, R. N., RIBA, R. D., ZACHAROULIS, S., BRAMLEY, A. H., VINCENT, L., COSTA, C., MACDONALD, D. D., JIN, D. K., SHIDO, K., KERNS, S. A., ZHU, Z., HICKLIN, D., WU, Y., PORT, J. L., ALTORKI, N., PORT, E. R., RUGGERO, D., SHMELKOV, S. V., JENSEN, K. K., RAFII, S. & LYDEN, D. (2005) VEGFR1-positive haematopoietic bone marrow progenitors initiate the pre-metastatic niche. *Nature,* 438**,** 820-7.

KAPPAS, N. C., ZENG, G., CHAPPELL, J. C., KEARNEY, J. B., HAZARIKA, S., KALLIANOS, K. G., PATTERSON, C., ANNEX, B. H. & BAUTCH, V. L. (2008) The VEGF receptor Flt-1 spatially modulates Flk-1 signaling and blood vessel branching. *J Cell Biol,* 181**,** 847-58.

KARKKAINEN, M. J., HAIKO, P., SAINIO, K., PARTANEN, J., TAIPALE, J., PETROVA, T. V., JELTSCH, M., JACKSON, D. G., TALIKKA, M., RAUVALA, H., BETSHOLTZ, C. & ALITALO, K. (2004) Vascular endothelial growth factor C is required for sprouting of the first lymphatic vessels from embryonic veins. *Nat Immunol,* 5**,** 74-80.

KEARNEY, J. B., KAPPAS, N. C., ELLERSTROM, C., DIPAOLA, F. W. & BAUTCH, V. L. (2004) The VEGF receptor flt-1 (VEGFR-1) is a positive modulator of vascular sprout formation and branching morphogenesis. *Blood,* 103**,** 4527-35.

KENDALL, R. L. & THOMAS, K. A. (1993) Inhibition of vascular endothelial cell growth factor activity by an endogenously encoded soluble receptor. *Proc Natl Acad Sci U S A,* 90**,** 10705-9.

KENDALL, R. L., WANG, G. & THOMAS, K. A. (1996) Identification of a natural soluble form of the vascular endothelial growth factor receptor, FLT-1, and its heterodimerization with KDR. *Biochem Biophys Res Commun,* 226**,** 324-8.

KIM, H., SHIN, J., KIM, S., POLING, J., PARK, H. C. & APPEL, B. (2008) Notch-regulated oligodendrocyte specification from radial glia in the spinal cord of zebrafish embryos. *Dev Dyn,* 237**,** 2081-9.

KRUPINSKI, J., KALUZA, J., KUMAR, P., KUMAR, S. & WANG, J. M. (1994) Role of angiogenesis in patients with cerebral ischemic stroke. *Stroke,* 25**,** 1794-8.

KRUSSEL, J. S., CASAN, E. M., RAGA, F., HIRCHENHAIN, J., WEN, Y., HUANG, H. Y., BIELFELD, P. & POLAN, M. L. (1999) Expression of mRNA for vascular endothelial growth factor transmembraneous receptors Flt1 and KDR, and the soluble receptor sflt in cycling human endometrium. *Mol Hum Reprod,* 5**,** 452-8.

KUBOTA, Y., TAKUBO, K., SHIMIZU, T., OHNO, H., KISHI, K., SHIBUYA, M., SAYA, H. & SUDA, T. (2009) M-CSF inhibition selectively targets pathological angiogenesis and lymphangiogenesis. *J Exp Med,* 206**,** 1089-102.

KUHNERT, F., KIRSHNER, J. R. & THURSTON, G. (2011) Dll4-Notch signaling as a therapeutic target in tumor angiogenesis. *Vasc Cell,* 3**,** 20.

LACKNER, D. H. & BAHLER, J. (2008) Translational control of gene expression from transcripts to transcriptomes. *Int Rev Cell Mol Biol,* 271**,** 199-251.

LAGOS-QUINTANA, M., RAUHUT, R., YALCIN, A., MEYER, J., LENDECKEL, W. & TUSCHL, T. (2002) Identification of tissue-specific microRNAs from mouse. *Curr Biol,* 12**,** 735-9.

LANDGREN, E., SCHILLER, P., CAO, Y. & CLAESSON-WELSH, L. (1998) Placenta growth factor stimulates MAP kinase and mitogenicity but not phospholipase C-gamma and migration of endothelial cells expressing Flt 1. *Oncogene,* 16**,** 359-67.

LAWSON, N. D., SCHEER, N., PHAM, V. N., KIM, C. H., CHITNIS, A. B., CAMPOS-ORTEGA, J. A. & WEINSTEIN, B. M. (2001) Notch signaling is required for arterial-venous differentiation during embryonic vascular development. *Development,* 128**,** 3675-83.

LAWSON, N. D. & WEINSTEIN, B. M. (2002) In vivo imaging of embryonic vascular development using transgenic zebrafish. *Dev Biol,* 248**,** 307-18.

LE NOBLE, F., FLEURY, V., PRIES, A., CORVOL, P., EICHMANN, A. & RENEMAN, R. S. (2005) Control of arterial branching morphogenesis in embryogenesis: go with the flow. *Cardiovasc Res,* 65**,** 619-28.

LE NOBLE, F., KLEIN, C., TINTU, A., PRIES, A. & BUSCHMANN, I. (2008) Neural guidance molecules, tip cells, and mechanical factors in vascular development. *Cardiovasc Res,* 78**,** 232-41.

LE NOBLE, F., MOYON, D., PARDANAUD, L., YUAN, L., DJONOV, V., MATTHIJSEN, R., BREANT, C., FLEURY, V. & EICHMANN, A. (2004) Flow regulates arterial-venous differentiation in the chick embryo yolk sac. *Development,* 131**,** 361-75.

LEE, H. K., CHAUHAN, S. K., KAY, E. & DANA, R. (2011) Flt-1 regulates vascular endothelial cell migration via a protein tyrosine kinase-7-dependent pathway. *Blood,* 117**,** 5762-71.

LESLIE, J. D., ARIZA-MCNAUGHTON, L., BERMANGE, A. L., MCADOW, R., JOHNSON, S. L. & LEWIS, J. (2007) Endothelial signalling by the Notch ligand Delta-like 4 restricts angiogenesis. *Development,* 134**,** 839-44.

LEWIS, J. (1998) Notch signalling and the control of cell fate choices in vertebrates. *Semin Cell Dev Biol,* 9**,** 583-9.

LEWIS, K. E. & EISEN, J. S. (2003) From cells to circuits: development of the zebrafish spinal cord. *Prog Neurobiol,* 69**,** 419-49.

LIM, A. H., SULI, A., YANIV, K., WEINSTEIN, B., LI, D. Y. & CHIEN, C. B. (2011) Motoneurons are essential for vascular pathfinding. *Development,* 138**,** 3847-57.

LIU, Z. J., SHIRAKAWA, T., LI, Y., SOMA, A., OKA, M., DOTTO, G. P., FAIRMAN, R. M., VELAZQUEZ, O. C. & HERLYN, M. (2003) Regulation of Notch1 and Dll4 by vascular endothelial growth factor in arterial endothelial cells: implications for modulating arteriogenesis and angiogenesis. *Mol Cell Biol,* 23**,** 14-25.

LOBOV, I. B., RENARD, R. A., PAPADOPOULOS, N., GALE, N. W., THURSTON, G., YANCOPOULOS, G. D. & WIEGAND, S. J. (2007) Delta-like ligand 4 (Dll4) is induced by VEGF as a negative regulator of angiogenic sprouting. *Proc Natl Acad Sci U S A,* 104**,** 3219-24.

LOUVI, A. & ARTAVANIS-TSAKONAS, S. (2006) Notch signalling in vertebrate neural development. *Nat Rev Neurosci,* 7**,** 93-102.

LU, X., LE NOBLE, F., YUAN, L., JIANG, Q., DE LAFARGE, B., SUGIYAMA, D., BREANT, C., CLAES, F., DE SMET, F., THOMAS, J. L., AUTIERO, M., CARMELIET, P., TESSIER-LAVIGNE, M. & EICHMANN, A. (2004) The netrin receptor UNC5B mediates guidance events controlling morphogenesis of the vascular system. *Nature,* 432**,** 179-86.

LUTTUN, A., TJWA, M., MOONS, L., WU, Y., ANGELILLO-SCHERRER, A., LIAO, F., NAGY, J. A., HOOPER, A., PRILLER, J., DE KLERCK, B., COMPERNOLLE, V., DACI, E., BOHLEN, P., DEWERCHIN, M., HERBERT, J. M., FAVA, R., MATTHYS, P., CARMELIET, G., COLLEN, D., DVORAK, H. F., HICKLIN, D. J. & CARMELIET, P. (2002) Revascularization of ischemic tissues by PlGF treatment, and inhibition of tumor angiogenesis, arthritis and atherosclerosis by anti-Flt1. *Nat Med,* 8**,** 831-40.

MARU, Y., HANKS, S. K. & SHIBUYA, M. (2001) The tubulogenic activity associated with an activated form of Flt-1 kinase is dependent on focal adhesion kinase. *Biochim Biophys Acta,* 1540**,** 147-53.

MATSUSHIME, H., YOSHIDA, M. C., SASAKI, M. & SHIBUYA, M. (1987) A possible new member of tyrosine kinase family, human frt sequence, is highly conserved in vertebrates and located on human chromosome 13. *Jpn J Cancer Res,* 78**,** 655-61.

MAZZONE, M., DETTORI, D., LEITE DE OLIVEIRA, R., LOGES, S., SCHMIDT, T., JONCKX, B., TIAN, Y. M., LANAHAN, A. A., POLLARD, P., RUIZ DE ALMODOVAR, C., DE SMET, F., VINCKIER, S., ARAGONES, J., DEBACKERE, K., LUTTUN, A., WYNS, S., JORDAN, B., PISACANE, A., GALLEZ, B., LAMPUGNANI, M. G., DEJANA, E., SIMONS, M., RATCLIFFE, P., MAXWELL, P. & CARMELIET, P. (2009) Heterozygous deficiency of PHD2 restores tumor oxygenation and inhibits metastasis via endothelial normalization. *Cell,* 136**,** 839-51.

MEDURI, G., BAUSERO, P. & PERROT-APPLANAT, M. (2000) Expression of vascular endothelial growth factor receptors in the human endometrium: modulation during the menstrual cycle. *Biol Reprod,* 62**,** 439-47.

MEHTA, D. & MALIK, A. B. (2006) Signaling mechanisms regulating endothelial permeability. *Physiol Rev,* 86**,** 279-367.

MELANI, M. & WEINSTEIN, B. M. (2010) Common factors regulating patterning of the nervous and vascular systems. *Annu Rev Cell Dev Biol,* 26**,** 639-65.

MOLONEY, D. J., PANIN, V. M., JOHNSTON, S. H., CHEN, J., SHAO, L., WILSON, R., WANG, Y., STANLEY, P., IRVINE, K. D., HALTIWANGER, R. S. & VOGT, T. F. (2000) Fringe is a glycosyltransferase that modifies Notch. *Nature,* 406**,** 369-75.

MOSES, M. A. (1997) The regulation of neovascularization of matrix metalloproteinases and their inhibitors. *Stem Cells,* 15**,** 180-9.

MUKOUYAMA, Y. S., SHIN, D., BRITSCH, S., TANIGUCHI, M. & ANDERSON, D. J. (2002) Sensory nerves determine the pattern of arterial differentiation and blood vessel branching in the skin. *Cell,* 109**,** 693-705.

MURAKAMI, M., IWAI, S., HIRATSUKA, S., YAMAUCHI, M., NAKAMURA, K., IWAKURA, Y. & SHIBUYA, M. (2006) Signaling of vascular endothelial growth factor receptor-1 tyrosine kinase promotes rheumatoid arthritis through activation of monocytes/macrophages. *Blood,* 108**,** 1849-56.

MYERS, P. Z. (1985) Spinal motoneurons of the larval zebrafish. *J Comp Neurol,* 236**,** 555-61.

NAGAMATSU, T., FUJII, T., KUSUMI, M., ZOU, L., YAMASHITA, T., OSUGA, Y., MOMOEDA, M., KOZUMA, S. & TAKETANI, Y. (2004) Cytotrophoblasts up-regulate soluble fms-like tyrosine kinase-1 expression under reduced oxygen: an implication for the placental vascular development and the pathophysiology of preeclampsia. *Endocrinology,* 145**,** 4838-45.

NERLOV, C. & GRAF, T. (1998) PU.1 induces myeloid lineage commitment in multipotent hematopoietic progenitors. *Genes Dev,* 12**,** 2403-12.

NILSSON, I., BAHRAM, F., LI, X., GUALANDI, L., KOCH, S., JARVIUS, M., SODERBERG, O., ANISIMOV, A., KHOLOVA, I., PYTOWSKI, B., BALDWIN, M., YLA-HERTTUALA, S., ALITALO, K., KREUGER, J. & CLAESSON-WELSH, L. (2010) VEGF receptor 2/-3 heterodimers detected in situ by proximity ligation on angiogenic sprouts. *EMBO J,* 29**,** 1377-88.

NISHI, J., MINAMINO, T., MIYAUCHI, H., NOJIMA, A., TATENO, K., OKADA, S., ORIMO, M., MORIYA, J., FONG, G. H., SUNAGAWA, K., SHIBUYA, M. & KOMURO, I. (2008) Vascular endothelial growth factor receptor-1 regulates postnatal angiogenesis through inhibition of the excessive activation of Akt. *Circ Res,* 103**,** 261-8.

OGUNSHOLA, O. O., ANTIC, A., DONOGHUE, M. J., FAN, S. Y., KIM, H., STEWART, W. B., MADRI, J. A. & MENT, L. R. (2002) Paracrine and autocrine functions of neuronal vascular endothelial growth factor (VEGF) in the central nervous system. *J Biol Chem,* 277**,** 11410-5.

OLSSON, A. K., DIMBERG, A., KREUGER, J. & CLAESSON-WELSH, L. (2006) VEGF receptor signalling - in control of vascular function. *Nat Rev Mol Cell Biol,* 7**,** 359-71.

ONG, C. T. & CORCES, V. G. (2011) Enhancer function: new insights into the regulation of tissue-specific gene expression. *Nat Rev Genet,* 12**,** 283-93.

OUTTZ, H. H., TATTERSALL, I. W., KOFLER, N. M., STEINBACH, N. & KITAJEWSKI, J. (2011) Notch1 controls macrophage recruitment and Notch signaling is activated at sites of endothelial cell anastomosis during retinal angiogenesis in mice. *Blood,* 118**,** 3436-9.

PALIS, J., MCGRATH, K. E. & KINGSLEY, P. D. (1995) Initiation of hematopoiesis and vasculogenesis in murine yolk sac explants. *Blood,* 86**,** 156-63.

PARK, H. C., HONG, S. K., KIM, H. S., KIM, S. H., YOON, E. J., KIM, C. H., MIKI, N. & HUH, T. L. (2000) Structural comparison of zebrafish Elav/Hu and their differential expressions during neurogenesis. *Neurosci Lett,* 279**,** 81-4.

PARK, J. E., CHEN, H. H., WINER, J., HOUCK, K. A. & FERRARA, N. (1994) Placenta growth factor. Potentiation of vascular endothelial growth factor bioactivity, in vitro and in vivo, and high affinity binding to Flt-1 but not to Flk-1/KDR. *J Biol Chem,* 269**,** 25646-54.

PARK, M. & LEE, S. T. (1999) The fourth immunoglobulin-like loop in the extracellular domain of FLT-1, a VEGF receptor, includes a major heparin-binding site. *Biochem Biophys Res Commun,* 264**,** 730-4.

PATAN, S., HAENNI, B. & BURRI, P. H. (1993) Evidence for intussusceptive capillary growth in the chicken chorio-allantoic membrane (CAM). *Anat Embryol (Berl),* 187**,** 121-30.

PATAN, S., HAENNI, B. & BURRI, P. H. (1996) Implementation of intussusceptive microvascular growth in the chicken chorioallantoic membrane (CAM): 1. pillar formation by folding of the capillary wall. *Microvasc Res,* 51**,** 80-98.

PATAN, S., MUNN, L. L., TANDA, S., ROBERGE, S., JAIN, R. K. & JONES, R. C. (2001) Vascular morphogenesis and remodeling in a model of tissue repair: blood vessel formation and growth in the ovarian pedicle after ovariectomy. *Circ Res,* 89**,** 723-31.

PELSTER, B. & BURGGREN, W. W. (1996) Disruption of hemoglobin oxygen transport does not impact oxygen-dependent physiological processes in developing embryos of zebra fish (Danio rerio). *Circ Res,* 79**,** 358-62.

PHNG, L. K. & GERHARDT, H. (2009) Angiogenesis: a team effort coordinated by notch. *Dev Cell,* 16**,** 196-208.

PHNG, L. K., POTENTE, M., LESLIE, J. D., BABBAGE, J., NYQVIST, D., LOBOV, I., ONDR, J. K., RAO, S., LANG, R. A., THURSTON, G. & GERHARDT, H. (2009) Nrarp coordinates endothelial Notch and Wnt signaling to control vessel density in angiogenesis. *Dev Cell,* 16**,** 70-82.

PILLOZZI, S., BRIZZI, M. F., BERNABEI, P. A., BARTOLOZZI, B., CAPORALE, R., BASILE, V., BODDI, V., PEGORARO, L., BECCHETTI, A. & ARCANGELI, A. (2007) VEGFR-1 (FLT-1), beta1 integrin, and hERG K+ channel for a macromolecular signaling complex in acute myeloid leukemia: role in cell migration and clinical outcome. *Blood,* 110**,** 1238-50.

PIOSSEK, C., SCHNEIDER-MERGENER, J., SCHIRNER, M., VAKALOPOULOU, E., GERMEROTH, L. & THIERAUCH, K. H. (1999) Vascular endothelial growth factor (VEGF) receptor II-derived peptides inhibit VEGF. *J Biol Chem,* 274**,** 5612-9.

PLATE, K. H., BREIER, G., WEICH, H. A., MENNEL, H. D. & RISAU, W. (1994) Vascular endothelial growth factor and glioma angiogenesis: coordinate induction of VEGF receptors, distribution of VEGF protein and possible in vivo regulatory mechanisms. *Int J Cancer,* 59**,** 520-9.

POESEN, K., LAMBRECHTS, D., VAN DAMME, P., DHONDT, J., BENDER, F., FRANK, N., BOGAERT, E., CLAES, B., HEYLEN, L., VERHEYEN, A., RAES, K., TJWA, M., ERIKSSON, U., SHIBUYA, M., NUYDENS, R., VAN DEN BOSCH, L., MEERT, T., D'HOOGE, R., SENDTNER, M., ROBBERECHT, W. & CARMELIET, P. (2008) Novel role for vascular endothelial growth factor

(VEGF) receptor-1 and its ligand VEGF-B in motor neuron degeneration. *J Neurosci,* 28**,** 10451-9.

QUINN, G., OCHIYA, T., TERADA, M. & YOSHIDA, T. (2000) Mouse flt-1 promoter directs endothelial-specific expression in the embyroid body model of embryogenesis. *Biochem Biophys Res Commun,* 276**,** 1089-99.

RAHIMI, N., GOLDE, T. E. & MEYER, R. D. (2009) Identification of ligand-induced proteolytic cleavage and ectodomain shedding of VEGFR-1/FLT1 in leukemic cancer cells. *Cancer Res,* 69**,** 2607-14.

RISAU, W. (1995) Differentiation of endothelium. *FASEB J,* 9**,** 926-33.

RISAU, W. (1997) Mechanisms of angiogenesis. *Nature,* 386**,** 671-4.

ROBINSON, C. J. & STRINGER, S. E. (2001) The splice variants of vascular endothelial growth factor (VEGF) and their receptors. *J Cell Sci,* 114**,** 853-65.

ROCA, C. & ADAMS, R. H. (2007) Regulation of vascular morphogenesis by Notch signaling. *Genes Dev,* 21**,** 2511-24.

ROECKL, W., HECHT, D., SZTAJER, H., WALTENBERGER, J., YAYON, A. & WEICH, H. A. (1998) Differential binding characteristics and cellular inhibition by soluble VEGF receptors 1 and 2. *Exp Cell Res,* 241**,** 161-70.

ROSSI, C. C., KAJI, T. & ARTINGER, K. B. (2009) Transcriptional control of Rohon-Beard sensory neuron development at the neural plate border. *Dev Dyn,* 238**,** 931-43.

ROTTBAUER, W., JUST, S., WESSELS, G., TRANO, N., MOST, P., KATUS, H. A. & FISHMAN, M. C. (2005) VEGF-PLCgamma1 pathway controls cardiac contractility in the embryonic heart. *Genes Dev,* 19**,** 1624-34.

ROYBAL, J. D., ZANG, Y., AHN, Y. H., YANG, Y., GIBBONS, D. L., BAIRD, B. N., ALVAREZ, C., THILAGANATHAN, N., LIU, D. D., SAINTIGNY, P., HEYMACH, J. V., CREIGHTON, C. J. & KURIE, J. M. (2011) miR-200 Inhibits lung adenocarcinoma cell invasion and metastasis by targeting Flt1/VEGFR1. *Mol Cancer Res,* 9**,** 25-35.

RUHRBERG, C. (2003) Growing and shaping the vascular tree: multiple roles for VEGF. *Bioessays,* 25**,** 1052-60.

RUHRBERG, C., GERHARDT, H., GOLDING, M., WATSON, R., IOANNIDOU, S., FUJISAWA, H., BETSHOLTZ, C. & SHIMA, D. T. (2002) Spatially restricted patterning cues provided by heparin-binding VEGF-A control blood vessel branching morphogenesis. *Genes Dev,* 16**,** 2684-98.

RUIZ DE ALMODOVAR, C., FABRE, P. J., KNEVELS, E., COULON, C., SEGURA, I., HADDICK, P. C., AERTS, L., DELATTIN, N., STRASSER, G., OH, W. J., LANGE, C., VINCKIER, S., HAIGH, J., FOUQUET, C., GU, C., ALITALO, K., CASTELLANI, V., TESSIER-LAVIGNE, M., CHEDOTAL, A., CHARRON, F. & CARMELIET, P. (2011) VEGF mediates commissural axon chemoattraction through its receptor Flk1. *Neuron,* 70**,** 966-78.

RUIZ DE ALMODOVAR, C., LAMBRECHTS, D., MAZZONE, M. & CARMELIET, P. (2009) Role and therapeutic potential of VEGF in the nervous system. *Physiol Rev,* 89**,** 607-48.

RYMO, S. F., GERHARDT, H., WOLFHAGEN SAND, F., LANG, R., UV, A. & BETSHOLTZ, C. (2011) A two-way communication between microglial cells and angiogenic sprouts regulates angiogenesis in aortic ring cultures. *PLoS One,* 6**,** e15846.

SAINSON, R. C., AOTO, J., NAKATSU, M. N., HOLDERFIELD, M., CONN, E., KOLLER, E. & HUGHES, C. C. (2005) Cell-autonomous notch signaling regulates endothelial cell branching and proliferation during vascular tubulogenesis. *FASEB J,* 19**,** 1027-9.

SANCHEZ, A., WADHWANI, S. & GRAMMAS, P. (2010) Multiple neurotrophic effects of VEGF on cultured neurons. *Neuropeptides,* 44**,** 323-31.

SAWAMIPHAK, S., SEIDEL, S., ESSMANN, C. L., WILKINSON, G. A., PITULESCU, M. E., ACKER, T. & ACKER-PALMER, A. (2010) Ephrin-B2 regulates VEGFR2 function in developmental and tumour angiogenesis. *Nature,* 465**,** 487-91.

SAWANO, A., IWAI, S., SAKURAI, Y., ITO, M., SHITARA, K., NAKAHATA, T. & SHIBUYA, M. (2001) Flt-1, vascular endothelial growth factor receptor 1, is a novel cell surface marker for the lineage of monocyte-macrophages in humans. *Blood,* 97**,** 785-91.

SCHEER, N. & CAMPOS-ORTEGA, J. A. (1999) Use of the Gal4-UAS technique for targeted gene expression in the zebrafish. *Mech Dev,* 80**,** 153-8.

SCHMIDT, T. & CARMELIET, P. (2010) Blood-vessel formation: Bridges that guide and unite. *Nature,* 465**,** 697-9.

SCOTTO-LAVINO, E., DU, G. & FROHMAN, M. A. (2006a) 3' end cDNA amplification using classic RACE. *Nat Protoc,* 1**,** 2742-5.

SCOTTO-LAVINO, E., DU, G. & FROHMAN, M. A. (2006b) 5' end cDNA amplification using classic RACE. *Nat Protoc,* 1**,** 2555-62.

SEETHARAM, L., GOTOH, N., MARU, Y., NEUFELD, G., YAMAGUCHI, S. & SHIBUYA, M. (1995) A unique signal transduction from FLT tyrosine kinase, a receptor for vascular endothelial growth factor VEGF. *Oncogene,* 10**,** 135-47.

SEGARRA, M., WILLIAMS, C. K., SIERRA MDE, L., BERNARDO, M., MCCORMICK, P. J., MARIC, D., REGINO, C., CHOYKE, P. & TOSATO, G. (2008) Dll4 activation of Notch signaling reduces tumor vascularity and inhibits tumor growth. *Blood,* 112**,** 1904-11.

SENGER, D. R., LEDBETTER, S. R., CLAFFEY, K. P., PAPADOPOULOS-SERGIOU, A., PERUZZI, C. A. & DETMAR, M. (1996) Stimulation of endothelial cell migration by vascular permeability factor/vascular endothelial growth factor through cooperative mechanisms involving the alphavbeta3 integrin, osteopontin, and thrombin. *Am J Pathol,* 149**,** 293-305.

SHALABY, F., HO, J., STANFORD, W. L., FISCHER, K. D., SCHUH, A. C., SCHWARTZ, L., BERNSTEIN, A. & ROSSANT, J. (1997) A requirement for Flk1 in primitive and definitive hematopoiesis and vasculogenesis. *Cell,* 89**,** 981-90.

SHALABY, F., ROSSANT, J., YAMAGUCHI, T. P., GERTSENSTEIN, M., WU, X. F., BREITMAN, M. L. & SCHUH, A. C. (1995) Failure of blood-island formation and vasculogenesis in Flk-1-deficient mice. *Nature,* 376**,** 62-6.

SHAWBER, C. J., FUNAHASHI, Y., FRANCISCO, E., VORONTCHIKHINA, M., KITAMURA, Y., STOWELL, S. A., BORISENKO, V., FEIRT, N., PODGRABINSKA, S., SHIRAISHI, K., CHAWENGSAKSOPHAK, K., ROSSANT, J., ACCILI, D., SKOBE, M. & KITAJEWSKI, J. (2007) Notch alters VEGF responsiveness in human and murine endothelial cells by direct regulation of VEGFR-3 expression. *J Clin Invest,* 117**,** 3369-82.

SHIBUYA, M. (2001) Structure and dual function of vascular endothelial growth factor receptor-1 (Flt-1). *Int J Biochem Cell Biol,* 33**,** 409-20.

SHIBUYA, M., ITO, N. & CLAESSON-WELSH, L. (1999) Structure and function of vascular endothelial growth factor receptor-1 and -2. *Curr Top Microbiol Immunol,* 237**,** 59-83.

SHIBUYA, M., YAMAGUCHI, S., YAMANE, A., IKEDA, T., TOJO, A., MATSUSHIME, H. & SATO, M. (1990) Nucleotide sequence and expression of a novel human

receptor-type tyrosine kinase gene (flt) closely related to the fms family. *Oncogene,* 5**,** 519-24.

SHIN, J., POLING, J., PARK, H. C. & APPEL, B. (2007) Notch signaling regulates neural precursor allocation and binary neuronal fate decisions in zebrafish. *Development,* 134**,** 1911-20.

SIEKMANN, A. F. & LAWSON, N. D. (2007) Notch signalling limits angiogenic cell behaviour in developing zebrafish arteries. *Nature,* 445**,** 781-4.

SONDELL, M., SUNDLER, F. & KANJE, M. (2000) Vascular endothelial growth factor is a neurotrophic factor which stimulates axonal outgrowth through the flk-1 receptor. *Eur J Neurosci,* 12**,** 4243-54.

STAINIER, D. Y., FOUQUET, B., CHEN, J. N., WARREN, K. S., WEINSTEIN, B. M., MEILER, S. E., MOHIDEEN, M. A., NEUHAUSS, S. C., SOLNICA-KREZEL, L., SCHIER, A. F., ZWARTKRUIS, F., STEMPLE, D. L., MALICKI, J., DRIEVER, W. & FISHMAN, M. C. (1996) Mutations affecting the formation and function of the cardiovascular system in the zebrafish embryo. *Development,* 123**,** 285-92.

STALMANS, I., NG, Y. S., ROHAN, R., FRUTTIGER, M., BOUCHE, A., YUCE, A., FUJISAWA, H., HERMANS, B., SHANI, M., JANSEN, S., HICKLIN, D., ANDERSON, D. J., GARDINER, T., HAMMES, H. P., MOONS, L., DEWERCHIN, M., COLLEN, D., CARMELIET, P. & D'AMORE, P. A. (2002) Arteriolar and venular patterning in retinas of mice selectively expressing VEGF isoforms. *J Clin Invest,* 109**,** 327-36.

STEFATER, J. A., 3RD, LEWKOWICH, I., RAO, S., MARIGGI, G., CARPENTER, A. C., BURR, A. R., FAN, J., AJIMA, R., MOLKENTIN, J. D., WILLIAMS, B. O., WILLS-KARP, M., POLLARD, J. W., YAMAGUCHI, T., FERRARA, N., GERHARDT, H. & LANG, R. A. (2011) Regulation of angiogenesis by a non-canonical Wnt-Flt1 pathway in myeloid cells. *Nature,* 474**,** 511-5.

STORKEBAUM, E., LAMBRECHTS, D., DEWERCHIN, M., MORENO-MURCIANO, M. P., APPELMANS, S., OH, H., VAN DAMME, P., RUTTEN, B., MAN, W. Y., DE MOL, M., WYNS, S., MANKA, D., VERMEULEN, K., VAN DEN BOSCH, L., MERTENS, N., SCHMITZ, C., ROBBERECHT, W., CONWAY, E. M., COLLEN, D., MOONS, L. & CARMELIET, P. (2005) Treatment of motoneuron degeneration by intracerebroventricular delivery of VEGF in a rat model of ALS. *Nat Neurosci,* 8**,** 85-92.

STRASSER, G. A., KAMINKER, J. S. & TESSIER-LAVIGNE, M. (2010) Microarray analysis of retinal endothelial tip cells identifies CXCR4 as a mediator of tip cell morphology and branching. *Blood,* 115**,** 5102-10.

SUCHTING, S., FREITAS, C., LE NOBLE, F., BENEDITO, R., BREANT, C., DUARTE, A. & EICHMANN, A. (2007) The Notch ligand Delta-like 4 negatively regulates endothelial tip cell formation and vessel branching. *Proc Natl Acad Sci U S A,* 104**,** 3225-30.

SUMOY, L., KEASEY, J. B., DITTMAN, T. D. & KIMELMAN, D. (1997) A role for notochord in axial vascular development revealed by analysis of phenotype and the expression of VEGR-2 in zebrafish flh and ntl mutant embryos. *Mech Dev,* 63**,** 15-27.

SUTO, K., YAMAZAKI, Y., MORITA, T. & MIZUNO, H. (2005) Crystal structures of novel vascular endothelial growth factors (VEGF) from snake venoms: insight into selective VEGF binding to kinase insert domain-containing receptor but not to fms-like tyrosine kinase-1. *J Biol Chem,* 280**,** 2126-31.

SWIFT, M. R. & WEINSTEIN, B. M. (2009) Arterial-venous specification during development. *Circ Res,* 104**,** 576-88.

TAKAHASHI, H. & SHIBUYA, M. (2005) The vascular endothelial growth factor (VEGF)/VEGF receptor system and its role under physiological and pathological conditions. *Clin Sci (Lond),* 109**,** 227-41.

TAMME, R., WELLS, S., CONRAN, J. G. & LARDELLI, M. (2002) The identity and distribution of neural cells expressing the mesodermal determinant spadetail. *BMC Dev Biol,* 2**,** 9.

TAMMELA, T. & ALITALO, K. (2010) Lymphangiogenesis: Molecular mechanisms and future promise. *Cell,* 140**,** 460-76.

TAMMELA, T., ZARKADA, G., WALLGARD, E., MURTOMAKI, A., SUCHTING, S., WIRZENIUS, M., WALTARI, M., HELLSTROM, M., SCHOMBER, T., PELTONEN, R., FREITAS, C., DUARTE, A., ISONIEMI, H., LAAKKONEN, P., CHRISTOFORI, G., YLA-HERTTUALA, S., SHIBUYA, M., PYTOWSKI, B., EICHMANN, A., BETSHOLTZ, C. & ALITALO, K. (2008) Blocking VEGFR-3 suppresses angiogenic sprouting and vascular network formation. *Nature,* 454**,** 656-60.

TARSITANO, M., DE FALCO, S., COLONNA, V., MCGHEE, J. D. & PERSICO, M. G. (2006) The C. elegans pvf-1 gene encodes a PDGF/VEGF-like factor able to

bind mammalian VEGF receptors and to induce angiogenesis. *FASEB J,* 20**,** 227-33.

TAYLOR, K. L., HENDERSON, A. M. & HUGHES, C. C. (2002) Notch activation during endothelial cell network formation in vitro targets the basic HLH transcription factor HESR-1 and downregulates VEGFR-2/KDR expression. *Microvasc Res,* 64**,** 372-83.

TEN DIJKE, P. & ARTHUR, H. M. (2007) Extracellular control of TGFbeta signalling in vascular development and disease. *Nat Rev Mol Cell Biol,* 8**,** 857-69.

TERMAN, B., KHANDKE, L., DOUGHER-VERMAZAN, M., MAGLIONE, D., LASSAM, N. J., GOSPODAROWICZ, D., PERSICO, M. G., BOHLEN, P. & EISINGER, M. (1994) VEGF receptor subtypes KDR and FLT1 show different sensitivities to heparin and placenta growth factor. *Growth Factors,* 11**,** 187-95.

TERMAN, B. I., DOUGHER-VERMAZEN, M., CARRION, M. E., DIMITROV, D., ARMELLINO, D. C., GOSPODAROWICZ, D. & BOHLEN, P. (1992) Identification of the KDR tyrosine kinase as a receptor for vascular endothelial cell growth factor. *Biochem Biophys Res Commun,* 187**,** 1579-86.

TESSIER-LAVIGNE, M. & GOODMAN, C. S. (1996) The molecular biology of axon guidance. *Science,* 274**,** 1123-33.

THERAPONTOS, C. & VARGESSON, N. (2010) Zebrafish notch signalling pathway mutants exhibit trunk vessel patterning anomalies that are secondary to somite misregulation. *Dev Dyn,* 239**,** 2761-8.

THISSE, B., HEYER, V., LUX, A., ALUNNI, V., DEGRAVE, A., SEILIEZ, I., KIRCHNER, J., PARKHILL, J. P. & THISSE, C. (2004) Spatial and temporal expression of the zebrafish genome by large-scale in situ hybridization screening. *Methods Cell Biol,* 77**,** 505-19.

THOMAS, C. P., ANDREWS, J. I. & LIU, K. Z. (2007) Intronic polyadenylation signal sequences and alternate splicing generate human soluble Flt1 variants and regulate the abundance of soluble Flt1 in the placenta. *FASEB J,* 21**,** 3885-95.

THOMAS, C. P., RAIKWAR, N. S., KELLEY, E. A. & LIU, K. Z. (2010) Alternate processing of Flt1 transcripts is directed by conserved cis-elements within an intronic region of FLT1 that reciprocally regulates splicing and polyadenylation. *Nucleic Acids Res,* 38**,** 5130-40.

THOMPSON, M. A., RANSOM, D. G., PRATT, S. J., MACLENNAN, H., KIERAN, M. W., DETRICH, H. W., 3RD, VAIL, B., HUBER, T. L., PAW, B., BROWNLIE, A. J., OATES, A. C., FRITZ, A., GATES, M. A., AMORES, A., BAHARY, N., TALBOT, W. S., HER, H., BEIER, D. R., POSTLETHWAIT, J. H. & ZON, L. I. (1998) The cloche and spadetail genes differentially affect hematopoiesis and vasculogenesis. *Dev Biol,* 197**,** 248-69.

TREVARROW, B., MARKS, D. L. & KIMMEL, C. B. (1990) Organization of hindbrain segments in the zebrafish embryo. *Neuron,* 4**,** 669-79.

TUNG, J. J., TATTERSALL, I. W. & KITAJEWSKI, J. (2012) Tips, Stalks, Tubes: Notch-Mediated Cell Fate Determination and Mechanisms of Tubulogenesis during Angiogenesis. *Cold Spring Harb Perspect Med,* 2**,** a006601.

VAN EEDEN, F. J., GRANATO, M., SCHACH, U., BRAND, M., FURUTANI-SEIKI, M., HAFFTER, P., HAMMERSCHMIDT, M., HEISENBERG, C. P., JIANG, Y. J., KANE, D. A., KELSH, R. N., MULLINS, M. C., ODENTHAL, J., WARGA, R. M., ALLENDE, M. L., WEINBERG, E. S. & NUSSLEIN-VOLHARD, C. (1996) Mutations affecting somite formation and patterning in the zebrafish, Danio rerio. *Development,* 123**,** 153-64.

VERLOHREN, S., HERRAIZ, I., LAPAIRE, O., SCHLEMBACH, D., MOERTL, M., ZEISLER, H., CALDA, P., HOLZGREVE, W., GALINDO, A., ENGELS, T., DENK, B. & STEPAN, H. (2012) The sFlt-1/PlGF ratio in different types of hypertensive pregnancy disorders and its prognostic potential in preeclamptic patients. *Am J Obstet Gynecol,* 206**,** 58 e1-8.

VILLEFRANC, J. A., AMIGO, J. & LAWSON, N. D. (2007) Gateway compatible vectors for analysis of gene function in the zebrafish. *Dev Dyn,* 236**,** 3077-87.

WALTENBERGER, J., CLAESSON-WELSH, L., SIEGBAHN, A., SHIBUYA, M. & HELDIN, C. H. (1994) Different signal transduction properties of KDR and Flt1, two receptors for vascular endothelial growth factor. *J Biol Chem,* 269**,** 26988-95.

WANG, E. T., SANDBERG, R., LUO, S., KHREBTUKOVA, I., ZHANG, L., MAYR, C., KINGSMORE, S. F., SCHROTH, G. P. & BURGE, C. B. (2008) Alternative isoform regulation in human tissue transcriptomes. *Nature,* 456**,** 470-6.

WANG, S. & OLSON, E. N. (2009) AngiomiRs--key regulators of angiogenesis. *Curr Opin Genet Dev,* 19**,** 205-11.

WANG, Y., NAKAYAMA, M., PITULESCU, M. E., SCHMIDT, T. S., BOCHENEK, M. L., SAKAKIBARA, A., ADAMS, S., DAVY, A., DEUTSCH, U., LUTHI, U., BARBERIS, A., BENJAMIN, L. E., MAKINEN, T., NOBES, C. D. & ADAMS, R. H. (2010) Ephrin-B2 controls VEGF-induced angiogenesis and lymphangiogenesis. *Nature,* 465**,** 483-6.

WEBBY, C. J., WOLF, A., GROMAK, N., DREGER, M., KRAMER, H., KESSLER, B., NIELSEN, M. L., SCHMITZ, C., BUTLER, D. S., YATES, J. R., 3RD, DELAHUNTY, C. M., HAHN, P., LENGELING, A., MANN, M., PROUDFOOT, N. J., SCHOFIELD, C. J. & BOTTGER, A. (2009) Jmjd6 catalyses lysyl-hydroxylation of U2AF65, a protein associated with RNA splicing. *Science,* 325**,** 90-3.

WESTERFIELD, M., MCMURRAY, J. V. & EISEN, J. S. (1986) Identified motoneurons and their innervation of axial muscles in the zebrafish. *J Neurosci,* 6**,** 2267-77.

WESTIN, J. & LARDELLI, M. (1997) Three novel Notch genes in zebrafish: implications for vertebrate Notch gene evolution and function. *Dev Genes Evol,* 207**,** 51-63.

WU, F. T., STEFANINI, M. O., MAC GABHANN, F., KONTOS, C. D., ANNEX, B. H. & POPEL, A. S. (2010) A systems biology perspective on sVEGFR1: its biological function, pathogenic role and therapeutic use. *J Cell Mol Med,* 14**,** 528-52.

XIANG, F., TANAKA, J., TAKAHASHI, J. & FUKUDA, T. (2001) Expression of vascular endothelial growth factor (VEGF) and its two receptors in diffusely infiltrating astrocytomas and relationship to proliferative activity of tumor cells. *Brain Tumor Pathol,* 18**,** 67-71.

YAMAGUCHI, S., IWATA, K. & SHIBUYA, M. (2002) Soluble Flt-1 (soluble VEGFR-1), a potent natural antiangiogenic molecule in mammals, is phylogenetically conserved in avians. *Biochem Biophys Res Commun,* 291**,** 554-9.

YOON, K. & GAIANO, N. (2005) Notch signaling in the mammalian central nervous system: insights from mouse mutants. *Nat Neurosci,* 8**,** 709-15.

YOSHIJI, H., GOMEZ, D. E., SHIBUYA, M. & THORGEIRSSON, U. P. (1996) Expression of vascular endothelial growth factor, its receptor, and other angiogenic factors in human breast cancer. *Cancer Res,* 56**,** 2013-6.

ZACCHIGNA, S., RUIZ DE ALMODOVAR, C. & CARMELIET, P. (2008) Similarities between angiogenesis and neural development: what small animal models can tell us. *Curr Top Dev Biol,* 80**,** 1-55.

ZECCHIN, E., CONIGLIARO, A., TISO, N., ARGENTON, F. & BORTOLUSSI, M. (2005) Expression analysis of jagged genes in zebrafish embryos. *Dev Dyn,* 233**,** 638-45.

ZELTNER, T. B., CADUFF, J. H., GEHR, P., PFENNINGER, J. & BURRI, P. H. (1987) The postnatal development and growth of the human lung. I. Morphometry. *Respir Physiol,* 67**,** 247-67.

ZHANG, Y. & FROHMAN, M. A. (1997) Using rapid amplification of cDNA ends (RACE) to obtain full-length cDNAs. *Methods Mol Biol,* 69**,** 61-87.

ZHONG, T. P., CHILDS, S., LEU, J. P. & FISHMAN, M. C. (2001) Gridlock signalling pathway fashions the first embryonic artery. *Nature,* 414**,** 216-20.

ZYGMUNT, T., GAY, C. M., BLONDELLE, J., SINGH, M. K., FLAHERTY, K. M., MEANS, P. C., HERWIG, L., KRUDEWIG, A., BELTING, H. G., AFFOLTER, M., EPSTEIN, J. A. & TORRES-VAZQUEZ, J. (2011) Semaphorin-PlexinD1 signaling limits angiogenic potential via the VEGF decoy receptor sFlt1. *Dev Cell,* 21**,** 301-14.

8 Abbreviations

ab	antibody
bp	base pair
BSA	bovine serum albumin
CBB	Coomassie brilliant blue
cDNA	complementary DNA
conc	concentration
DA	dorsal aorta
DAPT	N-[N-(difluorophenacetyl)-L-alanyl]-S-phenylglycine t-butyl ester
DEPC	diethyl pyrocarbonate
DIG	digoxigenin
DLAV	dorsal longitudinal anastomotic vessel
Dll1-4	delta-like 1-4
DMOG	dimethyloxalglycine
DNA	deoxyribonucleic acid
DNase	deoxyribonuclease
dNTP	deoxynucleoside triphosphate
DTT	dithiothreitol
EC	endothelial cell
EDTA	ethylenediamine tetraacetic acid
eGFP	enhanced green fluorescent protein
e	exon
FACS	fluorescence-activated cell sorting
f. c.	fold change
Flt1	Fms-like tyrosine kinase1/VEGFR-1
Flt4	Fms-like tyrosine kinase 4/VEGFR-3
GFP	green fluorescent protein
GFP+	green fluorescent protein positive
GFP-	green fluorescent protein negative
GSP1/2	gene specific primer 1/2
hpf	hour per fertilization
HUVEC	human umbilical vein endothelial cell
IC	intracellular

IF	immunofluorescence
Ig	immunoglobulin
IPTG	isopropylthio-β-D-galactoside
ISV	intersomitic vessel
Jag1-2	Jagged1-2
Kdra	kinase insert domain receptor-like/VEGFR-2
Kdrb	kinase insert domain receptor/VEGFR-2
MAPK	mitogen-activated protein kinases
mFlt1	membrane-bound Fms-like tyrosine kinase1/mVEGFR-1
MO	morpholino
mRNA	messenger RNA
NICD	Notch intracellular domain
Nrarpa/b	Notch-regulated ankyrin repeat protein a/b
o/n	over night
PAGE	polyacrylamide gel electrophoresis
PBS	phospate buffered saline
PBS-T	phospate buffered saline-Tween 20
PCR	polymerase chain reaction
PCV	posterior cardinal vein
PFA	paraformaldehyde
PLGF	placental growth factor
pre mRNA	precursor mRNA
PTK7	protein tyrosine kinase-7
PTU	1-phenyl-2-thiourea
PVDF	polyvinylidene difluoride
qRT-PCR	quantitative real-time PCR
RACE-PCR	rapid amplification of cDNA-ends with PCR
RNA	ribonucleic acid
RNase	ribonuclease
Rpm	revolution per minute
rbpsuh	recombining protein suppressor of hairless
RT-PCR	reverse transcription PCR
SDS	sodium dodecylsulfate
SEM	standard error of the mean

sFlt1	solube Fms-like tyrosine kinase1/sVEGFR-1
SIRT1	NAD^+-dependent deacetylase sirtuin 1
Taq	*Thermus aquaticus*
TEMED	N, N, N', N'-tetramethylethylendiamin
Tg	transgenic
TM	transmemnrane-spanning domain
Tris	tris(hydroxymethyl)-aminomethane
TyrKc	tyrosine kinase catalytic domain
VEGF	vascular endothelial growth factor
VEGFR	vascular endothelial growth factor receptor
WB	Western blotting
WISH	whole mount in situ hybridization
X-gal	5-bromo-4-chloro-3-indolyl-β-D-galactoside
YFP	yellow fluorescent protein
3` UTR	3` untranslated region
5` UTR	5` untranslated region

9 List of figures

10 List of tables

11 Curriculum vitae and publications

Der Lebenslauf ist in der Online-Version aus Gründen des Datenschutzes nicht enthalten.

Due to data privacy protection there is no curriculum vitae in the online version.

Der Lebenslauf ist in der Online-Version aus Gründen des Datenschutzes nicht enthalten.

Due to data privacy protection there is no curriculum vitae in the online version.